RUNX EXPRESSION IN NORMAL AND OSTEOARTHRITIC CARTILAGE: POSSIBLE FUNCTIONS OF RUNX PROTEINS IN CHONDROCYTES

A Dissertation Presented

By

Kimberly Taylor LeBlanc

Submitted to the Faculty of the

University of Massachusetts Graduate School of Biomedical Sciences, Worcester

in partial fulfillment of the requirements for the degree of

DOCTOR OF PHILOSOPHY

February 28, 2013

M.D./Ph.D Program in Biomedical Sciences

RUNX EXPRESSION IN NORMAL AND OSTEOARTHRITIC CARTILAGE:

POSSIBLE FUNCTIONS OF RUNX PROTEINS IN CHONDROCYTES

A Dissertation Presented
By

Kimberly Taylor LeBlanc

The signatures of the Dissertation Defense Committee signifies completion and approval as to style and content of the Dissertation

Jane Lian, Ph.D., Thesis Advisor

Paul Fanning, Ph.D., Member of Committee

Ellen Gravallese, M.D., Member of Committee

Anthony Imbalzano, Ph.D., Member of Committee

Louis Gerstenfeld, Ph.D., External Member of Committee

The signature of the Chair of the Committee signifies that the written dissertation meets the requirements of the Dissertation Committee

Paul Odgren Ph.D., Chair of Committee

The signature of the Dean of the Graduate School of Biomedical Sciences signifies that the student has met all graduation requirements of the school.

Anthony Carruthers, Ph.D.
Dean of the Graduate School of Biomedical Sciences

M.D./Ph.D Program in Biomedical Sciences
February 28, 2013

Acknowledgements

I would like to thank Dr. Jane Lian, my thesis advisor, for her outstanding support during my time in her laboratory. Despite her busy schedule, she always made time to sit down with me and discuss experimental design, results and conclusions. She was able to identify my weaknesses as a scientist and worked with me to overcome them. In addition to her endless support and encouragement, it was an amazing opportunity to work with a woman who made such outstanding contributions to the fields of bone and cancer biology.

Dr. Gary Stein, my co-mentor, deserves a great deal of thanks as well. His excitement about science was always inspirational, especially during the many times my experiments weren't working. He was always there with words of encouragement, ideas for the future of my projects, or a joke to lighten the mood. Dr. Stein truly balances his love of science and research, with his life outside of the laboratory and has been an inspiration throughout my graduate years.

In addition to Drs. Lian and Stein, I was fortunate enough to have two additional principal investigators who were always there to offer advice during the course of my project. I would like to thank Dr. Janet Stein and Dr. Andre van Wijnen for all of their input on experimental design, proper controls, and data analysis and interpretation. I deeply appreciate their input on my project, and their help with any question I ever came to them with.

The first two chapters of this thesis would not have been possible without the collaboration of Dr. Paul Fanning. Dr. Fanning taught me everything I know about analysis of cartilage samples. He helped me with everything from the technical aspects of experiments to data analysis and interpretation. In addition to being a great mentor, I enjoyed my conversations about running, baseball, and life in general (although I am secretly happy that my number didn't get picked for the Mt. Washington Road Race!)

I would also like to thank Dr. Marci Jones for her support, both in the lab, and as I pursue a career in orthopedics. She was always there to answer any questions I had about orthopedics, research, or balancing life as a mom/surgeon/wife/researcher. I am also very grateful that she allowed me to shadow her in the clinic and in the operating room, both of which were extremely valuable learning experiences.

I am very grateful to the members of my TRAC Dr. Ellen Gravallese, Dr. Tim Kowalik, and Dr. Paul Fanning for stimulating intellectual conversation, ideas, and advice on my various projects. I am especially thankful to my chair, Dr. Paul Odgren, for all of his support along the way, and for not seeming to mind my countless office visits asking him for advice, which he was always willing to give! I would like to thank Dr. Tony Imbalzano and Dr. Louis Gerstenfeld for taking time out of their busy schedules and agreeing to be on my DEC.

There are so many other members of the Stein/Lian/van Wijnen lab that deserve thanks as well. Dr. Julie Liu, a former lab member, took me under her

wing when I first joined the lab and was incredibly helpful in getting my project started. Dr. Tripti Gaur helped me with chondrocyte differentiation models, data analysis and interpretation, and MEF preparation. Dr. Kaleem Zaidi, Dr. Prachi Ghule, and Akhtar Ali were helpful with immunofluorescense studies and never seemed to mind when I pulled them away from their benches to look at my slides under the microscope. Dr. Mohammad Hassan taught me how to do EMSAs, and always gave great advice on life in general. Dr. Jonathan Gordon was always available to answer pretty much any question I had about any experiment I did. My fellow graduate students Sandhya Pande and Chris Dowdy were helpful with my Runx overexpression experiments, and always had helpful advice. I am especially thankful to my fellow graduate student Jason Dobson for being amazingly helpful with my ChIP experiments, IF experiments, and for letting me steal (borrow) all of his reagents. I am grateful to Shirwin Pockwinse, who is the driving force behind keeping the lab in order. I am also grateful to Marissa Johnson, who was incredibly accommodating with my tissue culture orders, and to Dana Frederick who always knew where to find everything I was looking for. I would like to thank Dr. Jack Wixted for allowing me to shadow him in the operating room, and for advice on pursuing a career in orthopedic surgery and research. I would like to thank Marta DeSourtes and Judy Rask for all of their editorial and administrative assistance. I am grateful to all members of the lab, past and present, because they have all helped me out with something along the way. Additionally, I would like to thank Matthew Mandeville, Marissa

Johnson, Kristie Kapinas, Gillian Browne, and Dana Frederick for being like family to me, and for providing endless hours of entertainment.

Lastly, I would like to thank my friends and family for their support throughout this journey. My parents Kenneth and Susan, despite not attending college, were very supportive of my choice to pursue an MD/PhD degree. My brothers Keith and Kenny have also always been there for anything I needed. I am also thankful to aunts, uncles, grandparents, and cousins for their endless support. There are many groups of friends who have kept me sane throughout my journey. I am grateful to my running friends (all the athletes I have coached, members of my relay team, Rachel Levitsky, Dyan Lally, and my triathlon coach Dan Graovac), my showchoir kids (along with Peter Carney and Greg “Bubba” Bussiere who inspired me to go to medical school), fellow UMass friends (Dr. Jennifer Laine, Alison Bright, Dr. Nikki Mehta, Dr. Michal Ganz, Dr. Miguel Concepcion, Dr. William Daya, Dr. Sam Ayala, and Dr. Brad Schwartz), fellow MD/PhD students (Liz Yu, Shira Fischer, Tom Flood, Joanna Chaurette), the book club ladies (Kate Gerber, Jennifer Audette, Angela Buccini, and Jennifer Rodeheffer), and Jillian Levasseur, Donny Moisan, Jessica McPartland, Leah Williams, Christine VanNort, Christine D’Eramo, and Michelle Charon, for being the most amazing, understanding, and supportive friends a girl could want! I would also like to give a special thanks to Oren Malka, for his kindness, generosity, patience, and support during this whole process, and also for driving anywhere from 20 minutes to 1 hour out of his way on multiple occasions to bring

me coffee or food while I was writing this dissertation; I could not have made it through this without him!

Abstract

The Runx family of transcription factors supports cell fate determination, cell cycle regulation, global protein synthesis control, and genetic as well as epigenetic regulation of target genes. Runx1, which is essential for hematopoiesis; Runx2, which is required for osteoblast differentiation; and Runx3, which is involved in neurologic and gut development; are expressed in the growth plate during chondrocyte maturation, and in the chondrocytes of permanent cartilage structures. While Runx2 is known to control genes that contribute to chondrocyte hypertrophy, the functions of Runx1 and Runx3 during chondrogenesis and in cartilage tissue have been less well studied.

The goals of this project were to characterize expression of Runx proteins in articular cartilage and differentiating chondrocytes and to determine the contribution of Runx1 to osteoarthritis (OA). Here, the expression pattern of Runx1 and Runx2 was characterized in normal bovine articular cartilage. Runx2 is expressed at higher levels in deep zone chondrocytes, while Runx1 is primarily expressed in superficial zone chondrocytes, which is the single cell layer that lines the surface of articular cartilage. Based on this finding, the hypothesis was tested that Runx1 is involved in osteoarthritis, which is a disease characterized by degradation of articular cartilage and changes in chondrocytes. These studies showed that Runx1 is upregulated in articular cartilage explants in response to mechanical compression. Runx1 was also expressed in chondrocytes found at the periphery of OA lesions in the articular cartilage of mice that underwent an

OA-inducing surgery. Runx1 was also upregulated in cartilage explants of human osteoarthritic knees, and IHC data showed that Runx1 is mainly expressed in chondrocyte “clones” characteristic of OA.

To ascertain the potential function of the upregulation of Runx1 in these cartilage stress conditions and disease states, the hypothesis was tested that Runx1 is upregulated in very specific chondrocyte populations in response to the cartilage damage in osteoarthritis. These studies addressed the properties of these cells that related to functions in cell growth and differentiation. In both the surface layer of normal articular cartilage, and in OA cartilage, Runx1 expression by IF co-localized with markers of mesenchymal progenitor cells, as well as markers of proliferation Ki-67 and PCNA. This finding indicated that Runx1 is found in a population of cells that represent a proliferative population of mesenchymal progenitor cells in osteoarthritis.

To further address Runx1 function and identify downstream targets of Runx proteins, a promoter analysis of genes that are known to be either downregulated or upregulated during chondrocyte maturation was done. These studies found that many of these genes have 1 or more Runx binding sites within 2kb of their transcription start site, indicating that they are potential downstream Runx target genes.

Lastly, some preliminary experiments were done to characterize novel roles of Runx proteins in the chondrocyte. Runx proteins have been shown to epigenetically regulate their target genes by remaining bound to them throughout

mitosis, “poising” them for transcription upon exit from mitosis. The hypothesis that Runx proteins also function by remaining bound to their target genes throughout mitosis in chondrocytes was tested. It was demonstrated by immunofluorescense imaging of Runx proteins on metaphase chromosomes of ATDC5 cells, that Runx2 remains bound to chromosomes during mitosis.

Cell proliferation and hypertrophy are both linked to increases in protein synthesis. Runx factors, which regulate rates of global protein synthesis, are expressed in both proliferating and hypertrophic chondrocytes. Thus, it was hypothesized that Runx proteins regulate rates of global protein synthesis during chondrocyte maturation. These studies showed that the overexpression of Runx proteins in a chondrocyte cell line (ATDC5) did not affect protein synthesis rates or levels of protein synthesis machinery. Additionally, Runx proteins did not affect proliferation rates in this chondrocyte cell line.

Table of Contents

List of Tables

List of Figures

List of Abbreviations

ALL – acute lymphocytic leukemia
AML – acute myelogenous leukemia
BMP – bone morphogenic protein
BSA – bovine serum albumin
dGEMRIC – delayed gadolinium-enhanced MRI of cartilage
DMEM – Dulbecco's Modified Eagle Medium
DMM – destabilization of the medial meniscus
DMOADs – disease-modifying osteoarthritis drugs
DTT – Dithiothreitol
DZ – deep zone
EDTA - ethylenediaminetetraacetic acid
FBS – fetal bovine serum
IF – immunofluorescence
IHC - immunohistochemistry
MEF – mouse embryonic fibroblast
MMP – matrix metalloproteinase
MPC – mesenchymal progenitor cell
MZ – middle zone
NSAIDs – non-steroidal anti-inflammatory drugs
OA - osteoarthritis
PBS – phosphate-buffered saline
PCNA – proliferating cell nuclear antigen
PIS – pressure-induced strain
SDS - sodium dodecyl sulfate
SZ – superficial zone

Runx nomenclature:
Runx1 = CBFA2 = AML1 = PEBP2aB
Runx2 = CBFA1 = AML3 = PEPB2aA
Runx3 = CBFA3 = AML2 = PEBP2aC

Preface

Chapters II and III, were a collaborative effort between the Stein/Lian/van Wijnen and Fanning Laboratories and the work is being submitted for publication under the title "Runx1 is Present in Superficial Zone Chondrocytes and Upregulated in Response to Compression in Human and Mouse Model Osteoarthritic Tissue". For this project, Dr. Marie Walcott did many of the human and mouse immunofluorescense experiments and repeated the qPCR on articular chondrocytes, as well as assisting with Destabilization of the Medial Meniscus (DMM) surgeries, articular cartilage isolation, figure preparation, and data analysis. Shannon L. O'Connell also assisted with DMM surgeries, articular cartilage isolation, and western blot analysis. Kirti Basil performed many of the double immunoflourescent experiments. Dr. Fanning performed double IF, western blots, IHC and imaging analysis. April Mason-Savas did all the paraffin embedding and tissue sectioning. Dr. Jason Silva assisted with DMM surgeries. I am very grateful for all of their work on this project it would not have been complete without their efforts.

CHAPTER I:

GENERAL INTRODUCTION

Osteoarthritis

Osteoarthritis is a major public health issue in the United States, and it is estimated that as many as 26.9 million adults exhibited some type of clinical OA in 2005, with as many as 9.3 million adults having symptomatic knee OA. The prevalence of osteoarthritis is of significant financial burden both on the US healthcare system and on patients with the disease. One study shows that OA increases insurer expenditures by as much as $149.4 billion/year, and out of pocket expenditures by $36.1 billion/year [1]. With the aging of the "Baby Boomer" generation, this cost is expected to increase with time. In fact, the cost of total hip and knee replacements alone is expected to exceed $100 billion annually by the year 2030 [2]. Thus it is of public health interest to explore more cost-effective ways to detect, treat, and prevent this disease. This necessitates an understanding of the molecular processes that are involved with disease initiation and progression.

This dissertation contributes to the molecular profiling of OA. The characterization of the expression of Runx1 in normal articular and osteoarthritic cartilage, and the preliminary experiments on some novel functions of Runx proteins in cartilage, begin to explore the role of Runx proteins in cartilage and osteoarthritis. By way of introduction, this is a general background on the current knowledge of gene expression during the disease process of osteoarthritis, as well as information about Runx family of transcription factors, and their role in the process of endochondral ossification, and permanent cartilage formation.

Osteoarthritis: Risk Factors, Diagnosis, and Current Treatment Options

There are many well-known risk factors for knee OA, including increased BMI, prior history of knee injury, certain occupations (such as farming, construction, and physical education instructors), increased bone mineral density (although increased bone mineral density is correlated with increased BMI, and so this may not be an independent risk factor), exercise, and previous menisectomy [3]. One of the most prevalent risk factors for development of OA is age, with an estimated 25% of asymptomatic patients over the age of 50 predicted to develop knee pain within three years [4]. It is important to understand the molecular basis behind these risk factors. It is well established that mechanical strain is a risk factor for development of OA, which explains why certain occupations and a history of knee injury are risk factors for its development. For many years, it was thought that the obesity resulted in increased mechanical strain on knee joints, which accounted for the increased incidence of OA in overweight or obese people. More recent literature shows that there is more than just increased mechanical strain that contributes to the development of OA in obesity [5-7]. Obesity is associated with an increase in systemic cytokines known as adipokines, which are released by adipose tissue. A chronic inflammatory state is associated with the development and progression of OA. Specifically, IGF-1, TGF-B, IL-1, IL-6, TNF-a, prostaglandin E2, and NO have all been associated with OA [5]. IL-1B has been shown to increase MMPs while certain mutations in the IL-1 receptor IL1RN result in resistance to OA [6].

Leptin, another molecule that is released by adipocytes, induces expression of MMP1 and MMP3 in cartilage explants [7]. The correlation between the release of cytokines by adipose tissue, and the role of these inflammatory cytokines in OA can help explain why there is an increased incidence of OA in weight-bearing joints (knee, hip), as well as non weight-bearing joints (hands) in obese patients. There does, however, still seem to be an association between obesity and impaired biomechanics. An increase in BMI is associated with an increase in the degree of knee malalignment [8], which is well-known to contribute to the pathogenesis of knee OA. Other studies show that an increase in BMI is only associated with joint space narrowing in people who have moderate malallignments already [9] . Additionally, Griffin et al. showed that obese mice have a higher incidence of OA, but that wheel running is protective [5]. This seems counter-intuitive given that wheel running results in a higher load on the knee joint. One theory is that cyclic loading is protective in OA, with repetitive loading promoting an increase in antioxidants which helps battle cartilage damage by removing damaging free radicals from chondrocytes [5]. Taken together, these data show that there is a multi-factorial contribution of obesity to OA.

The main risk factor for OA is age, and this is likely due to a composition of many of the above factors. For example, it is common to find evidence of incidental meniscal damage on MRI in the elderly, which leads to joint space immobility, altered biomechanics, and osteoarthritis [10]. Aged cartilage has

lower levels of antioxidant enzymes than younger cartilage [11]. With cartilage strain promoting free radical production and lower levels of antioxidants, OA is more likely to develop. As with obesity, cytokine signaling plays a role in the development of OA with age. In fact, elderly patients with lower circulating levels of IL-1B had a lower incidence of hip OA, while elderly patients with lower levels of IL-6 and IL-1A had lower incidence of hand OA [12].

Currently, osteoarthritis is difficult to monitor and to treat. Patients who present with joint pain and have joint space narrowing on X-ray are diagnosed with osteoarthritis. By the time there is joint space narrowing on X-ray, there is no way to reverse the disease process. In mice with surgically induced osteoarthritis, recombinant human PTH(1-34) was found to inhibit cartilage degeneration [13]. It is important to be able to monitor early disease progression in OA and to understand the molecular mechanisms that will inhibit and reverse cartilage damage. The recent implementation of delayed gadolinium enhanced magnetic resonance imaging (dGEMRIC) may make it possible for to detect changes in cartilage matrix composition that take place in early stages of OA, prior to the detection of joint space narrowing by X-ray. This imaging method is able to detect changes in cartilage matrix components in early OA, before there is cartilage destruction and joint space narrowing [14]. While this is promising, its widespread use is limited by cost and by the fact that even if OA changes were detected at an early stage, there are currently no treatment options in humans that are proven to halt the disease course.

Current treatment options for OA are extremely limited. The most common treatment options are acetaminophen or non-steroidal anti-inflammatory drugs (NSAIDs) to treat pain resulting from symptomatic OA [15]. The only treatment for advanced OA, accompanied by joint destruction, is a total joint replacement. Currently, 97% of total knee and 82% of total hip replacements are due to OA [2]. It is clear that we must develop better treatment strategies than pain management and joint replacement, and there is a push for development of disease modifying osteoarthritis drugs (DMOADs). Currently in clinical trials are items such as intra-articular stem cell injections, antioxidant therapy, IL1 receptor antagonists, and even BoTox therapy [16]. The most useful OA drugs would stop cartilage damage and even initiate cartilage repair. An important first step in the development of these drugs is the understanding of the biological processes that occur during disease progression of osteoarthritis.

Disease Mechanisms in Osteoarthritis

Although there is a genetic component to OA, there has been little progress identifying susceptibility loci that are linked to osteoarthritis. Most loci that are identified in specific genome wide association studies (GWAS) are not consistent among different ethnic groups; or when sample size is increased, associations become insignificant [17]. There are, however, some loci that seem to be associated with an increased risk for developing OA, including secreated

frizzled-related protein 3 (SFRP3), a cluster of genes located on chromosome 7q22, and the proteins growth/differentiation factor 5 (GDF5) and Iodothyronine-deiodinase enzyme type 2 (DIO2) [17, 18]. While there are not many known susceptibility loci, there has been much research exploring the molecular mechanisms of osteoarthritis.

Pathological characteristics of OA include chondrocyte clustering, an increase in the production of specific extracellular matrix components (usually different from those produced in normal articular cartilage), and increased degradation of cartilage which leads to fibrillation of the cartilage surface [19]. At a molecular level, many changes in gene expression mimic those that occur during the transition to chondrocyte hypertrophy in growth plate chondrocytes. Genes such as *SDC3* and *ANXA5* [20], *COL10A1* [21, 22], *ACAN* [22], *MMP-13* [23] and *ADAMTS5* [24] are upregulated during the disease progression of osteoarthritis. One study shows that increased hedgehog signaling leads to more severe OA [25], and another suggests that haploinsufficiency of Runx2 leads to less severe OA in mice [26]. One study also suggests that abnormal maturation of chondrocytes in osteoarthritis may be due to loss of TGF-beta signaling after degradation of Smad2 and Smad3 [27]. Additionally, epigenetic modifications occur in OA such as DNA methylation, histone acetylation, and histone methylation [28]. There are also changes in micro RNAs present in cartilage that target many genes for protection of normal cartilage from inflammation and degradation [29].

In addition to genetics, mechanical instability is a major cause of osteoarthritis. Chondrocytes have receptors that can respond directly to mechanical signals, including stretch activated ion channels, CD44, Anchorin 2, and Integrin receptors [30]. In response to mechanical loading, cell-matrix interactions are disrupted, water content is increased, and tensile strength of the extracellular matrix is decreased [31]. *In vitro* studies have shown that shear stress increases Integrin receptor binding to specific ligands: Integrin B_1 to fibronectin and Integrin B_2 to vitronectin [32]. Additionally, chondrocytes from normal cartilage respond to pressure induced strain (PIS) [30] by membrane hyperpolarization, in contrast to the response of membrane depolarization by osteoarthritic chondrocytes [30]. These changes in response to pressure-induced strain also lead to changes in gene expression, with normal chondrocytes increasing mRNA levels of aggrecan and decreasing levels of MMP-3 in response to PIS, and OA chondrocytes showing no change in these genes [30]. While there are differences in the ways that normal and diseased chondrocytes respond to PIS, it is known that PIS can cause an upregulation of genes that lead to the development of OA, such as ERK1/2 [33].

Understanding the molecular mechanisms during OA pathogenesis is an important step in identifying drugs that will both attenuate the severity of the disease and potentially reverse the cartilage damage that is a result of late stage OA. In addition, understanding the different types of chondrocytes in articular and growth plate cartilage will help with the identification of a sub-population of

chondrocytes that has the potential to re-populate articular cartilage in response to damage caused by trauma or arthritis.

Runx Family of Transcription Factors

The Runx proteins are a family of transcription factors containing the conserved 128 amino acid Runt homology domain [34]. All members of the Runx family, Runx1, Runx2, and Runx3, heterodimerize with Cbf β to enhance their DNA binding [34]. Runx proteins are able to both enhance and reduce transcription of their target genes [34]. Each member of the Runx family is a cell fate determining transcription factor and functional roles of Runx as master transcription factors have been well characterized. Runx1 (CBFA2, AML1, PEBP2 α B) is responsible for definitive hematopoiesis and mice lacking both alleles die before day E12.5 due to hemorrhaging [35]. Runx2 (CBFA1, AML3, PEBP2 α A) is required for osteoblast development and Runx2 -/- mice have a cartilaginous skeleton and die shortly after birth as a result of asphyxiation [36]. Runx2 interacts with a number of co-regulatory factors such as C/EBP, Smads, YAP, and Hes to regulate genes required for osteoblastogenesis (Lian 2003 [37]). Runx3 (CBFA3, AML2, PEBP2 α C) is involved in neurologic and gut development. Different strains of *Runx3* -/- mice show different phenotypes. In an inbred background, *Runx3* -/- mice do not survive longer than 10 days and it is hypothesized that they die of starvation as their blood sugar is low and their gastric mucosa is thickened as a result of increased proliferation and apoptosis [38]. In a *Runx3* -/-

strain that was generated on a mixed background, mice live for several months but exhibit severe limb ataxia, consistent with the expression of Runx3 in the dorsal root ganglia [39].

In humans, all three Runx proteins are involved in disease. Haploinsufficiency of *RUNX1* results in familial thrombocytopenia, characterized by a low platelet count [40]. Haploinsufficiency or genetic mutations of *RUNX2* result in cleidocranial dysplasia, a disease characterized by absence of clavicles, failure in closure of fontanelles, extra teeth, and short stature [41, 42]. Additionally, all three Runx factors are involved in cancers. Runx1 is one of the most common proteins involved in chromosomal translocations resulting in leukemias. 20% of acute lymphoblastic leukemias (ALL) and 13% of acute myelogenous leukemias (AML) contain a chromosomal translocation involving *RUNX1* [43]. Commonly, the (8:21) translocation resulting in a fusion protein containing the DNA-binding domain of Runx1 fused to the entire ETO protein or the (12:21) translocation resulting in a fusion protein containing the N-terminus of Runx1 and TEL are found in the M2 subtype of AML and childhood pre-B cell ALL, respectively [44, 45]. Runx2 is commonly expressed at higher levels in osteosarcoma, prostate cancer, and breast cancer. Runx2 is expressed abnormally in both breast and prostate cancer cell lines and its expression is increased in those cell lines derived from metastatic primary tumors and tumors that metastasize to bone [46]. Additionally, Runx2 activates many metastasis related genes and disruption of Runx2 function decreases the formation of

osteolytic lesions, showing that expression of Runx2 is important in the metastatic potential of primary breast and prostate cancers [47-49]. Runx3 has been implicated in a wide variety of cancers and is known to be a potent tumor suppressor in normal gastric epithelium [38]. One study shows that *RUNX3* is hypermethylated in 64% of gastric cancers, 73% of hepatocellular carcinomas, 62% of larynx cancers, and 46% of lung cancers [50]. Interestingly, Runx3 is also increased in pancreatic tumors, indicating that it can function as an oncogene when expressed aberrantly in normal cells, in addition to functioning as a tumor suppressor [51]. From the detrimental effects of Runx deletions in mice, and their altered expressions in many human cancers, it is clear that proper functioning and expression of Runx proteins is critical to maintain normal cellular function. In this thesis, the roles of Runx factors, with a focus of Runx1 and cartilage tissue, have been examined. Further presentation of the Runx factors in the skeletal relationship to chondrogenesis and articular cartilage is found in each chapter exploring Runx function in chondrocytes.

Endochondral Ossification and Mechanisms of Chondrocyte Hypertrophy

During development, bones of the skeleton form by either intramembranous ossification (lateral clavicles and bones of the cranium) or endochondral ossification (medial clavicles, vertebrae, facial bones, ribs, and all long bones). During intramembranous ossification, mesenchymal progenitors differentiate directly into osteoblasts while during endochondral ossification, mesenchymal

cells condense and form a cartilage anlagen of the skeleton which is replaced by bone. During endochondral ossification, mesenchymal progenitor cells condense to form the template for a long bone. Cells at the center of the cartilage anlagen begin to differentiate into chondrocytes, expressing markers such as Collagen2a1, while cells located at distal portions of the anlagen proliferate at a slower rate and become resting zone chondrocytes. Cells in the center then exit the cell cycle and increase greatly in size. These hypertrophic chondrocytes are responsible for growth of the axial and apendicular skeleton. Hypertrophic chondrocytes begin to downregulate Col2a1 and upregulate Col10a1, alkaline phosphatase, osteopontin, and fibronectin. Late stage hypertrophic chondrocytes express vascular endothelial growth factor (VEGF) and matrix degrading enzymes such as Mmp13, allowing for degradation of the cartilage matrix, and invasion of blood vessels, which carry osteoblasts to replace the cartilage skeleton with bone [52, 53].

The process of chondrocyte maturation during endochondral ossification is tightly controlled by a number of transcription factors and regulatory pathways. The most important transcription factor for cartilage formation is Sox9, which is required for mesenchymal condensation to occur [54]. Additionally, *Sox9* +/- mice mimic the phenotype of humans with Campomelic Dysplasia, characterized by underdevelopment of all skeletal elements [55]. Sox5 and Sox6 also play an important role in cartilage differentiation. While *Sox5* -/- and *Sox6* -/- mice have only minor skeletal phenotypes, the *Sox5/Sox6* double knockout shows marked

delays in chondrocyte proliferation and a decrease in the levels of many cartilage markers, including extracellular matrix components [56]. This indicates that while Sox5 and Sox6 may be functionally redundant, they are important components of chondrocyte differentiation.

The transition from proliferating to hypertrophic chondrocyte is complex and involves many signaling pathways. The Indian Hedgehog (IHH)/Parathyroid Hormone Related Peptide (PTHrP) pathway is an important regulator of chondrocyte hypertrophy. *Ihh* -/- mice show no deficiency in the initial cartilage condensation, however there is a vast decrease in the number of proliferating chondrocytes in these mice [57]. Additionally, conditional *Ihh* knockout mice, in which *Ihh* is deficient only in Col2 producing cells, show an increase in mineralization and a decrease in chondrocyte proliferation, providing evidence that IHH promotes chondrocyte proliferation and inhibits chondrocyte hypertrophy [58]. IHH, which is expressed in pre-hypertrophic chondrocytes, induces expression of PTHrP in chondrocytes of the resting zone. PTHrP promotes chondrocyte proliferation, and also inhibits expression of IHH in pre-hypertrophic chondrocytes, providing a negative feedback loop to regulate proliferation of chondrocytes in the growth plate [59].

Another important signaling pathway during chondrocyte maturation is the Bone Morphogenic Protein (BMP) signaling pathway. BMP binding to its receptor induces the phosphorylation of receptor Smads 1, 5, and 8. These then dimerize with Smad4 and are transported to the nucleus where they can regulate

gene transcription [60]. BMP signaling increases the transition from resting to proliferating chondrocytes while inhibiting the transition to chondrocyte hypertrophy [61]. Studies also show that IHH increases BMP signaling in proliferating chondrocytes and in the perichondrium, indicating that these two pathways work together to promote chondrocyte proliferation [62]. TGF-beta, which is part of the same family as BMP, also contributes to the pathogenesis of osteoarthritis via Smad signaling. TGF-beta signaling via the ALK1 pathway leads to phosphorylation of Smads 1, 5, and 8 while TGF-beta signaling via the ALK5 pathway leads to phosphorylation of Smads 2 and 3 [63]. The balance between these two pathways is important in maintaining cartilage homeostasis and is disrupted in osteoarthritis [63].

Fibroblast growth factor (specifically FGF2 and FGFR3) signaling antagonizes the IHH and BMP signaling pathways by promoting chondrocyte hypertrophy and inhibiting chondrocyte proliferation, in part by increasing expression of the cell cycle inhibitor p21 [64, 65]. FGF signaling also negatively regulates IHH and BMP signaling, although the direct mechanisms remain unknown. *In vitro*, FGF signaling decreases Smad phosphorylation, which leads to a decrease in BMP signaling; however, this phenomenon has not been seen *in vivo* [60].

In addition to the complex network of signaling pathways regulating chondrocyte maturation, an additional transcription factor is important for the transition from proliferation to hypertrophy. Runx2, the essential transcription

factor for osteoblast differentiation, also regulates chondrocyte hypertrophy, as evidenced by the fact that Runx2 -/- mice only exhibit hypertrophic chondrocytes in distal skeletal elements [66]. Runx2/Runx3 double knockout mice, however, exhibit no hypertrophic chondrocytes, suggesting a functionally redundant role for these proteins during chondrocyte maturation [67]. Mice deficient for Runx1 in all non-hematopoietic lineages develop normal skeletons, with the exception that their sterna fail to mineralize [68]. However, a recent study shows that mice with a 50% reduction in Runx1 activity have growth plate irregularities and delayed fracture healing, as well as decreased expression of Runx2 and Runx3 in the growth plate [69]. This eludes to a possible function for Runx1 in cartilage, as it has been shown that Runx factors can regulate their own transcription, and the transcription of other Runx family members [70]. A summary of the growth plate, with its transcriptional regulators, phenotypic markers, and signaling pathways, can be seen in Figure 1.1.

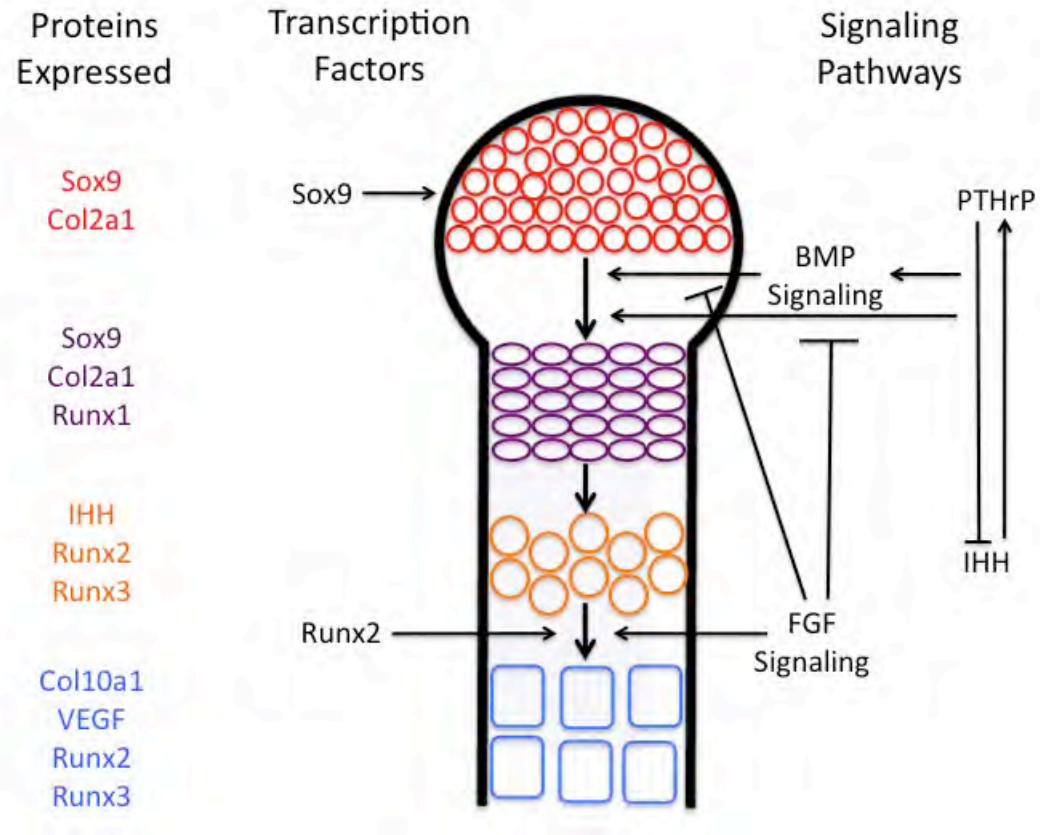

Figure 1.1: Mechanisms of Control and Proteins Expressed during Chondrocyte Maturation
A summary of mechanisms controlling each stage of chondrocyte maturation in the growth plate, along with proteins expressed at each stage of chondrogenesis. Red = resting chondrocytes, Purple = proliferating chondrocytes, Orange = pre-hypertrophic chondrocytes, Blue = hypertrophic chondrocytes.

Runx Proteins in Skeletal Development

In addition to functioning as cell fate determining transcription factors, all three Runx proteins are found in cartilage during skeletal development. Runx1, 2, and 3 are present in the mesenchymal condensation and are downregulated for commitment to the chondrocyte lineage. Runx1 is expressed in proliferating chondrocytes of the growth plate and in chondrocytes of permanent cartilage

structures, while Runx2 and Runx3 are present in pre-hypertrophic and hypertrophic chondrocytes. [36].

The most well studied Runx protein during cartilage development is Runx2. Runx2 is important for chondrocyte hypertrophy and mice lacking functional Runx2 contain hypertrophic chondrocytes only in some skeletal elements (radius/ulna and tibia/fibula) [36]. Overexpression of Runx2 during development results in joint fusion and decreased length of long bones as a result of premature terminal chondrocyte hypertrophy [71]. Runx2 also controls many genes that are involved in chondrocyte hypertrophy, such as ColX, Ihh, and Mmp13 [72] [73] [74]. The expression of Runx2 and Runx3 in the same populations of growth plate chondrocytes suggests a possible functional redundancy of these proteins during development. Interestingly, while Runx2 -/- mice still have hypertrophic chondrocytes in some skeletal elements, Runx2 -/-, Runx3 -/- mice have no ColX expressing hypertrophic chondrocytes [67].

Many recent studies have demonstrated a role for Runx1 during skeletal development. Runx1 is expressed in the mesenchymal condensation, resting and proliferating zone chondrocytes, suture lines of the calvaria, periosteum, and hyaline cartilage [75]. Runx1 -/- mice, that have Runx1 restored in the hematopoietic and endothelial systems to bypass embryonic lethality exhibit a relatively normal skeleton; however they fail to develop a mineralized sternum and show some skeletal abnormalities [68]. In mesenchymal specific Runx1 knockout mice, mesenchymal cells condense normally but have delayed

commitment to the chondrocyte lineage, while cartilage specific Runx1 knockout mice exhibit normal skeletal development [76]. This indicates that Runx1 is involved in, but not required for commitment to the chondrocyte lineage.

Conclusions

Many questions remain relating to the underspecified role of Runx1 during endochondral bone formation and in disorders associated with cartilage and bone disregulation. Additionally, there is a need for a better understanding of the molecular basis of osteoarthritis. This dissertation aims to characterize the expression of Runx1 in osteoarthritis, and begins to explore the possible role of Runx1 in healthy and diseased cartilage. It also preliminarily explores some novel functions of Runx proteins including global protein synthesis control and epigenetic regulation of target genes.

CHAPTER II:

Runx Expression in Normal and Osteoarthritic Cartilage

Abstract

Runx1 is the only Runx factor that is expressed in the chondrocytes of permanent cartilage structures during development; however its role in normal joint functioning and cartilage disease is not known. To gain a basic understanding of Runx expression in non-diseased cartilage, IHC was done on full thickness immature bovine knee joints, showing Runx1 expression at greatest levels in superficial zone chondrocytes, and Runx2 expression at greatest levels in deep zone chondrocytes. Runx1 protein and mRNA levels were quantified in response to static mechanical compression of bovine articular cartilage, and found to be upregulated under compression conditions. To determine Runx1 expression during OA disease progression, a mouse model of experimental OA, induced by surgical destabilization of the medial meniscus (DMM), was used. To determine the expression of Runx1 in human osteoarthritis, the spared and diseased compartments in knees of OA patients were examined for Runx1 expression by immunohistochemistry and Runx1 protein levels by Western blot analysis. In human osteoarthritis, Runx1 expression is increased, and is visualized in chondrocyte clones in human disease. In some, but not all, mouse OA tissue sections, the Runx1-expressing chondrocytes appear to cluster at the peripheries of the OA lesions.

Introduction

During development of cartilage tissue in the process of endochondral ossification, all three Runx proteins are expressed in precursor cells in the condensing mesenchyme [77, 78]. Several studies have shown that in mouse embryonic fibroblasts, as well as in early mesenchymal cells, Runx2 protein must be downregulated for commitment to the chondrocyte lineage. Experimental evidence suggests that the transcription factor Nkx3.2 [79] directly downregulates Runx2 [80, 81], with a concomitant upregulation of Sox9, a transcription factor critical for chondrogenic progression [54]. In committed chondrocytes, Runx1 continues to be expressed only in proliferating chondrocytes [75], while Runx2 and Runx3 are expressed in pre-hypertrophic and hypertrophic chondrocytes [71]. Runx2 in chondrocytes controls the transcription of hypertrophy-specific genes [67, 72, 74, 77], but the functions of Runx1 and Runx3 during chondrogenesis are less well understood.

Deficiency of Runx3 causes chondrocyte maturation to be slightly delayed [82], and Runx3 may help compensate for haploinsufficiency of Runx2 [67]. During development, Runx1, a master regulator of the hematopoietic lineage [26, 83], is the only Runx factor that is expressed in permanent cartilage structures [75, 78]. Mice deficient for Runx1 in non-hematopoietic lineages develop normal skeletons but their sterna fail to mineralize [68]. These findings suggest a role for

Runx1 in normal cartilage development. However, the status of Runx1 during the progression of OA has not been examined.

During osteoarthritis, many hypertrophic markers, such as MMP13, are upregulated leading to tissue degradation [84]. MMP's are direct Runx targets [85, 86]. In the late stages of osteoarthritis, Runx2 is upregulated and is thought to play a role in the transcription of genes that lead to tissue destruction during late stages of the disease [25, 87]. Consistent with this hypothesis, haploinsufficiency of Runx2 leads to less aggressive OA in mice challenged with DMM surgery, indicating that Runx2 promotes OA progression [26]. The involvements of Runx1 and Runx3 in osteoarthritis have not been widely studied. As there is some evidence for redundancy of Runx2 and Runx3 function during chondrogenesis, the present studies aimed to explore the expression of Runx1 during osteoarthritis.

There are many cell culture models to facilitate the study of chondrogenesis; however, the study of osteoarthritis requires *in vivo* or *ex vivo* models. To better understand protein regulation in response to mechanical stress, compression of bovine cartilage explants has been used extensively. Both static and cyclic compression can result in upregulation of inflammatory cytokines and a decrease in matrix synthesis [88]. The static compression model used in Dr. Fanning's laboratory allows us to monitor for the upregulation of genes in response to mechanical compression within 6-24 hours. This model

was chosen as it allows for the detection of changes that happen shortly after the induction of mechanical compression.

There are also many animal models currently in use for the study of osteoarthritis. Mice and rats are especially advantageous due to their low cost and ease of genetic manipulation to study particular genes involved in OA pathogenesis. The disadvantages are the thin cartilage and increased calcified cartilage in the mouse, as well as the pain response in osteoarthritic rats [89]. There are very few animal models of naturally occurring osteoarthritis. There are a number of experimental models targeted at inducing mechanical and structural joint instability. Inducing structural instability involves direct damage to the cartilage (e.g. surgical trauma, freezing, ionizing radiation, etc.) to look for a direct response to cartilage damage, while mechanical instability involves disruption of the knee-stabilizing ligaments (e.g. patella dislocation, ACL transection, menisectomy, etc.), resulting in altered loads on knee cartilage [90]. A mouse model using destabilization of the medial meniscus (DMM) to induce OA was chosen for these studies. This surgery involves transecting the medial meniscotibial ligament, leading to knee joint instability that produces a focal lesion on the medical side of the knee, while mostly sparing the lateral side, a pattern that mimics the vast majority of human osteoarthritis [91]. This model is also advantageous as the changes occur rapidly, with apoptosis occurring by 2 weeks post-surgery Changes in gene expression were detected as early as 8 days post-surgery, making this an ideal model to study gene expression changes

during osteoarthritis progression. The goal of this study was to identify the expression pattern of Runx1 in mouse, bovine, and human normal and osteoarthritic cartilage, and to determine the response of Runx1 expression to cartilage stress conditions.

Materials and Methods

Bovine Studies

A. Isolation of Articular Cartilage Zones

Superficial (SZ), middle (MZ), and deep zone (DZ) chondrocytes were harvested from the femoropatellar groove of 1-week-old male calves as previously described [92]. Briefly, the SZ cartilage was harvested from the 100 μm of tissue at the articular surface using a scalpel (final volume is approx. 5% by weight), while the MZ and DZ tissues were harvested from the next 60% and 35% of tissue, respectively (by wet weight) moving toward the sub-chondral bone.

B. Compression Experiments

Full thickness cartilage plugs were isolated from a 2-10 day old bovine knee joint using a hollow drill-bit measuring 1cm in diameter. The plugs were sliced into 1mm thick sections and a 3mm biopsy punch was used to obtain discs with final measurements of 3mm in diameter x 1mm. One bovine knee joint generates more than 36 plugs for experimental use (n=12/group). 12 cartilage discs were

cultured in either one well of a 6-well plate (free swelling control) or under conditions of 25% or 50% compression for 3 days in Dulbecco's Modified Eagle Medium (DMEM) supplemented with insulin-transferrin-sodium selenite (ITS)(Sigma) and Pen/Strep (Gibco). For compression experiments, discs were cultured in compression apparatus that holds 12 discs in individual compartments under conditions of constant compression. In each set, medium was changed the first day after harvest, and every three days thereafter. Repetitive experiments were performed with 36 discs from 2 calves. Statistics were performed in 24 samples comparing 0%, 25%, and 50% compression groups.

Mouse Osteoarthritis Model

Osteoarthritis was surgically induced in the right leg of 10-week old male 129 S6/SvEv mice by destabilization of the medial meniscus (DMM) as previously described [91]. Briefly, mice were anesthetized using inhaled Isofluorane (HaloCarbon Corp, NJ) titrated to the appropriate effect. Unilateral joint instability was induced by aseptically preparing the knee with iodine and alcohol, opening the joint capsule medial to the patellar tendon, and transecting the anterior attachment of the medial meniscotibial ligament. The joint capsule was closed using a running 7-0 Vicryl (Ethicon) suture and the skin incision was closed using an interrupted 7-0 Vicryl suture. In sham-operated animals, the skin and joint capsule were surgically opened but the medial meniscotibial ligament was left intact. Two mice were harvested at each time point for both DMM animals and

one mouse was harvested at each time point for Sham-operated animals. Immunofluorescense and immunohistochemical analysis were repeated at least twice for each study.

Mice

129S6/SvEv mice were obtained from Taconic Farms (Germantown, NY), housed in cages with a maximum of five animals per cage, and allowed free access to food and water. They were cared for in accordance with the National Institutes of Health and American Association of Laboratory Animal Care regulations, in addition to the University of Massachusetts Medical School's Institutional Animal Care and Use Committee protocols.

Samples from Human Osteoarthritic Patients

Knee joints were obtained from osteoarthritic patients with varus malalignments undergoing total knee replacements at the time of surgery, in accordance with the institution's policy on discarded samples. For protein data, patient samples, gender, and age are presented in Table 2.1. For immunohistochemistry and immunofluorescense, samples were obtained from 6 patients (2 male and 4 female) ranging in age from 46 to 79, with a mean age of 67 and a median age of 68. At the time of surgery, the tibial plateau and medial and lateral condyles of the femur were removed and placed into phosphate buffered saline. Full thickness articular cartilage samples (from surface to bone) were removed from

the tibial plateau and from both the medial and lateral condyles of the femur. Each of these tissues was divided into serial samples to be used for immunohistochemistry and western blotting.

Immunohistochemistry and Immunofluorescense

Human cartilage samples were isolated as described above. Intact right knees of mice were removed by performing a hemi-pelvectomy. Samples from human and mouse were fixed in freshly prepared 4% paraformaldehyde in cacodylate buffer for 24 hours, with a change in buffer after 16 hours, dehydrated through a series of graded ethanols to citrusol (Fisher Scientific) and then embedded in paraffin for sectioning at a thickness of 6μm.

Safranin O staining was performed as previously described [93]. For immunohistochemistry (IHC) to detect Runx1 and PCNA, paraffin sections were rehydrated through a series of graded alcohols to phosphate buffered saline. Blocking of endogenous peroxidase was carried out using 3% hydrogen peroxide in methanol. Antigen retrieval was performed using citrate buffer at high temperature in a pressure-cooking apparatus, the 2100 Retriever apparatus, according to the manufacturer's specifications (Pick Cell Laboratories). Non-specific sites for antibody binding were blocked by 5% BSA in PBS for 1 hour, sections were then incubated in primary antibody overnight. The next day, sections were washed three times in wash buffer (0.1% BSA, 0.2% gelatin, 0.05% saponin in PBS), then incubated in secondary antibody for 2 hours, and

washed three times in wash buffer. Staining was visualized using the DAB detection system (Dako).

Immunofluorescense [94] studies were used to detect Runx1 in bovine, human, and mouse cartilage sections. Paraffin sections were rehydrated through a series of graded alcohols to phosphate buffered saline. To reduce autofluorescense, sections were washed 3 times, for 10 minutes each, in 1mg/mL sodium borohydride, and washed 3 times in 1% Tween in phosphate buffered saline. Antigen retrieval was performed using citrate buffer at high temperature in a pressure-cooking apparatus, the 2100 Retriever apparatus, according to the manufacturer's specifications (Pick Cell Laboratories). Proteins were blocked for non-specific dye binding using the Image-iT FX Image Enhancer Solution (Invitrogen) according to the manufacturer's specification, blocked for non-specific antibody binding in 6% BSA in PBS for 1 hour, and then incubated in primary antibody overnight. Sections were washed then 3 times in 1% Tween in phosphate buffered saline, incubated in secondary antibody for 2 hours, and nuclei were counter-stained with DAPI (0.1ug/mL) to visualize cell nuclei. Sections were visualized on a Zeiss Axioplan fluorescence microscope using MetaMorph imaging software.

The Runx1 antibody used for bovine, mouse, and human sections for both IF and IHC was AML-1, raised in rabbit (1:200 Cat# 4334, Cell Signaling Technologies). The secondary antibody used for immunohistochemistry was goat anti-rabbit, HRP conjugate (1:800 Cat# SC-2004, Santa Cruz). The secondary antibody

used for immunofluorescense was avidin, Alexa Flour 488 Conjugate (1:800 Cat# A21370, Invitrogen).

Western Blot Analysis

Cartilage samples from human and bovine knee joints to be used for western blotting were flash-frozen in liquid nitrogen, pulverized with a Bessman tissue pulverizer (Fischer Scientific), chilled in liquid nitrogen, and put into Lysis Buffer (50mM Tris pH 8.8, 150mM NaCl, 1% NP-40, 1% SDS, 10% glycerol, 0.5% deoxycholic acid, 0.6M DTT, 100mM NaF, 2mM Na_3VO_4, 1X Complete Mini Protease Inhibitor (Roche), 25μM MG132) for protein extraction. For bovine experiments, 12 cartilage discs were harvested from the same compression chamber and pooled together for protein isolation. Cartilage from human patients was obtained at the time of surgery. Data on western blots from human samples were an average from 5 patients. Proteins were separated by SDS-PAGE, transferred to a nitrocellulose membrane, and probed for the presence of Runx1. Antibodies used were AML-1, rabbit polyclonal (1:1000, Cat# 4334, Cell Signaling Technologies), Pan-Runx antibody 2B5 mouse monoclonal, a generous gift from Dr. Kosei Ito (1:1000, Kyoto University Hospital, Kyoto, Japan), and GAPDH, goat polyclonal (1:5000, Cat# SC-31915 Santa Cruz).

qPCR

Bovine cartilage samples (n=12 plugs/sample) to be used for RNA isolation were flash-frozen in liquid nitrogen, and pulverized as above. Each sample was homogenized in 1mL of Trizol using a Polytron PT1200 homogenizer for 20 seconds on level 1. RNA isolation was carried out by phenol/chloroform extraction followed by ethanol precipitation. DNA contamination was removed using the DNase-free RNA kit (Zymo) according to the manufacturer's specifications. Nucleic acid quantification was carried out using a Nano-drop spectrophotometer, and RNA purity was assessed using the 260/280 ratio. One µg of RNA was reverse transcribed into cDNA with the First Strand cDNA synthesis kit (Invitrogen) using random hexamers according to the manufacturer's protocol. RT-PCR was preformed on a 7500 fast RT-PCR machine (Applied Biosystems). Samples were run in duplicate using 20ng of cDNA, 5µM forward and reverse primer, and SybrGreen Master Mix (Bio Rad) in a 20 µL reaction. Values were normalized to B-actin. Primers used were as follows: Runx1 Forward 5' AACCCTCAGCCTCAGAGTCA 3';
Runx1 Reverse 5' GCGATGGATCCCAGGTACT 3'; B-actin Forward 5'CTGCGGCATTCACGAAACTA 3'; B-actin Reverse: 5' ACCGTGTTGGCGTAGAGGTC 3'.

Results

Runx1 and Runx 2 are Expressed in Immature Bovine Articular Cartilage

To determine baseline Runx levels in healthy cartilage, full thickness cartilage sections were obtained from immature bovine knee joints. Immunohistochemical analysis demonstrated that, at this stage of cartilage development, both Runx1 and Runx2 were expressed throughout the cartilage (Figure 2.1). However, Runx1 immunohistochemical staining was highest in the most superficial zone chondrocytes (Figure 2.1 A-E), while the staining for Runx2 was stronger in deep zone chondrocytes (Figure 2.1 D-F). Runx1 expression was analyzed in chondrocytes isolated from the superficial, middle, and deep zones of bovine articular cartilage (thickness shown in figure 2.2A, lower). Quantitative RT-PCR analysis shows that expression levels of Runx1 are highest in the superficial zone and diminish through the deep zone (Figure 2.2A, upper), with levels of Runx1 being significantly different between the superficial and deep zones ($p<0.05$).

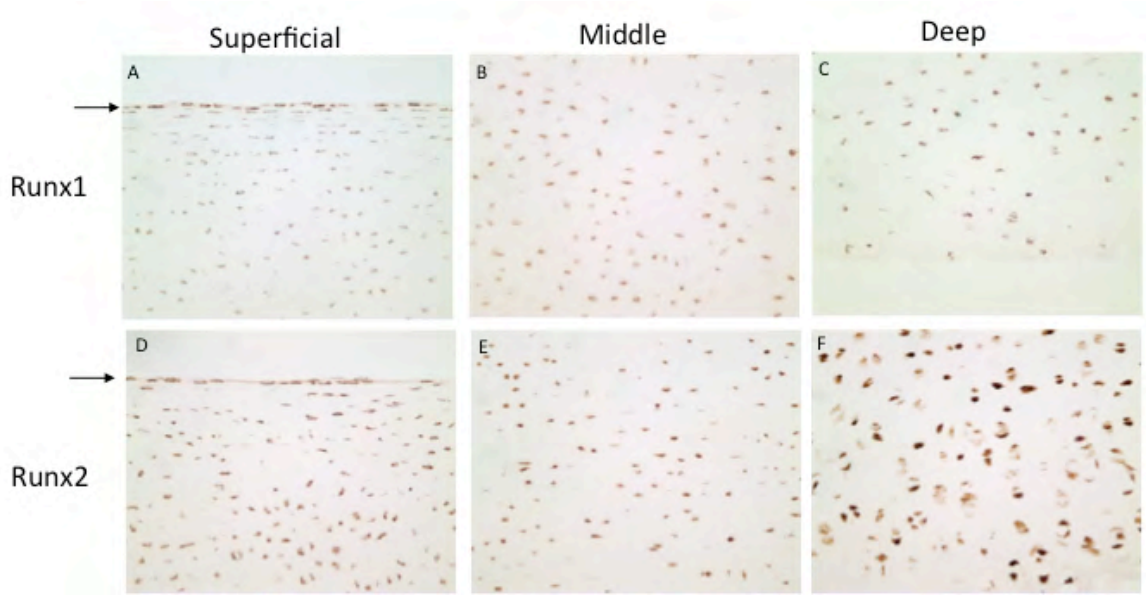

Figure 2.1: Runx1 and Runx2 Expression in Immature Bovine Knee Cartilage.

Immunohistochemistry of Runx1 (A,B,C) and Runx2 (D,E,F) in the superficial (A,D), middle (B,E), and deep (C,F) zones of immature bovine articular cartilage shows Runx1 expression most strongly in the superficial zone (denoted by the arrow) and Runx2 expression most strongly in the deep zone.

Runx1 is Upregulated in Response to Mechanical Compression

Since OA is a disease that results from chronic overloading of articular cartilage, it is of interest to determine if Runx1 responds directly to mechanical compression. Bovine cartilage plugs (see Methods) that underwent 3 days of compression began to show loss of extracellular matrix as evidenced by loss of Safranin-O staining, indicating that compression of these plugs mimics the disease process of OA (data not shown). Quantitative PCR analysis shows that Runx1 mRNA levels are upregulated in response to graded degrees of tissue strain after as little as 6 hours of mechanical compression. Runx1 levels continue to increase through 16 hours of compression (Figure 2.2B). Western blot analysis of protein samples shows that Runx1 protein is upregulated in cartilage plugs after undergoing three days of either 25% or 50% strain when compared to control plugs that remained uncompressed during culture (Figure 2.2C, upper panel, n=3). The lower panel shows a corresponding representative immunoblot that reveals a clear Runx1 doublet band, both of which are included in the densitometry measurements for figure 2D. As it is a Runx1 specific antibody that is detecting this doublet, it is possible that these doublet bands represent different Runx1 isoforms. However, the identity of each individual band was not determined. Thus, the elevated Runx1 that occurs in normal bovine cartilage in response to compression suggests that the increased Runx1 observed in human OA samples is a consequence of mechanical strain on the diseased joints.

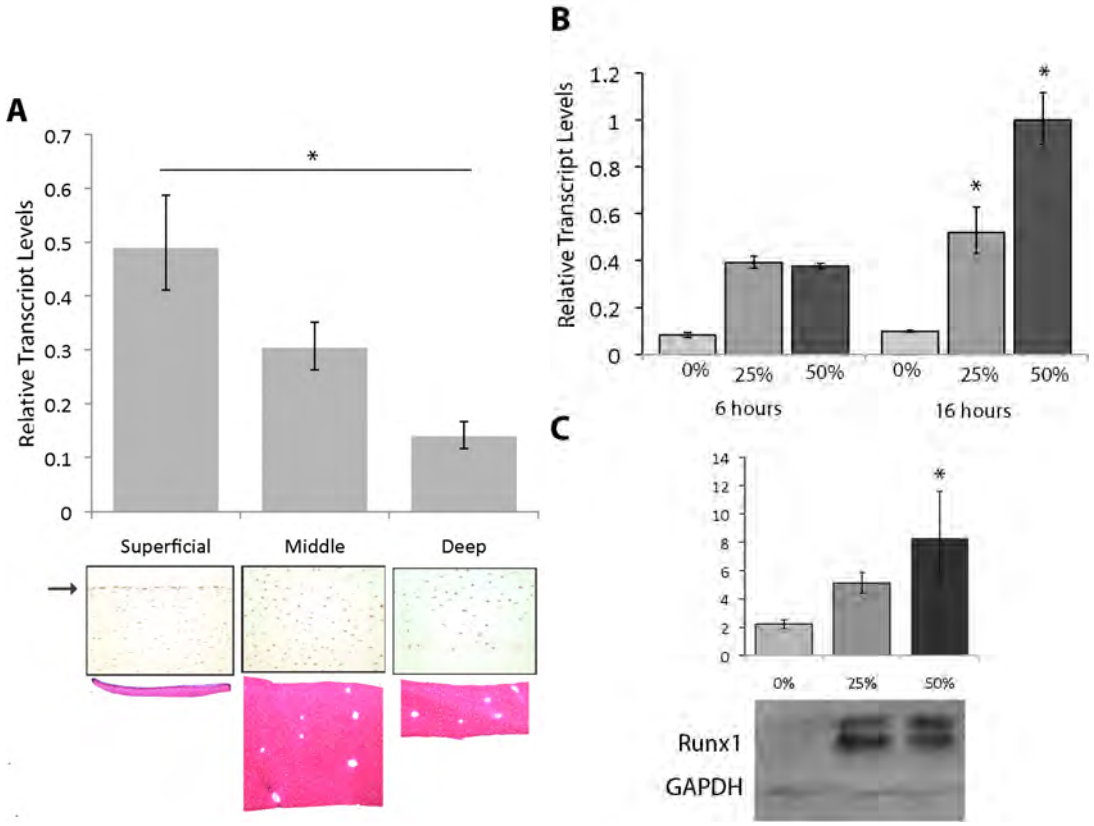

Figure 2.2: Runx1 is Upregulated in Bovine Cartilage in Response to Mechanical Compression.

(A) Upper: Quantitative RT-PCR analysis of Runx1 mRNA in the superficial, middle and deep zones of normal bovine articular cartilage were compared using Tukey's test, *=p<0.05. Middle: Immunohistochemistry showing the zonal distribution of Runx1 in bovine articular cartilage (100x). The arrow indicates Runx1 in the superficial zone. Lower: Safranin O staining showing isolation of cartilage zones. (B) Quantitative Real Time PCR of Runx1 mRNA in samples undergoing 0%, 25%, or 50% compression for 6 or 16 hours (n=12 pooled samples per group; duplicate assay of samples). Data from 25% or 50% compression was compared to 0% compression using Tukey's test, *=p< 0.05. (C) Upper: Quantitation of immunoblot analysis shows a significant increase of Runx1 protein levels in response to 25% or 50% compression when compared to uncompressed samples (Tukey's test, *=p<0.05). Lower: Representative immunoblots of Runx1 protein and GAPDH (loading control) in compressed cartilage samples.

Runx1 is Expressed in a Subpopulation of Chondrocytes in a Mouse Model of OA

To better characterize the changes in Runx1 gene expression in osteoarthritis, as related to compression of the diseased tissue, OA was generated in a mouse model by destabilization of the medial meniscus (Glasson, 2007 [91]). This surgery creates a focal osteoarthritic lesion on the medial side of the joint, while sparing the lateral side of the joint, allowing for examination of Runx1 during the progressive degeneration of articular cartilage over a 3-week period. In sham-operated animals, no arthritic lesions were observed and Runx1 was detected in the population of chondrocytes that are present near the joint surface (Figure 2.3 sham). In the damaged cartilage tissue, Runx1 immunostaining began to drop out of the area of the lesion at day 4. However, by day 8, Runx1 was observed in chondrocyte clusters located at the periphery of the OA lesions. These clusters remained present throughout the time course (Figure 2.3). The presence of Runx1 in the normal surface layer of articular cartilage suggests a role in maintaining the surface integrity of normal articular cartilage. Runx1 is depleted in OA lesions, but induced in chondrocyte clusters at lesion peripheries.

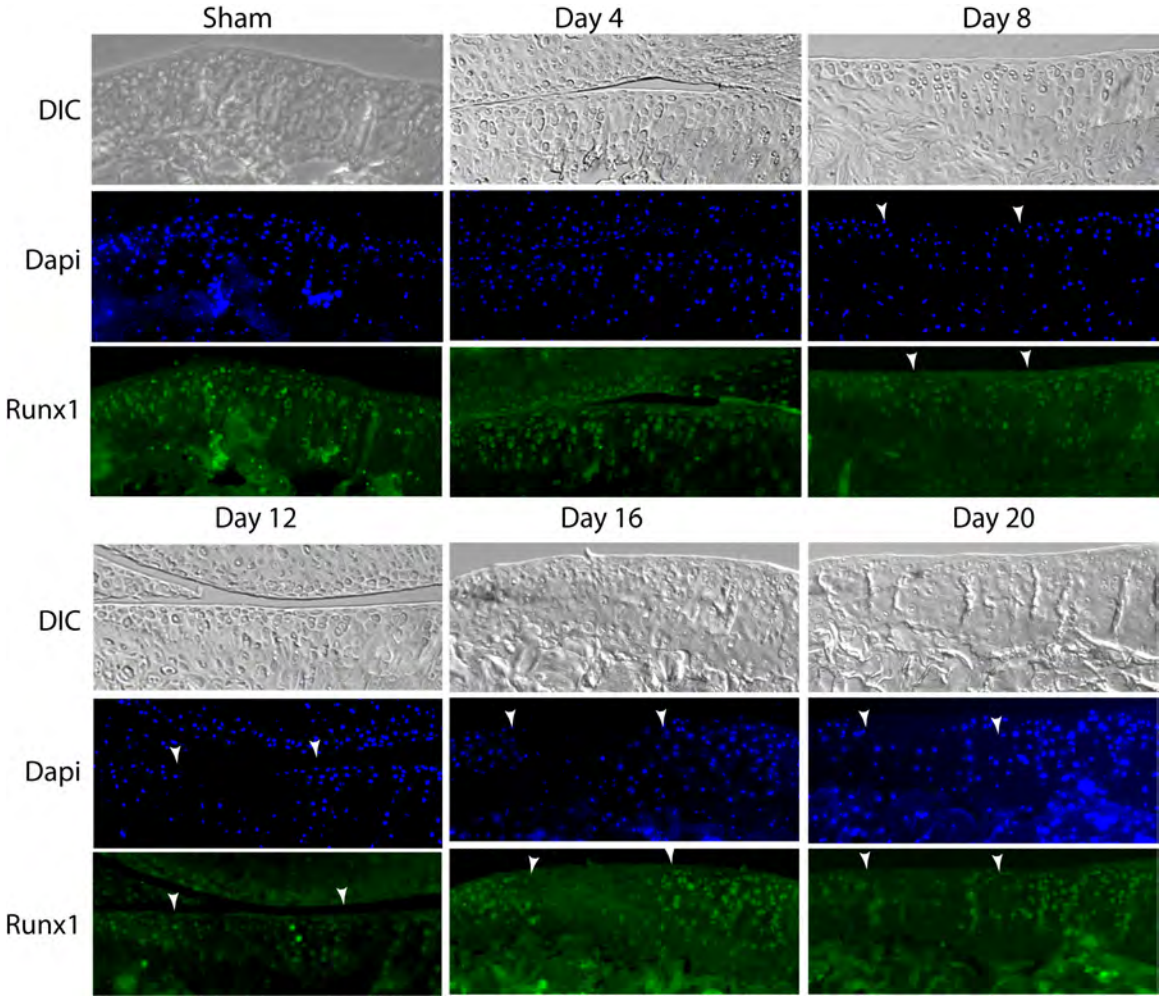

Figure 2.3: Runx1 is Expressed at the Periphery of OA Lesions in a Mouse Model of OA.
DIC (differential interference contrast) and immunofluorescense showing the progression of Runx1 development around the sites of an osteoarthritic lesion (40x). Images show the medial side of a mouse knee joint, with the femoral cartilage at the top, and the tibial cartilage at the bottom of the picture. Note the droupout of Runx1 in the area of the lesion, followed by the presence of Runx1 [95] in clusters of chondrocytes at the lesion periphery by day 16 (indicated by arrows). Nuclei are stained using DAPI (blue).

Runx1 is Upregulated in Human Osteoarthritis.

In patients with varus knee malalignments, osteoarthritis is more severe on the medial side (OA) of the knee than on the lateral side (spared), as can be seen in Figure 2.4A by the loss of Safranin O staining, severe fibrillation, and chondrocyte cloning in the medial compartment of this malalligned knee. Also observed are the typical clustered chondrocytes, or “clones”, in the affected OA area (arrows in Figure 2.4A, right panel). Since Runx1 expression predominates in articular cartilage, and is differentially expressed during mouse OA, it was hypothesized that its expression would be modified in human OA tissue as well. Immunoblot analysis of cartilage from both compartments using a Runx1 specific antibody shows an upregulation of Runx1 protein levels in n=5 knees. The medial tibial and femoral compartment samples are increased 2-fold and 2.5-fold, when compared to lateral tibial and femoral compartment samples, respectively ($p<0.05$, Table 2.1 and Figure 2.4B, left). Two representative immunoblots from two different patients are shown for Runx and GAPDH protein in contiguous slices of each compartment using Runx1 antibodies from two sources (see methods, figure 2.4B right). Immunohistochemical analysis of additional tissue samples from the same patient knees indicates the cellular localization of Runx1 in articular cartilage. Runx1 protein is detected in normal chondrocytes of the spared compartment (figure 2.4C, left). Chondrocytes expressing Runx1 observed in the spared compartment are located mainly in the superficial zone. There are some clusters of chondrocytes in the spared compartment, indicating

that there is evidence of disease even on the spared side of an OA joint. These clusters, characteristic of fibrillated OA cartilage, are enriched in the medial diseased compartment of the joint and show the presence of Runx1 (Figure 2.4C, right). Taken together, these data indicate that Runx1 is upregulated in response to the cartilage damage in human osteoarthritis.

		Lateral Femur			Medial Femur			Tibia	
Age	Gender	Anterior Femur	Posterior Femur	Combined LF	Anterior Femur	Posterior Femur	Combined MF	Lateral Tibia	Medial Tibia
52	F			0.17 (0.1)			1.37 (0.31)	NC	NC
81	F	0.92 (0.25)	0.11 (0.06)	0.14 (0.05)	0.50 (0.11)	0.24 (0.04)	0.22 (0.08)	0.52 (0.05)	0.74 (0.28)
52	F	0.05 (0.01)	1.18 (0.2)	1.71 (0.42)	1.35 (0.48)	1.28 (0.11)	1.60 (0.65)	0.55 (0.09)	0.95 (0.09)
66	F			0.68 (0.09)			1.24 (0.44)	NC	NC
64	F	0.01 (0.08)	0.55 (0.25)	0.25 (0.08)	1.18 (0.15)	1.02 (0.13)	1.01 (0.51)	0.44 (0.08)	0.63 (0.06)

Table 2.1: Summary of Runx1 Experimental and Patient Data from Human OA Knees
NC = Not collected. In some combined samples, anterior and posterior tissues were not separated. Densitometry measurements of Runx1 protein levels by Western blot are expressed as mean (+/- SEM)

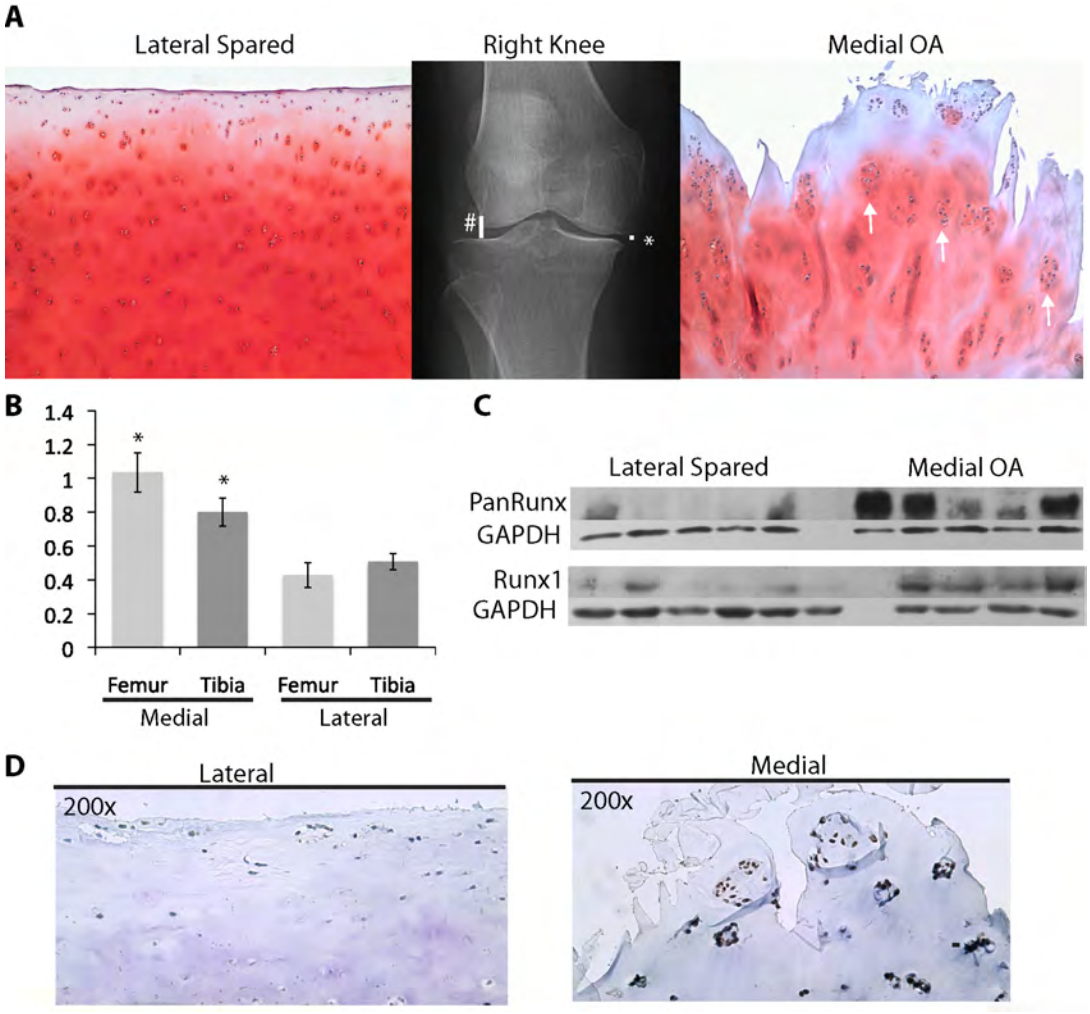

Figure 2.4: Runx1 is Upregulated in Human Osteoarthritis.
(A) X-ray from a patient with a malalligned right knee showing compression in the medial compartment (*) of the knee and a normal joint space in the lateral compartment (#) (Sample K1 in Table 1). Safranin O staining shows loss of extracellular matrix on the medial side of the joint versus normal extracellular matrix on the lateral side. Arrows indicate “clones”. (B) Graph shows mean +/- SEM quantitation of western blots stained for Runx1 of cartilage tissue from 5 patients. Data from the medial and lateral compartments were compared using Tukey’s test, *=p<0.05. (C) Representative western blots from human knees using a pan-Runx antibody (upper) and a Runx1-specific antibody show increased Runx1 on the medial (OA) side of the joint when compared to the lateral side. Different lanes are sections of cartilage from the medial and lateral sides from one human knee. (D) Immunohistochemical staining using a Runx1 specific antibody on the lateral (spared) and medial (OA) compartments.

Conclusion

In articular cartilage, Runx1 is expressed at the highest levels in the superficial zone, the 1-2 cell layer closest to the joint surface of articular cartilage, while immunohistochemical staining for Runx2 is strongest in deep zone chondrocytes. As previously mentioned, superficial and deep zone chondrocytes exhibit different properties. Superficial zone chondrocytes have higher proliferation rates, a smaller size, and higher Sox9 expression than their deep zone counterparts [92]. The Runx expression patterns also reflect what is seen in the growth plate, with Runx1 expressed at higher levels in the proliferating chondrocytes, which are smaller in size and express higher levels of Sox9 than hypertrophic chondrocytes, which have high Runx2 expression.

Runx1 expression is upregulated in osteoarthritic cartilage in humans, and in a mouse model of OA. *In vitro* compression of bovine cartilage explants demonstrates that this upregulation could be a direct response to the cartilage compression that occurs in osteoarthritic joints. In human OA cartilage, Runx1 is localized to chondrocyte “clones”, while in mouse OA cartilage, Runx1 expressing chondrocytes can be found in clusters at the periphery of OA lesions. The expression pattern in the superficial zone chondrocytes, and at the border of mouse OA lesions suggests a possible protective role of Runx1, possibly establishing a barrier of healthy cartilage around the diseased cartilage.

CHAPTER III:

Runx1 is expressed with Markers of Mesenchymal Progenitor Cells and Proliferation in Osteoarthritic Cartilage

Abstract

Runx1 functions as a critical hematopoietic transcription factor for normal cellular differentiation of hematopoietic lineage cells. Runx1 is expressed in periosteum, perichondrium, and early osteo-chondral progenitor cells [77]. However, the tissue related functions of Runx1 in articular cartilage are poorly understood. The most superficial layer of articular chondrocytes has been shown to express markers for mesenchymal progenitor cells [96]. Additionally, in growth plate chondrocytes, Runx1 is found in proliferating cells. To gain insight into the potential role of Runx1 in articular cartilage, a series of immunofluorescense experiments was carried out. The hypothesis was tested that since Runx1 is found in superficial zone chondrocytes, it may be co-expressed with markers of mesenchymal progenitor cells in both normal and OA cartilage. It was also hypothesized that the clonal populations containing Runx1 positive cells may be a result of proliferation and that Runx1 may function to support the activity of these populations. Runx1 is expressed in cells that also express VCAM-1, which is a marker for mesenchymal progenitor cells, in both normal and osteoarthritic cartilage. Further, in osteoarthritic cartilage, Runx1 is expressed with the markers for proliferation Ki-67 or PCNA. Overexpression of Runx1 in ATDC5 cells, which are described in more

detail in Chapter IV did not result in increased proliferation in these cells. Finally, a candidate gene approach was used to identify Runx binding sites in promoters of genes that are differentially expressed during chondrogenesis. Based on this study, candidate genes were chosen for analysis on the basis of their functions during OA; however the expression levels of these genes were not significantly changed by overexpression of Runx1.

Introduction

The superficial zone of articular cartilage, which shows expression of Runx1 (Figure 2.1), is different from the middle and deep zones in both morphology with respect to organization of collagen fibrils, and gene expression [97]. When cultured, cells of the superficial zone have higher rates of proliferation than cells of the deep and middle zones [92]. In addition, these superficial zone cells have been shown to express markers of mesenchymal progenitor cells such as Notch-1, Endoglin (CD105), ALCAM (CD166), and VCAM-1 (CD106) [97-99]. Interestingly, the clones of osteoarthritic cartilage have properties similar to the cells of the superficial zone. Certain osteoarthritic “clones” have been shown to express markers for mesenchymal progenitor cells, including VCAM-1[96, 100, 101]; and many studies show that these clones represent a proliferative cell population [20, 102].

The expression of Runx1 in the most superficial layer of articular cartilage is not surprising. Runx1 is also expressed in the epithelium of skin, nails, oral mucosa, hair follicles, and at the base of colonic crypts [103]. These populations of cells, like the most superficial layer of articular cartilage, contain progenitor cells [93, 103]. The role of Runx1 in progenitor cells has been studied in a wide variety of cell types, and is related to both proliferation and differentiation. A short isoform of Runx1, AML1a, is responsible for expansion of hematopoetic progenitor cells [104]. Overexpression of Runx1 promotes proliferation by stimulating the G1/S cell cycle transition [105, 106]. In hair follicle stem cells, downregulation of Runx1 causes decreased proliferation by upregulation of p21 [107]. Additionally, Runx1 overexpression can overcome contact-dependent inhibition of proliferation in *p53-/-,* but not normal MEFs [108]. In contrast Runx1 overexpression causes a decrease in proliferation in microglial cells, showing that it can have pro- or anti-proliferative properties depending on the cell type [95]. In addition to being associated with proliferation and progenitor cells, Runx1 is upregulated in response to injury in a number of cell types. For example, Runx1 is upregulated in microglia in response to nerve injury [95], and injury to the inter-follicular epidermis of the hair follicle results in an increase in both proliferation and Runx1 expression [103]. Because of the proliferative and progenitor cell properties of the superficial zone cells, and because of the association of Runx1 with proliferation and progenitor cell markers, the aim of this study was to further characterize the Runx1 positive chondrocytes in normal

articular and osteoarthritic cartilage, specifically characterizing the progenitor cell properties and proliferation potential of these cells.

Materials and Methods

Samples from Human Osteoarthritic Patients

Knee joints were obtained from osteoarthritic patients with varus malalignments undergoing total knee replacements at the time of surgery, in accordance with the institution's policy on discarded samples, as described in Chapter II. Full thickness articular cartilage samples (from surface to bone) were removed from the tibial plateau and from both the medial and lateral condyles of the femur. Each of these tissues was divided into serial samples to be used for immunohistochemistry and western blotting.

Mouse Osteoarthritis Model

Osteoarthritis was surgically induced in the right leg of 10-week old male 129 S6/SvEv mice by destabilization of the medial meniscus (DMM) as described in Chapter II. Two mice were harvested at each time point for both DMM animals and one mouse was harvested at each time point for Sham-operated animals. Immunofluorescense and immunohistochemical analysis were repeated at least twice for each study.

Mice

129S6/SvEv mice were obtained from Taconic Farms (Germantown, NY), housed in cages with a maximum of five animals per cage, and allowed free access to food and water. They were cared for in accordance with the National Institutes of Health and American Association of Laboratory Animal Care regulations, in addition to the University of Massachusetts Medical School's Institutional Animal Care and Use Committee protocols.

Immunohistochemistry and Immunofluorescense

Human cartilage samples were isolated as described above. Intact right knees of mice were removed by performing a hemi-pelvectomy. Samples from human and mouse were fixed in freshly prepared 4% paraformaldehyde in cacodylate buffer for 24 hours, with a change in buffer after 16 hours, dehydrated through a series of graded ethanols to citrusol (Fisher Scientific) and then embedded in paraffin for sectioning at a thickness of 6μm.

Immunofluorescense [94] studies were used to detect Runx1, VCAM-1, and Ki-67. Paraffin sections were rehydrated through a series of graded alcohols to phosphate buffered saline. To reduce autofluorescense, sections were washed 3 times, for 10 minutes each, in 1mg/mL sodium borohydride, and washed 3 times in 1% Tween in phosphate buffered saline. Antigen retrieval was done in Antigen Retrieval buffer (Dako) in a 2100 Retriever (Pick Cell Laboratories). Proteins were blocked for non-specific dye binding using the

Image-iT FX Image Enhancer Solution (Invitrogen) according to the manufacturer's specification, blocked for non-specific antibody binding in 6% BSA in PBS for 1 hour, and then incubated in primary antibody overnight. Sections were washed then 3 times in 1% Tween in phosphate buffered saline, and incubated in secondary antibody for 2 hours, and stained with DAPI (0.1ug/mL) to visualize cell nuclei. Sections were visualized on a Zeiss Axioplan fluorescence microscope.

The Runx1 antibody used for mouse and human sections for both IF and IHC was AML-1, rabbit polyclonal (1:200, Cat# 4334, Cell Signaling Technologies). For IF, VCAM-1 (1:200, Cat# 1504, Santa Cruz), and Ki-67 (1:200, Cat# ab8191, Abcam) were used and for IHC, PCNA (1:200, Cat# ab29, Abcam). Secondary antibodies used for immunohistochemistry were goat anti-mouse, HRP conjugate (Cat# SC-2005, Santa Cruz), and goat anti-rabbit, HRP conjugate (Cat# SC-2004, Santa Cruz). Secondary antibodies used for immunofluorescense were Alexa Fluor 488 donkey anti-rabbit (Cat# A21206, Invitrogen), Alexa Fluor 594 donkey anti-goat (Cat# A11058, Invitrogen), and Alexa Fluor 594 donkey anti-mouse (Cat# A21203, Invitrogen). All secondary antibodies were used at a dilution of 1:800.

Cell Culture Conditions

ATDC5 cells were maintained in DMEM/F12 Medium supplemented with 2mM L-glutamine, 100 U/mL penicillin, 100 µg/mL streptomycin, 10% FBS, 10µg/mL

transferrin, and $3x10^{-8}$M sodium selenite, and passaged at 80% confluence to maintain cells in a pre-chondrocyte state until they were used for transfection experiments. Cells were cultured at 37^{o}C in the presence of 5% CO_2.

Runx1 Overexpression

For Runx overexpression, vectors containing full-length mouse Runx1 in a pcDNA backbone was generated. For transformation experiments, ATDC5 cells were plated at 100,000 cells/well in a 6-well plate or 666,666 cells/plate in a 100mm plate. Cells were transfected with either an empty vector or a vector containing Runx1 using X-treme gene transfection reagent (Roche, Mannheim, Germany) according to the manufacturer's protocol, using 1µg of plasmid and 3µL of transfection reagent. Cells were grown up to 48h post-transfection and cells were harvested at the time points specified below.

Results

Runx1 Co-localizes with Markers of Mesenchymal Progenitor Cells in Normal and Osteoarthritic Cartilage

To determine if Runx1 is expressed in the same populations of chondrocytes that express markers of mesenchymal progenitor cells, knee joints were harvested from mice undergoing DMM surgery as well as control mice at the time points listed above, and Runx1 and the MPC marker VCAM-1 were detected by IF. At the surface of normal articular cartilage, Runx1 and VCAM-1 are found in the same population of chondrocytes (Figure 3.1A right). Interestingly, Runx1 and VCAM-1 are also found in the same characteristic clustered cells at the periphery of osteoarthritic lesions (Figure 3.1A left). To determine if this co-expression was also present in human disease, sections of cartilage from human osteoarthritic patients were also stained for Runx1 and VCAM-1. Interestingly, neither Runx1 nor VCAM-1 positive cells were found in the spared lateral compartment (data not shown). However, chondrocytes present in clonal populations on the medial side of the joint were positive for both Runx1 and VCAM-1 (Figure 3.1B). These results suggest that Runx1 positive chondrocytes represent a progenitor cell population that is capable of responding to cartilage damage.

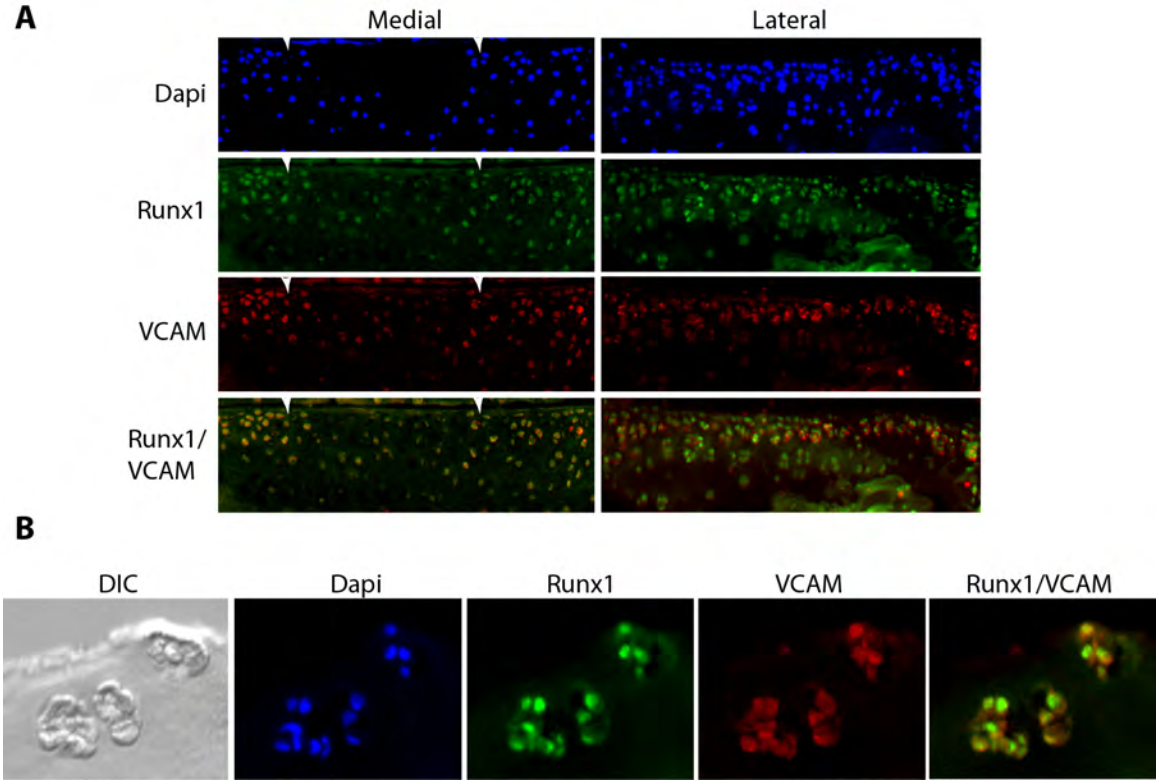

Figure 3.1: Runx1 and VCAM-1 Co-localize in Normal and Osteoarthritic Cartilage. (A) Immunofluorescense for Runx1 [95], VCAM1 (red), and DAPI (blue) in articular cartilage on the lateral (spared) and medial (OA) side of the knee joint after induction of osteoarthritis in a mouse (40x). (B) Immunofluorescense for Runx1 [95], VCAM1 (red), and DAPI (blue) on sections from the medial (OA) side of a human osteoarthritic knee joint (40x).

Runx1 Co-localizes with Markers of Proliferation in Osteoarthritic Cartilage.

Runx1 positive cells are detected in chondrocyte clones in human osteoarthritis, and in clusters of cells at the periphery of OA lesions in the mouse, both populations of cells that may be a result of proliferation. To test if these Runx1 positive cells also express markers of proliferation, sections of mouse and human OA knees were stained for Runx1 and proliferation markers. Immunohistochemical analysis showed PCNA, a marker for proliferation, to be present in chondrocyte clusters at the periphery of OA lesions (Figure 3.2A, right) in a mouse model of osteoarthritis. Immunoflourescense analysis of human sections showed that both Runx1 and Ki-67, an additional marker for proliferation, were co-expressed in the clones of human OA (Figure 3.2B).

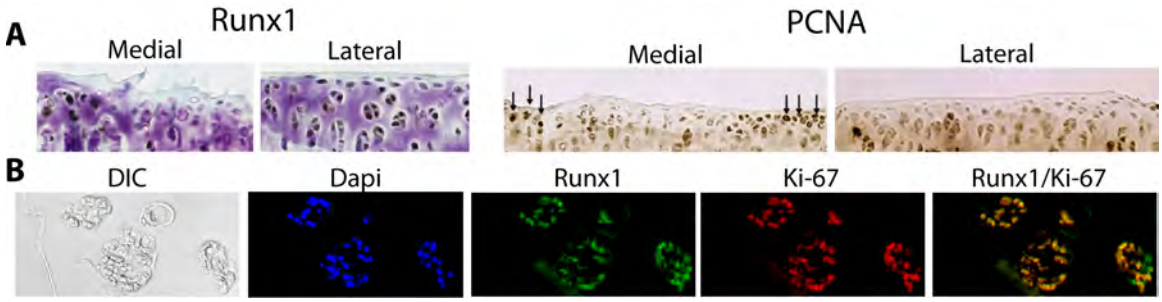

Figure 3.2: Runx1 and proliferation markers are expressed in the same population of Cells in OA Lesions.
(A) Immunohistochemistry for Runx1 (left) and PCNA in articular cartilage of a mouse after OA-inducing surgery (200x). Positive cells are denoted by arrows. (B) Immunofluorescense for Runx1 [95], Ki-67 (red) and Dapi (blue) in human osteoarthritic cartilage from the medial (OA) compartment (40x).

Runx1 does not Promote Proliferation in an in vitro Chondrocyte Model.

Because Runx1 is associated with proliferating cells in osteoarthritic cartilage, the hypothesis that Runx1 overexpression may result in increased proliferation in an *in vitro* chondrocyte model was tested. ATDC5 cells overexpressing Runx1, or an empty vector control were plated at an equivalent density, and counted every 12 hours for 2 days. In three independent wells, there was no significant change in cell number due to Runx1 overexpression at any of the time points, indicating that proliferation rates are the same for all cells tested (Figure 3.3A). Additionally, cell morphology did not change with overexpression of Runx1 (Figure 3.3B).

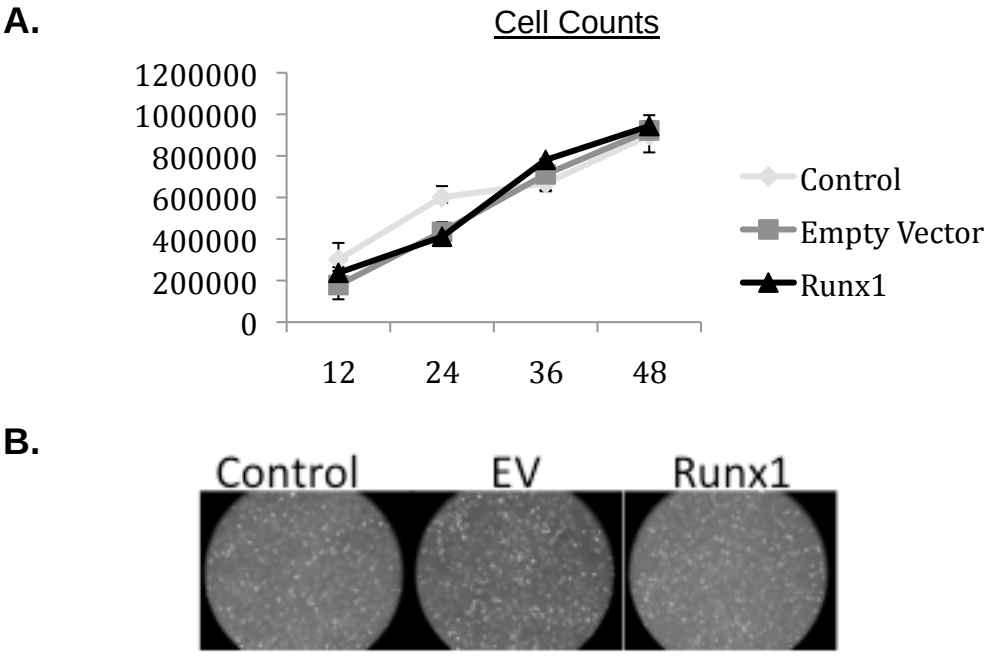

Figure 3.3: Runx1 does not Affect Cell Proliferation in ATDC5 Cells
(A) Graph of cell number 12, 24, 36, and 48 hours after overexpression of Runx1 proteins in ATDC5 cells. Graph average counts from three independent wells, and error bars represent standard deviation. (B) Phase images of ATDC5 cells 24 hours after overexpression of Runx1 proteins.

Promoter Analysis of Genes Differentially Regulated during Chondrogenesis

To gain insight into the potential role of Runx1 in cartilage, a candidate gene approach was used to identify its potential downstream targets. A 2005 study that profiled expressed cDNA by a microarray analysis identified 144 genes that were upregulated 10-fold or greater, and 66 genes that were downregulated 10-fold or greater during *in vitro* chondrocyte differentiation of limb bud micromass cultures, with some data validated in ATDC5 cells [109]. To test the hypothesis that these genes had the potential to be regulated by Runx proteins, each of the 210 genes that were differentially regulated during chondrogenesis

was searched for Runx binding sites in their proximal promoter (2kb from the transcription start site to 200bp after the transcription start site). The consensus Runx binding site (ACC A/G C A/T) or its complement (T/A G C/T GGT) was found in 131 genes that are upregulated and 61 genes that are downregulated during chondrogenesis. Table 3.1 summarizes the results. The 18 remaining genes contained no Runx binding sites in their proximal promoters. The number of Runx sites ranged from as few as one to as many as ten, indicating that most genes that are differently expressed during chondrogenesis have the potential to be directly regulated by Runx proteins. To determine if Runx1 regulated some of the genes, ATDC5 cells transfected with either empty vector controls or a Runx1 overexpression vector were analyzed for differential regulation of some of these genes that also play a role in osteoarthritis. Samples of these cells from 3 independent experiments were analyzed in duplicate wells by qPCR. For this preliminary experiment, genes that haven been previously shown to have functions in OA were chosen for analysis. These genes were *Cp*, *BMP7*, *Sox11*, *Wisp2*, *Dcn*, and *Cxcl10.* Additionally*, ItgB2* was chosen as a representative gene containing the maximum number of Runx binding sites in its proximal promoter found during the initial analysis. None of these genes showed a significant change in mRNA levels with overexpression of Runx1 (n=3 independent experiments with duplicate wells for RT-PCR analysis from each experiment).

Table 3.1. Identification of Runx Binding Sites in Genes Differentially Expressed during Chondrocyte Maturation

Gene Name	Gene Description	Chromosome	Fold Change	# of Runx Sites	Location of Runx Sites
Cxcl16	Chemokine (C-X-C motif) ligand 16	11	10	7	-1275, -992, -781, -514, -118, +26, +163
Avil	Advillin	10	10	2	-351, -25
Sepp1	Selenoprotein P, plasma, 1	15	10	2	-1952, -1621
Fgf21	Fibroblast growth factor 21	7	11	2	-1572, -817
Gpr49	G protein-coupled receptor 49	10	11	3	-1159, -1012, -948
Igfbp6	Keratin complex 2, basic, gene 8	15	11	3	-1972, -1485, -644
Dspg3	Dermatan sulphate proteoglycan 3	10	11	6	-1893, -847, -589, -540, -374, +37
Cilp2	Cartilage intermediate layer protein 2	8	11	3	-435, -418, -129
Ddx60	DEAD box polypeptide 60	8	11	7	-1994, -1198, -1115, -1018, -1009, +71, +141
Dcn	Decorin	10	11	2	-1683, -397
Tcfec	Transcription factor EC	6	11	4	-1290, -990, -221, -134
Esm1	Endothelial cell-specific molecule 1	13	11	1	-1244
Emp2	Epithelial membrand protein 2	16	11	1	-1928
Cpxm2	Carboxypeptidase X 2 (M14 family)	7	11	2	-764, -742
Vit	Vitrin	17	11	2	-741, +117
Ptpns	Protein tyrosine phosphatase, non receptor type substrate 1	2	11	2	-1658, -795
Serpina3n	Serine (or cysteine) protease inhibitor, clade A, member 3N	12	11	6	-1699, -977, -793, -739, +122, +271
Krtdap	Keratinocyte differentiation associated protein provided	7	11	6	-1971, -1612, -1255, -650, -425, +75
Ctss	Cathepsin S	3	12	4	-1524, -785, -684, +95
Cxcl15	Chemokine (C-X-C motif) ligand 15		12	1	
Chrdl1	Chordinlike 1	X	12	6	-1921, -1713, -1017, -560, -392, -77
Lmo2	LIM domain only 2	2	12	3	-1756, -1041, -914
Hpgd	Hydroxyprostaglandin dehydrogenase 15 [36]	8	12	2	-1645, -682
Fndc1	Fibronectin type III domain containing 1	17	13	1	-1124
Wisp2	WNT1 inducible signaling pathway protein 2	2	13	8	-1498, -1392, -1209, -765, -711, -437, -46, +189
C1s	Complement component 1, s subcomponent	6	13	1	-1314
Ccr5	Chemokine (C-C motif) receptor 5	9	13	6	-1906, -1837, -1694, -1381, -1316, -1098
C1qb	Complement component 1, q subcomponent, beta polypeptide	4	13	1	-942

Table 3.1 Continued

Gene Name	Gene Description	Chromosome	Fold Change	# of Runx Sites	Location of Runx Sites
Plek	Pleckstrin	11	13	5	-1590, -1047, -674, -372, +103
Tspan17	Tetraspanin 17	13	14	5	-1990, -1836, -1019, -682, +23
Rassf5	Ras association (RalGDS/AF-6) domain family 5	1	14	4	-1657, -1506, -1031, -877
Alox5ap	Arachidonate 5-lipoxygenase activating protein	5	14	4	-1836, -1164, -647, -498
AK018126	RIKEN cDNA 6330406I15 gene	5	14	1	-140
Blvrb	Biliverdin reductase B (flavin reductase (NADPH))	7	15	6	-1742, -1497, -1025, -927, -576, -389
Fxyd2	FXYD domain-containing ion transport regulator 2	9	15	5	-1952, -736, -499, -168, +126
Slfn8	Schlafen 8	11	15	4	-1851, -504, -19, +12
Casp11	Caspase 11, apoptosis-related cysteine proteiase	9	15	4	-1961, -1844, -1081, -628
Nr1d1	Nuclear receptor subfamily 1, group D, member 1	11	15	4	-1511, -1395, -607, -401
Ugt1a1	UDP-glucuronosyltransferase 1 family, member 1		15	5	-1552, -741, -529, -460, +48
Jcam2	Junction adhesion molecule 2	16	15	5	-1538, -849, -841, -237, -118
Car6	Carbonic anhydrase 6		16	4	-1552, -1187, -780, -606
Ebi3	Epstein-Barr virus induced gene 3	17	16	4	-1893, -1292, -1187, -184
Ms4a7	Membrane-spanning 4-domains, subfamily A, member 7	19	16	8	-1437, -1397, -1346, -1273, -1250, -787, -444, -361
C1qg	Complement component 1, q subcomponent, gamma polypeptide	4	16	5	-1470, -642, -338, -109, +19
Fermt3	Fermintin family homolog 3	19	16	5	-1993, -903, -260, -61, -24
C207 antigen	Langerin	6	16	4	-1813, -1492, -1364, -422
Fcgr3	Fc receptor, IgG, low-affinity Iib	1	16	10	-1830, -1714, -1171, -1152, -1067, -599, -481, -137, +24, +74
Gpnmb	Glycoprotein (transmembrane) nmb	6	17	4	-1880, -1206, -711, -175
Slpi	Secretory leukocyte protease inhibitor	2	17	4	-1126, -1046, -643, -628
Ly86	Lymphocyte antigen 86	13	17	5	-1835, -1598, -1321, -1183, -828

Table 3.1 Continued

Gene Name	Gene Description	Chromosome	Fold Change	# of Runx Sites	Location of Runx Sites
Kcnn4	Potassium intermediate/small conductance calcium-activated channel, subfamily N, member 4	7	17	10	-1498, -1115, -960, -346, -279, -226, -213, -190, -102, +11
Itgbl1	Integrin beta like 1	14	17	2	-1676, -1456
Csf1r	Colony stimulating factor 1 receptor	18	17	6	-1462, -1259, -907, -560, -293, +116
Evi2a	Ecotropic viral integration site 2a	11	17	6	-1181, -969, -707, -653, -376, +87
Vav	Vav 1 oncogene	17	18	3	-1207, -293, -1
Slc1a6	Solute carrier family 1, member 6	10	18	4	-1653, -1560, -334, -262
Prg	Proteoglycan, secretory granule		18	4	-1700, -1318, -809, -312
Cp	Ceruloplasmin	3	18	3	-1605, -832, -491
Msr1	Macrophage scavenger receptor 1	8	19	3	-1657, -850, -322
Pira6	Paired-Ig-like receptor A6	7	19	4	-1948, -1917, -979, -314
Thbs4	Thrombospondin 4	13	19	2	-1820, -1792
Nt5e	5' nucleotidase, ecto	9	19	3	-638, -549, -493
Itgb2	Integrin beta 2	10	19	10	-1894, -1787, -1697, -1205, -1068, -1014, -1003, -663, -376, +124
P2ry6	Pyrimidinergic receptor P2Y, G-protein coupled, 6	7	19	2	-750, -390
LOC226421	RIKEN cDNA 5430435G22 gene	1	19	9	-831, -813, -796, -770, -765, -753, -735, -722, -691
Fyb	FYN-binding protein	15	19	1	-311
Clecsf10	C-type (calcium-dependent, carbohydrate recognition domain) lectin, superfamily member 10	6	19	4	-1995, -1456, -446, -420
Lpl	Lipoprotein lipase	8	20	2	-1822, -1274
Cd68	CD68 antigen	11	20	2	-1883, +123
Lcp1	Lymphocyte cytosolic protein 1	14	20	4	-1457, -517, +67, +115
Icsbp	Interferon consensus sequence binding protein 1	8	20	1	-889
Cxcl10	Chemokine (C-X-C motif) ligand 10	5	21	2	-623, +23
Tnfaip2	Tumor necrosis factor, alpha-inducen protein 2	12	21	5	-998, -866, -197, -2, -115
Cxcl4	Chemokine (C-X-C motif) ligand 4	5	21	2	-1684, -354
Hcph	Hemopoietic cell phosphatase	6	22	1	-1988
Ci1	Solute carrier family 15, member 3	19	22	6	-1826, -824, -407, -143, -24, +51
Lrrc33	Leucine-rich repeat containing 33	16	22	5	-1837, -1692, -1441, -854, -174

Table 3.1 Continued

Gene Name	Gene Description	Chromosome	Fold Change	# of Runx Sites	Location of Runx Sites
Ms4a6d	Membrane-spanning 4-domains, subfamily A, member 6d	19	22	5	-1975, -1369, -1208, -915, -562
Ndr1	N-myc downstream regulated 1	15	22	5	-957, -645, -365, -294, +100
Tyrobp	TYRO protein tyrosine kinase binding protein	7	23	3	-1274, -711, +23
Sp100	Nuclear antigen Sp100	7	23	2	-1785, -583
Stab1	Stabilin1	14	23	3	-1502, -713, -490
Laptm5	Lysosomal-associated protein transmembrane 5	14	23	7	-1847, -1233, -953, -813, -789, -757, +18
Ccl9	Chemokine (C-C motif) ligand 9	11	23	9	-1990, -1839, -1785, -991, -725, -709, -591, -472, -352
Fam26e	Family with seuence similarity 26, member E gene	10	24	4	-1540, -1488, -1252, -657
Adh7	Alcohol dehydrogenase 7 (class IV), mu or sigma polypeptide	3	24	8	-1380, -1349, -1261, -433, -410, -354, -130, +75
C1qa	Complement component 1, q subcomponent, alpha polypeptide	4	24	4	-949, -366, -104, +106
Comp	Cartilage oligometric matrix protein	8	24	5	-1483, -1215, -921, -517, -231
Cxcl5	Chemokine (C-X-C motif) ligand 5	5	24	3	-1746, -1355, -443
Ptprc	Protein tyrosine phosphatase, receptor type, C	1	25	6	-1897, -1042, -760, -586, -141, +33
Cd53	CD53 antigen	3	25	2	-1103, -250
Prelp	Proline arginine-rich end leucine-rich repeat	1	25	1	-666
Apobec1	Apolipoprotein B editing complex 1	6	25	6	-1515, -1089, -668, -626, -246, +74
Clecsf8	C-type (calcium-dependent, carbohydrate recognition domain) lectin, superfamily member 8	6	26	3	-1828, -1677, -715
C1r	Complement component 1, r subcomponent	6	27	2	-1912, -1058
Clec4a2	C-type lectin domain, family 4, member a2 gene	6	27	3	-1178, -731, -297
Dock2	Dedicator of cyto-kinesis 2	11	27	2	-1698, -881
Rarres2	Retinoic acid receptor responder 2	6	29	2	-1736, +27
Csf2rb1	Colony stimulating factor 2 receptor	15	29	3	-1927, -745, -314
Bst1	Bone marrow stromal cell antigen 1	5	29	1	140
Lst1	Leukocyte-specific transcript 1	17	31	7	-1693, -1665, -1450, -1216, -849, -316, -283
Ccl3	Chemokine (C-C motif) ligand 3	11	32	6	-1572, -1040, -438, -389, -145, +90

Table 3.1 Continued

Gene Name	Gene Description	Chromosome	Fold Change	# of Runx Sites	Location of Runx Sites
Pirb	Paired-Ig-like receptor B	7	32	6	-1810, -1790, -1744, -1713, -422, -277
Fcer1g	Fc receptor, IgE, high affinity I, gamma polypeptide	1	33	5	-1732, -1185, -190, -125, +25
Adam23	A disintegrin and metalloprotease domain 23	1	35	2	-1194, -552
Mpeg1	Macrophage expressed gene 1	19	35	3	-1832, -1078, -529
Hp	Haptoglobin	8	37	6	-1736, -1545, -955, -938, -158, -43
Car9	Carbonic anhydrase 9	4	38	1	-111
Epsti1	Epithelial stromal interaction 1	14	39	6	-1734, -971, -902, -843, -672, +142
C1qr1	Complement component 1, q subcomponent, receptor 1	2	42	4	-1431, -1369, -244, +8
Fabp4	Fatty acid binding protein 4, adipocyte	3	43	2	-1973, -999
Evi2b	Ecotropic viral integration site 2b	11	45	6	-1231, -1019, -757, -703, -426, +37
Ccl6	Chemokine (C-C motif) ligand 6	11	45	7	-1121, -1102, -1089, -1068, -951, -624, -185
Pfc	Properdin factor, complement	X	47	3	-1318, -681, -552
Igsf6	Immunoglobulin superfamily, member 6	7	47	3	-1006, -523, +133
Xdh	Xanthine dehydrogenase	17	48	4	-1496, -1010, -897, -773
Ncf1	Neutrophil cytosolic factor 1	5	51	7	-1550, -1073, -987, -839, -422, -111, -16
Ifi203	Interferon-activated gene 203	1	53	3	-851, -753, -93
Ifi202b	Interferon-activated gene 202b	1	53	2	-1805, -1613
Trem2b	Triggering receptor expressed on myeloid cells 2b	17	57	4	-1772, -1357, -1303, -1073
Psmb8	Proteosome subunit, beta type 8	17	57	2	-1539, -1337
Cd48	CD48 antigen	1	59	3	-1903, -93, -79
Ifi205	Interferon-activated gene 205	1	64	5	-798, -530, -393, -176, -6
Lyzs	Lysozyme	10	64	3	-1708, -752, -17
Fgl2	Fibrinogenlike protein 2	5	68	4	-1866, -1209, -548, +128
Casp1	Caspase 1	9	80	3	-1815, -951, +104
Fcgr2b	Fc receptor, IgG, low-affinity Iib	1	80	3	-1187, -818, +114
Sod3	Superoxide dismutase 3, extracellular	5	85	9	-1907, -1845, -1800, -1330, -1295, -1253, -583, -115, -47
Pkib	Protein kinase inhibitor beta, cAMP dependent, testis specific	10	105	2	-923, -116

Table 3.1 Continued

Gene Name	Gene Description	Chromosome	Fold Change	# of Runx Sites	Location of Runx Sites
Mmp13	Matrix metalloproteinase 13	9	126	5	-1223, -908, -604, -542, -40
Ibsp	Integrin-binding sialoprotein	5	241	1	-1224
Tmem46	Transmembrane protein 4	14	-10	9	-1940, -1643, -1416, -1289, -1050, -863, -501, -376, -117
Pitx2	Pairedlike homeodomain transcraption factor 2	3	-10	4	-1891, -1283, -252, -211
Nespas	Neuroendocrine sceretory protein antisense	2	-10	6	-1715, -1373, -846, -540, -154, +30
Nmyc1	Neuroblastoma myc-related oncogene 1	12	-11	4	-1980, -877, -660, -570
Ccni	Cyclin I	5	-11	1	-1345
Cd24a	CD24a antigen	10	-11	3	-1226, -986, -313
Ank1	Ankyrin 1, erythroid	8	-11	7	-1473, -1378, -1147, -1073, -711, -605, -332
Sart3	Squamous cell carcinoma antigen recognized by T-cells 3	5	-11	6	-1890, -1683, -1290, -1115, -275, -144
Rxrg	Retinoid X receptor gamma	1	-12	6	-1759, -1484, -762, -569, -481, -16
Nipsnap 1	4-nitrophenylphosphatase domain and non-neuronal SNAP25-like protein homolog 1 (C. elegans)	11	-12	5	-1689, -1633, -1333, -676, +149
Asb4	Ankyrin repeat and SOCS box-containing protein 4	6	-13	2	-1670, -646
Pcdh8	Protocadherin 8	14	-13	2	-1526, -1213
Fjx1	Four-jointed box 1 (Drosophila)	2	-13	3	-1935, -1841, -389
Ttn	Titin	2	-13	6	-1969, -1964, -713, -245, +55, +73
Bex2	Brain expressed X-linked 2	X	-14	4	-1437, -1147, -169, -81
Gdf5	Growth differention factor 5	2	-15	2	-1996, -330
Peg3	Paternally expressed 3	7	-15	4	-1535, -890, -667, -559
Tnnt1	Troponin T1, skeletal, slow	7	-15	7	-1504, -1225, -1078, -730, -705, -695, -324
Sln	Sarcolipin	9	-15	2	-1410, -235
Myod1	Myogenic differentiation 1	7	-16	3	-1739, -1011, +37
Tmem100	Transmembrane protein 100	11	-16	4	-1790, -860, -791, -34
Myla	Myosin, light polypeptide 4	11	-16	3	-1728, -883, -594
Chrna1	Cholinergic receptor, nicotinic, alpha polypeptide 1 (muscle)	2	-17	2	-1935, -595
Tmem8c	Transmembrane protein 8c	2	-18	5	-1492, -863, -642, -42, +54
Igsf9	Immunoglobulin superfamily, member 9	1	-19	4	-1417, -1022, -976, +135
Acta1	Actin, alpha1, skeletal muscle	8	-19	3	-1794, -1170, -478
Pde9a	Phosphodiesterase 9A	17	-20	1	-1169

Table 3.1 Continued

Gene Name	Gene Description	Chromosome	Fold Change	# of Runx Sites	Location of Runx Sites
Mybph	Myosin -binding protein H	1	-21	3	-720, -585, -154
Sema6a	Sema domain, transmembrane domain [110],and cytoplasmic domain, (semaphorin) 6A	1	-21	3	-1858, -655, -178
Sox11	SRY-box containing gene 11	12	-21	2	-1081, -755
Lrp4	Low-density lipoprotein receptor-related protein 4	2	-22	2	-1703, -930
Il17b	Interleukin 17B	18	-22	1	-763
Gcat	Glycine C-acetyltransferase (2-amino-3-ketobutyrate-coenzyme A ligase)	15	-22	2	-416, -365
Sostdc1	Sclerostin domain containing 1	12	-22	5	-1817, -685, -667, -274, +162
Siat7c	Sialyltransferase 7 ((alpha-N-acetylneuraminyl 2,3-betagalactosyl-1,3)-N-acetyl galactosamidine alpha-2,6-siayltransferase) C	3	-24	3	-477, -207, -56
BC005730	RIKEN cDNA A330049M08 gene	4	-26	2	-1998, -679
Cacna1s	Calcium channel, voltage-dependent, L-type, aplha 1s subunit	1	-26	2	-1302, -1203
Tnni2	Troponin L, skeletal, fast 2	7	-26	4	-1580, -1349, -774, -615
Bcl11a	B-cell CLL/lymphoma 11A (zinc finger protein)	11	-26	2	-1372, -1343
Prom1	Prominin 1	5	-26	5	-1270, -1174, -856, -759, -703
Hba-a1	Hemoglobin alpha, adult chain 1	11	-28	2	-807, -198
Mb	Myoglobin	15	-28	4	-1404, -837, -95, -55
Grip1	Glutamate receptor-interacting protein 1	10	-29	5	-1825, -1472, -1122, -1094, -1072
Tncc	Troponin C, cardiac/slow skeletal	14	-30	5	-1637, -1390, -1135, -75, +63
Chrng	Cholinergic receptor, nicotinic, gamma polypeptide	1	-36	6	-696, -675, -492, -378, -367, -142
Csaq2	Calsequestrin 2	3	-38	4	-1637, -1295, -893, -626
Actn2	Actinin alpha 2	13	-38	7	-1972, -1566, -1429, -1289, -1104, -60, +91
Nnat	Neuronatin	2	-40	5	-1991, -1885, -1332, -1282, -1071
BMP7	Bone morphogenic protein 7	2	-40	3	-1675, -681, -175
Actc1	Actin, alpha, cardiac	2	-42	2	-1312, -1279
Dusp9	Dual specificity phosphatase 9	X	-43	2	-1274, -650
Dcx	Doublecortin	X	-44	1	-1691
Rex3	Reduced expression 3	X	-50	2	-1578, -1153

Table 3.1 Continued

Gene Name	Gene Description	Chromosome	Fold Change	# of Runx Sites	Location of Runx Sites
Lrrn1	Leucine-rich repeat protein 1, neuronal	6	-84	6	-742, -685, -468, -92, -54, +120
Myog	Myogenin	18	-85	3	-541, -530, -524
Tnnt2	Troponin T2, cardiac	1	-98	3	-1787, -954, -856
Tnni1	Troponin I, skeletal, slow 1	1	-111	1	-1672
Mylpf	Myosin light chain, phosphorylatable, fast skeletal muscle	7	-141	4	-1553, -1176, -909, -389
Hbb-y	Hemoglobin Y, betalike embryonic chain	7	-245	1	+15
Myh3	Myosin, heavy polypeptide 3, skeletal muscle, embryonic	11	-392	6	-1375, -869, -648, -344, -94, -39
Mylf	Myosin, light polypeptide 1	1	-339	7	-1895, -1766, -1235, -797, -743, -153, -102

Table 3.1 Identification of Runx Binding Sites in Genes Differentially Expressed during Chondrocyte Maturation

Genes that are differentially expressed during chondrogenesis and have Runx binding sites in their proximal promoters are listed in order of fold change in expression between proliferating and hypertrophic chondrocytes (a positive number indicates upregulation during chondrogenesis and a negative number indicates downregulation). The locations of the Runx sites are listed relative to the transcription start site. This table is adapted from [109].

Conclusion

In characterizing the clonal populations of Runx1 positive cells in osteoarthritic cartilage, it was discovered that they also express VCAM1, a marker for mesenchymal progenitor cells, and the proliferation markers Ki67 and PCNA. As stated above, Runx1 is involved in cell proliferation in hematopoietic cells [105], and it is possible that it contributes to the regulation of mesenchymal progenitor cells in response to articular cartilage damage. Although Runx1 is associated with markers of proliferation, our *in vivo* studies do not show that the increased proliferation rates in cartilage cells are a result of Runx1 expression. The *in vitro* experiments show that Runx1 does not cause increased proliferation rates in ATDC5 cells. This is possibly due to the fact that ATDC5 cells already proliferate at a rapid rate. It is possible that an increase in Runx1 in an already rapidly proliferating cell line would not be enough to increase proliferation rates further. Recent data from our laboratory shows that MEFs with decreased levels of Runx1 proliferate more slowly than their wild-type counterparts. A knockdown of Runx1 in ATDC5 cells may show decreased proliferation as well. Additional studies need to be done in a cell line that is more representative of articular chondrocytes, and these experiments should be repeated in Runx1 expressing cells isolated from immature cartilage tissues such as MEFs or immature bovine articular cartilage before any conclusions can be drawn. To try to gain insight into genes that are potential downstream targets of Runx1 in cartilage, using a published gene profile of chondrocyte expressed genes [109], the sequence of

the proximal promoter of each gene as published in GenBank was examined manually for all variations of consensus Runx binding sites 5'-3' (A/G)ACC(A/G)C(A/T). The purpose of this was to establish a population of candidate genes that are both expressed in cartilage, and have the potential to be regulated by Runx1. Candidate genes were chosen based on their role in osteoarthritis. 2 genes that are upregulated, 2 genes that are downregulated, and 2 genes that may be protective in OA were chosen for preliminary analysis, in addition to a gene that had 10 Runx binding sites in its promoter. Cp and Dcn are upregulated during the disease process of OA [111, 112]. Sox11 and Wisp2 are downregulated in response to mechanical strain [113, 114]. BMP7 and Cxcl10 were chosen for their potential protective effect during osteoarthritis. BMP7 decreases joint inflammation at low concentrations while Cxcl10 stimulates progenitor cell migration [115, 116]. In ATDC5 cells, none of these genes showed changes in expression as a result of overexpression of Runx1. As with the proliferation studies, it is important to confirm these findings in primary chondrocytes.

CHAPTER IV:

Runx Functions in Cartilage

Pilot Studies: Identifying Novel Mechanisms Runx Proteins in Regulation of Protein Synthesis and Epigenetic Control of Chondrogenesis

Abstract

In addition to functioning as phenotypic transcription factors, Runx genes have been shown to promote differentiation by controlling cell cycle progression and global protein synthesis in some cells. Changes in protein synthesis rates are associated with both cell proliferation and cellular hypertrophy – both processes that take place during chondrogenesis. To determine if Runx proteins regulate protein synthesis, Runx1, Runx2, or Runx3 was overexpressed in a chondrogenic cell line and assayed transcription levels of ribosomal machinery and protein synthesis rates by ^{35}S incorporation. Preliminary experiments show that Runx1, Runx2, and Runx3 overexpression do not cause changes in pre-rRNA or 28S levels and do not cause changes in protein synthesis rates. Additionally, a preliminary experiment shows that Runx proteins are not associated with rDNA repeats in ATDC5 cells at any stage during *in vitro* chondrocyte differentiation.

Runx1, Runx2, and Runx3 are all expressed in growth plate cartilage during distinct stages of chondrocyte maturation. While Runx2 is well known to control genes expressed during chondrocyte hypertrophy, the functions of Runx1 and Runx3 during this process are less well understood. Immunofluorescense studies showed that Runx2, but not Runx1 or Runx3, remains bound to DNA throughout mitosis, indicating that it has the potential to function epigenetically during chondrogenesis by bookmarking its target genes throughout the cell cycle, for later expression in post-proliferative hypertrophic chondrocytes.

Introduction

Regulation of protein synthesis is an important factor in the determination of cellular growth rates, and the amount of protein per cell contributes to cell size. The cellular protein content can be controlled by changing rates of protein synthesis and/or rates of protein turnover [117]. The control of global protein synthesis is determined by the amount of ribosomes available for translation, and this is directly controlled by ribosomal DNA (rDNA) transcription [118]. The ribosome is composed of a 40S subunit containing 18S rRNA and approximately 33 proteins, and a 60S subunit containing 5S, 28S, and 5.8s rRNA and approximately 49 proteins [119]. The 18S, 5.8S, and 28S rDNA components are transcribed as a single messenger RNA that is then processed into the component parts [120]. Transcription of pre-rRNA is controlled by a transcription initiation complex consisting of RNA Polymerase I, Selectivity Factor 1 (SL1), and Upstream Binding Factor (UBF) which is required for activated transcription [118]. All three Runx proteins can bind to ribosomal DNA repeats with UBF to control global protein synthesis regulation [121-123]. In osteoblasts, overexpression of Runx2 causes a decrease in global protein synthesis by repressing rDNA transcription [123].

Increased cell growth can result in either increased proliferation (as cells need to double in size before they divide) or cellular hypertrophy. In proliferating cells, an increase in RNA content leads to more rapid cell division [124]. Additionally, hypertrophy of cardiac myocytes results from an increase in protein

synthesis rates, which is directly associated with an increase in rDNA transcription [125]. Thus, an increase in ribosomal biogenesis results in an increase in overall protein synthesis, which can lead to cell division or hypertrophy, depending on cell context. Therefore in chondrocytes, regulation of global protein synthesis rates may be required for both the processes of proliferation and hypertrophy.

During endochondral bone formation, the chondrocyte goes through stages of both rapid division and cellular hypertrophy. While both of these cellular events are regulated by an increase in rates of protein synthesis, there must be some other factors regulating the decision between proliferation and hypertrophy. During chondrocyte hypertrophy, C/EBP ß directly controls $p57^{Kip2}$ expression causing exit from the cell cycle and leading to hypertrophy [126]. The protein $p57^{Kip2}$ is a member of the Cip/Kip family of cell cycle inhibitors and functions by binding to cyclin/CDK complexes and inhibiting the transition to G1/S phase [127].

Epigenetics is the process by which genetic information is transferred from parent to progeny cell without changes in DNA sequence. Epigenetics commonly refers to gene silencing or gene activation, and there are certain epigenetic marks associated with each of these. For example, DNA methyltransferases are enzymes that add methyl groups (CH_3) to regions of DNA that contain many CpG sites known as CpG islands [128, 129]. The methylations of CpG islands result in transcriptional repression by the displacement of

transcription factors along with recruitment of proteins involved in gene silencing [130].

Histone modifications provide another important mechanism of epigenetic regulation. In chromatin, DNA is associated with histones in complexes known as nucleosomes, each of which contain ~146 base pairs of DNA wrapped around a histone octamer containing two copies each of histones H2A, H2B, H3, and H4 [131]. The most common types of histone modifications are acetylation and methylation. Table 4.1 (adapted from [132]) lists some common histone modifications and their association with either activated or repressed chromatin. While this table is generally accurate, there are certain instances where the number of methyl groups added to a histone determines its association with active or inactive chromatin. For example, H3K9me1 (one methylation of lysine) is associated with active chromatin while H3K9me3 (three methylations of lysine) is associated with repressed chromatin [133].

In addition to the well-studied DNA methylations and histone modifications, “bookmarking” by transcription factors is emerging as a novel mechanism for epigenetic regulation of genes. This involves the retention of transcription factors on the promoters of their target genes throughout mitosis, when active transcription is not taking place. It is theorized that the presence of transcription factors on target gene promoters poises certain genes for transcription immediately upon exit from mitosis [128]. In addition to regulating the transcription of their target genes, Runx proteins possess epigenetic

functions. Runx1, Runx2, and Runx3 remain bound to the promoters of their target genes during mitosis, as a novel epigenetic mechanism poising these genes so that they can be transcribed upon exit from mitosis [76, 121]. Runx2 is also responsible for a number of histone modifications in osteoblasts [134].

Because of the novel functions of Runx proteins in protein synthesis control and epigenetic regulation of target genes, this study addresses the hypothesis that Runx factors may regulate these functions in chondrocytes. The unique expression of Runx1 in proliferating cells (both in the growth plate and in osteoarthritic cartilage) and Runx2 in hypertrophic cells allows for the possibility of these transcription factors to regulate protein synthesis during chondrogenesis. In addition, because of their known role as epigenetic regulators of their target genes in a variety of cell types, the aim of these experiments was to discover whether the Runx proteins also functioned epigenetically in chondrocytes.

Activating Modifications	Repressing Modifications
Lysine Acetylation H3K9, H3K14, H3K18, HeK56 H4K5, H4K8, H4K13, H4K16 H2A, H2B	CpG Island Methylations
Serine/Threonine Phosphorylation H3T3, H3S10, H3S28 H2A, H2B	Lysine Methylation H3K9, H3K27 H4K20
Arginine Methylation H3R17, H3R23 H4R3	Lysine Ubiquitination H2AK119
Lysine Methylation H3K4, H3K36, H3K79	Lysine Sumoylation H2BK6, H2BK7 H2AK126
Lysine Ubiquitination H2BK120	

Table 4.1: Common Epigenetic Modifications and Their Association with Activated or Repressed Chromatin (Adapted from [132])

Chondrocyte Cell Lines

One of the major problems with studying chondrocytes is that there are no cell lines that reliably reproduce the natural resting chondrocyte or the events of chondrogenesis as they happen *in vivo*. Many primary chondrocyte cultures de-differentiate after a few passages, making *in vitro* experiments difficult. For the pilot experiments discussed in this section, as well as for the proliferation

experiments in the previous section, a combination of three different chondrocyte differentiation models were used which will be described here.

N1511 is a chondrogenic cell line that was isolated from the rib cartilage of P53-null mice [135]. The addition of BMP2 and insulin to these cells at confluence induces differentiation to hypertrophic chondrocytes [135]. However, when BMP2 and insulin were added to the N1511 isolate that was obtained by our laboratory, cell death occurred within 48hours. Because this cell line was unable to be differentiated, it could not be used to study targets of Runx genes during chondrocyte differentiation. This cell line did express a high level of Runx2 in its proliferating state (Figure 4.1), making it useful for the knockdown experiments. In N1511 cells, proliferation is inhibited by re-introducing p53 [135], indicating that the absence of p53 is responsible for the rapid rate of proliferation in this cell line. The strong contribution of p53 to proliferation rates in this cell line made it a poor choice for studying the contribution of Runx factors to proliferation and protein synthesis in chondrogenesis, and may be one of the reasons there was no change in protein synthesis machinery observed in response to Runx2 knockdown.

Another cell type that can be used for the study of chondrocyte differentiation is the mouse embryonic fibroblast. These primary cells, when grown in high-density micromass cultures, reproducibly go through the stages of chondrocyte differentiation [136]. One of the drawbacks to the MEF micromass culture of chondrogenic differentiation is that it is difficult to obtain the amount of

cells needed for chromatin immunoprecipitation experiments. Also, it is difficult to transfect these cells when they are in high-density micromass cultures, making overexpression experiments difficult. The advantage to these primary cells is they can be isolated from different strains of mice. Thus, the ^{35}S incorporation experiments done on these cells are able to compare normal levels of Runx2 to a complete Runx2 knockout. Unfortunately, it is known that Runx2 -/- MEFs do not progress to hypertrophic chondrocytes, and therefore these cells can only be studied in monolayer culture.

The cell line that was used for a majority of this research was ATDC5. This is a cell line that is derived from a teratocarcinoma, and is able to mature to a chondrocyte that expresses many markers of hypertrophy when plated under differentiation conditions in medium containing insulin [137]. However, there is debate in the field regarding whether or not these cells actually reach chondrocyte hypertrophy, as determined by the expression of Collagen 10. In many studies, including these, Collagen 10 expression is not increased substantially during *in vitro* differentiation. However, these cells do produce a mineralized matrix as evidenced by positive alkaline phosphatase staining. An advantage to these cells is that they are easily transfectable, and that they can be differentiated in monolayer, making them a good choice for overexpression studies.

Materials and Methods

Cell Culture Conditions

ATDC5 cells were maintained in DMEM/F12 medium supplemented with 2mM L-glutamine, 100 U/mL penicillin, 100 µg/mL streptomycin, 10% FBS, 10µg/mL transferrin, and $3x10^{-8}$M sodium selenite. N1511 cells were maintained in α-MEM supplemented with 2mM L-glutamine, 100 U/mL penicillin, 100 µg/mL streptomycin, and 10% FBS. Both cell lines were cultured at 37^{o}C in the presence of 5% CO_2.

For ATDC5 differentiation, cells were plated at a concentration of 350,000 cells/plate in a 100mm plate, 133,636 cells/plate in a 60mm plate, or 24,182 cells/well in a 6-well plate. Cells were maintained in DMEM/F12 medium supplemented with 2mM L-glutamine, 100 U/mL penicillin, 100 µg/mL streptomycin, 10% FBS, 10µg/mL transferrin, and $3x10^{-8}$M sodium selenite for 7 days, with medium changes 4 and 6 days after plating. 7 days after plating, the medium was changed to DMEM/F12 supplemented with 2mM L-glutamine, 100 U/mL penicillin, 100 µg/mL streptomycin, 2% FBS, 10µg/mL transferrin, and $3x10^{-8}$M sodium selenite, and 10µg/mL insulin. Medium was changed every 2-3 days during the time course, and cells were harvested for up to 28 days.

Isolation of Mouse Embryonic Fibroblasts

For isolation of MEFs, mice with a targeted disruption of Runx2 on a C57/Bl6, Dba/2 background were used [36]. As mice homozygous for the mutation die at birth, heterozygous mice were bred to obtain litters containing wild type, heterozygous, and Runx2-/- embryos. Pregnant mice were sacrificed at day 12.5 by CO_2 asphyxiation and cervical dislocation. The abdomen was opened and the uterus was removed. Single embryos were removed by opening the uterus wall and puncturing the embryonic sac. Embryos were washed with phosphate buffered saline (PBS) and digested by adding 1mL of 0.25% Trypsin-EDTA, passing each embryo through an 18Ga needle 20 times, and incubating the resulting cell suspension for 15 minutes at room temperature. Nine mL of DMEM + 2mM L-glutamine, 100 U/mL penicillin, 100 µg/mL streptomycin, and 15% FBS were added to each sample and the mixture was plated on a 100mm plate and cultured at 37^{o}C in the presence of 5% CO_2. After 24 hours, cells were washed with PBS to remove the non-adherent cells and given fresh growth medium. Medium was changed every other day and cells were passaged 1:5 at 70% confluence.

Runx Overexpression

For Runx overexpression, vectors containing full-length mouse Runx1 and Runx3 in a pcDNA backbone, and full-length mouse Runx2 in a pLENTI CMV/TO GFP-Zeo DEST backbone were generated. For transformation experiments, ATDC5 cells were plated at 100,000 cells/well in a 6-well plate or 666,666 cells/plate in a 100mm plate. Cells were transfected with either an empty vector, or a vector containing Runx1, Runx2, or Runx3 using X-treme gene transfection reagent (Roche, Mannheim, Germany) according to the manufacturer's protocol, using 1µg of plasmid and 3µL of transfection reagent. Cells were grown up to 48h post-transfection and cells were harvested at the time points specified below.

Quantitative Real Time PCR Analysis

For RNA preparation, cells from a 100mm plate were rinsed with PBS, and then harvested in 1mL Trizol. RNA isolation was carried out by phenol/chloroform extraction followed by ethanol precipitation. DNA contamination was removed using the DNase-free RNA kit [138] according to the manufacturer's specifications. Nucleic acid quantification was carried out using a Nano-drop spectrophotometer, and RNA purity was assessed using the 260/280 ratio. One µg of RNA was reverse transcribed into cDNA with the First Strand cDNA synthesis kit (Invitrogen) using random hexamers according to the manufacturer's protocol. RT-PCR was performed on a 7300 Real Time PCR System (Applied Biosystems). Samples were run in duplicate using 20ng of

cDNA, 5μM forward and reverse primer, and SybrGreen Master Mix (Bio Rad) in a 25 μL reaction. Primers used can be found in Table 4.2.

Gene	Forward Primer	Reverse Primer
Cp	CATGGGGTAACGTACACCAAG	GCACATACACATACTGTTGTCCG
Dcn	CCCTACCGATGCCAGTGTC	GCAGGTCTAGCAAGGTTGTGT
Wisp2	TGCCCCGAGTGGGTGTGTGA	GGGCCATCGGCAGATGCAGG
Itgb2	TGCACCAAGTACAAAGTCAGC	GCGCAAGGAGTCAGGTTCT
Cxcl10	CCAAGTGCTGCCGTCATTTTC	GGCTCGCAGGGATGATTTCAA
Sox11	CCCTGTCGCTGGTGGATAAG	GGTCGGAGAAGTTCGCCTC
Bmp7	ACGGACAGGGCTTCTCCTAC	ATGGTGGTATCGAGGGTGGAA

Table 4.2: Genes Chosen and Primers used for Quantitative RT-PCR Analysis after Runx1 Overexpression

Chromatin Immunoprecipitation

Chromatin immunoprecipitation experiments were carried out as previously described [139]. ATDC5 cells were induced to undergo chondrocyte maturation using the differentiation protocol described above. On days 0 and 7, cells were rinsed once in PBS, and 10mL of DMEM/F12 was added back to the plates. On days 14, 21, and 28, cells were rinsed in PBS and treated with Collagenase P for 5 minutes. Cells were rinsed once more in PBS and 10mL of DMEM/F12 was added back to the plates. To crosslink proteins and DNA, 1mL of formaldehyde solution (50mM HEPES-KOH buffer pH 7-7.5, 100mM sodium chloride, 1mM

EDTA, 0.5mM ethylene-glycol-bis (2-aminoethylether)-N-N-N'-N'-tetraacetic acid, 2.57% (w/v) formaldehyde, in nuclease-free water) was added to each plate and plates were incubated for 10 minutes at room temperature. To quench the reaction, 0.5mL of 2.5M glycine was added to each plate and plates were incubated at room temperature for 10 minutes. Plates were washed with ice-cold PBS Wash Buffer (0.2µM-filtered PBS, 25µM MG132 (proteasome inhibitor), 1x complete EDTA-free protease inhibitor cocktail tablet solution), then harvested in 500µl of PBS Wash Buffer and transferred to a microcentrifuge tube. Cells were spun at 700xg for 5 minutes at 4^{o}C, resuspended in 1mL ice-cold PBS Wash Buffer, and spun again 700xg for 5 minutes at 4^{o}C. At this point, cells were flash-frozen in liquid nitrogen and stored at -80^{o}C.

Cells were thawed and resuspended in 1mL of ChIP Buffer C (10mM Tris-HCl pH 8.0, 100mM sodium chloride, 1mM EDTA, 1mM ethylene-glycol-bis(2-aminoethylether)-N-N-N'-N'-tetraacetic acid, 0.1% (w/v) sodium deoxycholate, 0.5% (w/v) N-lauroylsarcosine sodium salt solution, 25µM MG132, 1x complete EDTA-free protease inhibitor cocktail tablet solution, in nuclease free water) and cells were allowed to thaw in buffer for 20 minutes on ice. Cells were sonicated as follows: On Time: 1 second, Off Time: 2 seconds, Total On Time: 20 seconds; and this program was repeated 3 times with 20 seconds rest between. After sonication, 600U each of HaeIII and PstI-HF were added to each tube and incubated for 1h at 32^{o}C. Following this incubation, 109µL of Triton X-100 solution was added to each tube (final concentration = 1%). Tubes were spun for

15 minutes at 16,100 x g at 4^{o}C, and supernatants were transferred to a new microcentrifuge tube. One mL of chromatin prep was used for each IP. 5ug of antibody were added to each respective tube and cells were placed on a vertical rotor at 4^{o}C for 16h. 35µL each of Dynabeads Protein A and Protein G were added to each tube, and tubes were placed back on the vertical rotor at 4^{o}C for 5 hours. Beads were washed 1x in Buffer C + 1% triton X-100, and 3x in ChIP Wash Buffer (50mM HEPES-KOH pH 7-7.5, 150mM lithium chloride solution, 1mM EDTA, 0.5% (w/v) nonindet P40 solution, 0.25% (w/v) sodium deoxycholate, in nuclease-free water), and 1x in TE Buffer (10mM Tris-HcL pH 8.0, 1% (w/v) SDS solution, in nuclease-free water). Protein was eluted by adding 100uL of ChIP Elution Buffer (100mM sodium bicarbonate, 1% (w/v) SDS, in nuclease-free water) and placing tubes on the Micro Tube Mixer for 15 minutes, and this step was repeated after adding an additional 100uL of ChIP elution buffer. 160µL of ChIP Elution Buffer was added to the input sample, and all tubes were placed in a 65^{o}C hybridization oven for 16 hours. 200µL of TE buffer, and 8µL of RNase A were added to each tube and incubated at 37^{o}C for 2 hours. 4µL of proteinase K was added to each tube and incubated at 55^{o}C for 2 hours. Chromatin was then isolated by adding 400µL phenol/chloroform/isoamyl alcohol (25:24:1) solution to each tube, mixing thoroughly, and transferring to a MaXtract High Density 2mL tube, and spinning at 10,000rpm for 10 minutes to isolate the chromatin in the aqueous phase. 400µL of chloroform/isoamyl alcohol (24:1) was added to each tube and spun again at 10,000rpm for 10 minutes. The

aqueous layer was transferred to a new tube and 2µL of glycogen and 40µL of 3M sodium acetate pH 5.5 was added to each tube and DNA was precipitated using isopropanol. DNA pellets were resuspended in 200µL of nuclease-free water. DNA was quantified and equal concentrations were used in qPCR. Antibodies used for IP are described in Figure 4.3.

Metaphase Spreads

N1511 cells were passaged 1:20 every other day in the medium described above. Cells were blocked in metaphase as previously described [123]. One day after passaging, colcemid was added to a 100mm plate at a concentration of 30ng/µL and plates were incubated for 16h, at which point cells were harvested by mitotic shakeoff and pelleted by centrifugation at 1000 RPM for 5 minutes. Cells were resuspended in 5mL of 75mM KCl warmed to 37^{o}C and incubated for 15-20 min at 37^{o}C, and then pelleted by centrifugation at 2500 rpm for 5 min. Cells were washed with 1mL PBS, transferred a microcentrifuge tube, and pelleted at 4000rpm for 4 minutes. Cells were washed with an additional 400uL of PBS and Cytospun onto slides at 220 rpm for 10 min (~200uL/slide).

Immunofluorescense

Immunofluorescense experiments were carried out as previously described [123]. Slides were dried for 1-2 minutes, washed in PBS for 5 minutes, and fixed in 1% formaldehyde for 10 minutes. Cells were washed again for 5 minutes in PBS and

permeabilized using 0.25% Triton in PBS for 20 minutes. Cells were washed twice in PBS and then blocked in 0.5% BSA in PBS for 30 minutes. Cells were incubated for 1h at 37^{o}C in primary antibody. Cells were washed three times in PBS before incubation for 1h at 37^{o}C in secondary antibody. Cells were washed three times in PBS and stained with DAPI solution (1:5000 in triton+PBSA) for 3 minutes. Cells were washed with PBSA+triton, PBS, and PBSA before mounting with Pro-Long Gold Anti-fade reagent. Slides were visualized on a Zeiss Axioplan Fluorescence microscope using MetaMorph imaging software. Antibodies used were Runx1 rabbit polyclonal (1:100, Ab50541, Abcam), Runx2 Mouse Monoclonal (1:200), and Runx3 rabbit polyclonal (1:200, Ab 11905, Abcam). Secondary antibodies used were Alexa Fluor 488 goat anti-rabbit (1:800) and Alexa Fluor 594 goat anti-mouse (1:800).

Co-Immunoprecipitation

N1511 cells were grown to confluence and harvested in 1mL of PBS. Cells were pelleted by centrifugation at 4000rpm for 5 min in a tabletop microcentrifuge. Cells were resuspended in 1mL of sonication buffer and incubated on ice for 10 minutes before sonication at 10% for 5x10 seconds with 20 seconds rest in between. Lysate was separated into equal parts and 4µg of primary antibody was added. Samples were incubated at 4^{o}C for 16 hours before 50µL of Protein A/G beads were added. Samples were incubated at 4^{o}C for an additional 2

hours. Beads were pelleted at 3000rpm for 3 minutes, and washed 4x with 500µL Wash Buffer. Samples were eluded with 1X Gel Loading Buffer and analyzed by western blot. Antibodies used for IP were: Runx2 M70 (rabbit polyclonal, Santa Cruz) and UBF H300 (rabbit polyclonal, Santa Cruz). Antibodies used for Western Blot were Runx2 mouse monoclonal (1:2000) and UBF F9 mouse monoclonal (1:1000, Santa Cruz).

^{35}S Incorporation Assays

ATDC5 cells were plated at 100,000 cells/well in a 6-well plate. 24 hours later, cells were transfected with either an empty vector, or a vector containing *Runx1*, *Runx2*, or R*unx3* using X-treme gene transfection reagent according to the manufacturer's protocol, using 1µg of plasmid and 3µL of transfection reagent. 24 and 48 hours after transfection, cells were washed 2x with PBS, 2mL of pulse-labeling medium (DMEM –met, -cys, +10% dialyzed FBS + 25mM HEPES) were added to each well, and cells were incubated for 15 min at 37^{o}C at 5% CO_2. Medium was removed from the cells, and 0.5mL of [^{35}S]-methionine working solution (pulse-labeling medium + 0.1mCi/mL [^{35}S]-methionine) was added to each well. Cells were incubated for 20 minutes at 37^{o}C at 5% CO_2. Medium was removed from the cells, and the cells were washed twice with ice cold PBS and scraped into direct lysis buffer (2% sodium dodecyl sulfate, 10mM dithiothreitol, 10% glycerol, 2M urea, 1x Roche complete proteinase inhibitor, 10mM tris pH 7.5, 1x MG132). Total protein content was determined using the Coomassie

Plus (Bradford) Assay Kit (Thermo Scientific) according to the manufacturer's protocol. Equal amounts of protein were loaded on a 4-20% Ready Gel Tris-HCl Gel (Biorad). The gel was dried and exposed for 6-16 hours on BioMax Chemiluminescense film to determine ^{35}S incorporation.

For MEF experiments, mouse embryonic fibroblasts were isolated as described above from wild type or Runx2 -/- embryos. Cells were plated at 100,000 cells/plate on 60mm dishes and the pulse labeling was carried out as described above, however; cells were harvested in ice-cold PBS instead of direct lysis buffer. 10µL of the labeled cell suspension was added to 100µL of BSA/sodium azide and placed on ice. 1mL of ice-cold 10% (w/v) TCA solution was added to each sample. The mixture was vortexed and incubated on ice for 30 minutes. The suspension was filtered onto 2.5cm glass microfiber filter disks and washed twice with 5mL ice-cold 10% TCA and twice with ice-cold ethanol. 10uL of the labeled cell suspension was also spotted on an additional glass microfiber disc. All discs were allowed to air-dry for 30 minutes. Discs were transferred to 20mL scintillation vials, 5 mL of scintillation fluid was added, and radioactivity was measured in a scintillation counter. The ratio of TCA-precipitable label to total radioactivity was calculated.

Results

Characterization of Chondrocyte Cell Lines

Different chondrocyte cell lines and MEFs used in these experiments were compared for transcription factor levels to identify the most appropriate cell for the Runx functional studies. Messenger RNA was isolated from each cell type for qPCR analysis to determine levels of Runx1, Runx2, and Sox9. Both ATDC5 cells and N1511 cells represent more committed chondrocytes when compared to MEFs, as evidenced by their Sox9 expression (Figure 4.1). N1511 cells showed very high levels of Runx2 mRNA when compared with the other cell lines (Figure 4.1). To assess the progression of ATDC5 cells through chondrogenesis, mRNA was taken weekly for qPCR analysis during ATDC5 differentiation. Figure 4.2 shows changes in gene expression during differentiation. *Runx2* and *Runx3* mRNA levels increased 3.5 and 2 fold, respectively during ATDC5 differentiation. Interestingly, *Runx1* levels remained relatively constant throughout the time course, in contrast to what is seen *in vivo*. Phenotypic chondrocyte markers also showed changes in expression that mimic what is seen during *in vivo* chondrocyte maturation. *Sox9* levels increased 4-fold between days 0 and 7, then began to decline during further maturation. *Col2a1* levels began to increase on day 7 and reached maximal levels by day 14 (>60 fold increase) before they began to decline again at day 28. Alkaline phosphatase, a marker of hypertrophic chondrocytes, continued to increase through ATDC5 differentiation, reaching maximal levels at day 28 (>350 fold). These data indicate that ATDC5

cells exhibit the characteristics of proliferating chondrocytes between day 0 and 7, pre-hypertrophic chondrocytes at day 14, and a cell that expresses many hypertrophic markers after day 21.

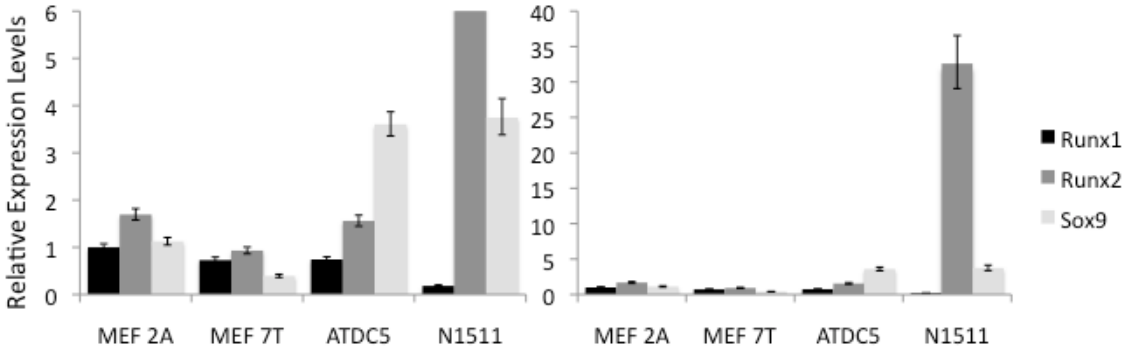

Figure 4.1: A Comparison of Runx1, Runx2, and Sox9 Expression in *in vitro* Chondrocyte Models

A comparison of Runx1, Runx2, and Sox9 mRNA levels in MEF cells isolated from 2 different mice, ATDC5 cells, and N1511 cells. The left panel shows a close-up version of the panel on the right, due to the high expression of Runx2 in N1511 cells. This graph represents one independent experiment and error bars represent standard deviation of duplicate samples

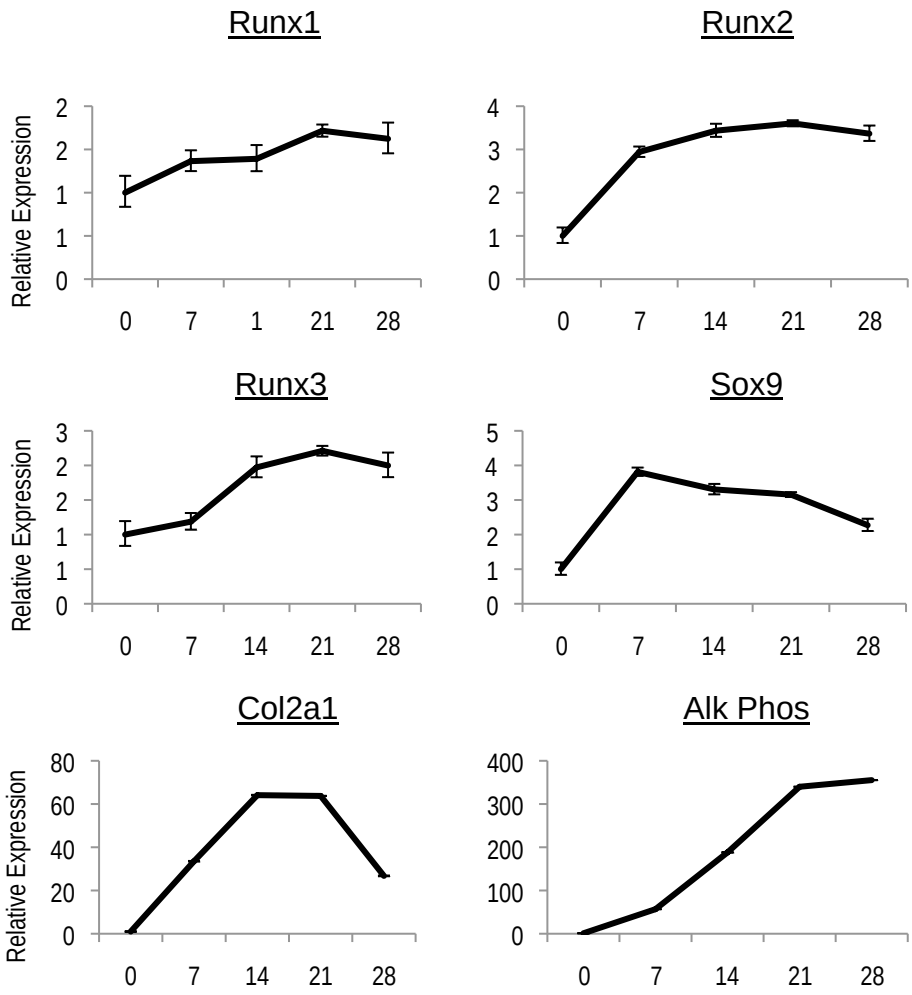

Figure 4.2: Expression of Runx Proteins and Phenotypic Chondrocyte Markers during ATDC5 Differentiation

Quantitative RT-PCR analysis shows expression of chondrocyte markers during ATDC5 differentiation. Values are normalized to GAPDH and expressed relative to day 0 values. This data is from 1 independent experiment with 2 replicate samples analyzed by qPCR. Error bars represent standard deviation of replicate samples.

Runx Overexpression does not affect Levels of Protein Synthesis Machinery or Change Levels of Global Protein Synthesis.

As reviewed in the introduction, both cellular proliferation and hypertrophy are associated with increases in protein synthesis. Runx proteins, which regulate global protein synthesis in other cell types, are expressed in distinct populations of growth plate chondrocytes, and chondrocytes of articular cartilage. To determine if global protein synthesis rates were changed in response to Runx overexpression, ^{35}S incorporation assays were performed. In ATDC5 cells, expression of neither Runx1, 2, nor 3 resulted in changes of protein synthesis rates (Figure 4.3 B,C), providing preliminary evidence that Runx proteins do not control global protein synthesis in this chondrogenic cell line. Although there was no change in protein synthesis rates with overexpression of Runx proteins in ATDC5 cells, osteoblasts derived from Runx2-/- mice show increased protein synthesis compared to wild-type osteoblasts [123]. To determine if MEFs derived from the same mice show increased protein synthesis compared to wild-type MEFs, ^{35}S incorporation assays were done on MEFs isolated from these mice. In comparison to wild-type MEFs, Runx2 -/- showed no significant change in ^{35}S incorporation, indicating comparable protein synthesis rates in both cell types (Figure 4.3A). Additionally, significant knockdown of Runx2 (Figure 4.4A) in a chondrocytic cell line that expresses high levels of Runx2 during proliferation resulted in no changes to pre-rRNA or 28S levels, although infection with virus alone caused a decrease in both levels (Figure 4.4B).

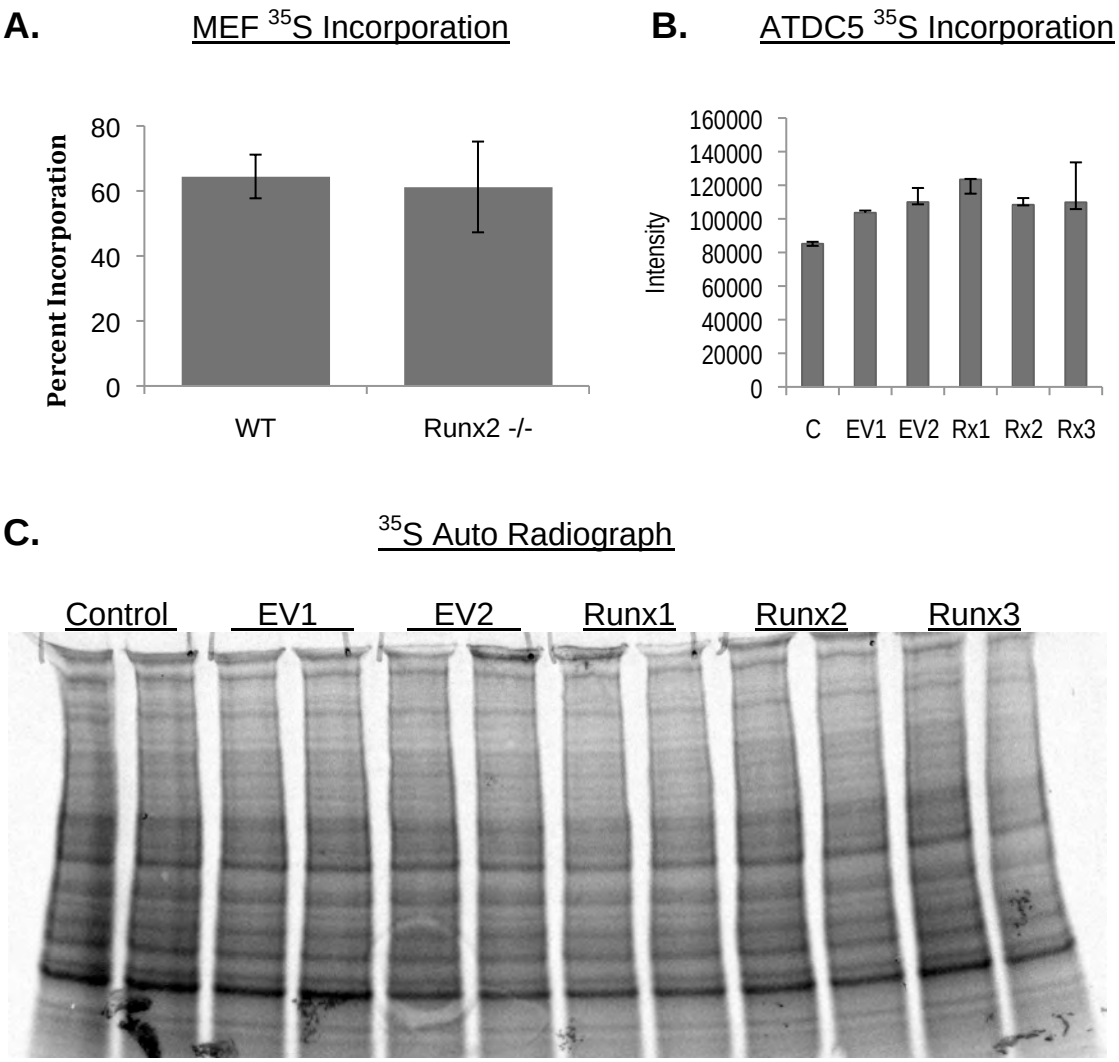

Figure 4.3: Runx Proteins do not Affect Global Protein Synthesis in Chondrogenic Cells
(A) Percent of ^{35}S incorporation into wild type or Runx2 -/- MEFs after a 30-minute ^{35}S-Met pulse. Graph represents one independent experiment, error bars represent standard deviation of triplicate samples. (B) Quantitation of autoradiograph shown in (C). (C) Autoradiograph of ^{35}S incorporation into ATDC5 cells transfected with empty vector controls (EV1 = backbone for Runx1 and Runx3 overexpression, EV2 = backbone for Runx2 overexpression), Runx1, Runx2 or Runx3 protein.

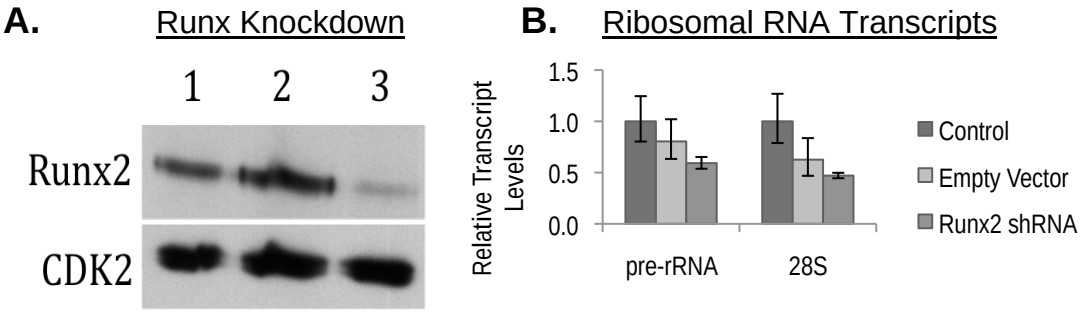

Figure 4.4: Runx2 Downregulation does not affect Levels of Protein Synthesis Machinery
(A) Western blot showing knockdown of Runx2 in N1511 cells. Lane 1 – Control, Lane 2 – Empty Vector, Lane 3 – Runx2 shRNA. (B) Quantitative RT-PCR analysis of 28S and pre-rRNA transcript levels after knockdown of Runx2 in N1511 cells. Values were normalized to mCox and expressed relative to control levels. Graph is from 1 independent experiment and error bars represent standard deviation of duplicate samples

Runx Proteins are not Directly Associated with rDNA Repeats or UBF in a Chondrogenic Cell Line

To further confirm the absence of Runx control of protein synthesis in chondrocytes, it is necessary to demonstrate that Runx is not associated with ribosomal DNA repeats, or with Upstream Binding Factor (UBF) which is essential for the control of all RNA PolI-mediated gene transcription. Chromatin immunoprecipitation analysis demonstrates that Runx proteins are not bound to ribosomal DNA repeats at any stage of chondrogenesis, although pulldown with UBF shows robust enrichment of between 3 and 7.5 fold over input levels, depending on the stage of chondrocyte maturation (Figure 4.5A). In co-immunoprecipitation experiments using endogenous Runx2 and UBF, no

association of these two proteins is observed (Figure 4.5B). These data together provide evidence that Runx proteins do not associate with protein synthesis machinery during chondrogenesis, indicating that global protein synthesis may be under the control of a different protein or group of proteins during chondrocyte maturation. Interestingly, pre-rRNA and 28S levels are downregulated during the transition from proliferating to pre-hypertrophic chondrocyte (Figure 4.5C) and that UBF binding to rDNA repeats follows the same pattern (Figure 4.5A). These experiments are preliminary studies and were not repeated; however they may indicate that there are higher rates of protein synthesis in proliferating and hypertrophic chondrocytes when compared to pre-hypertrophic chondrocytes.

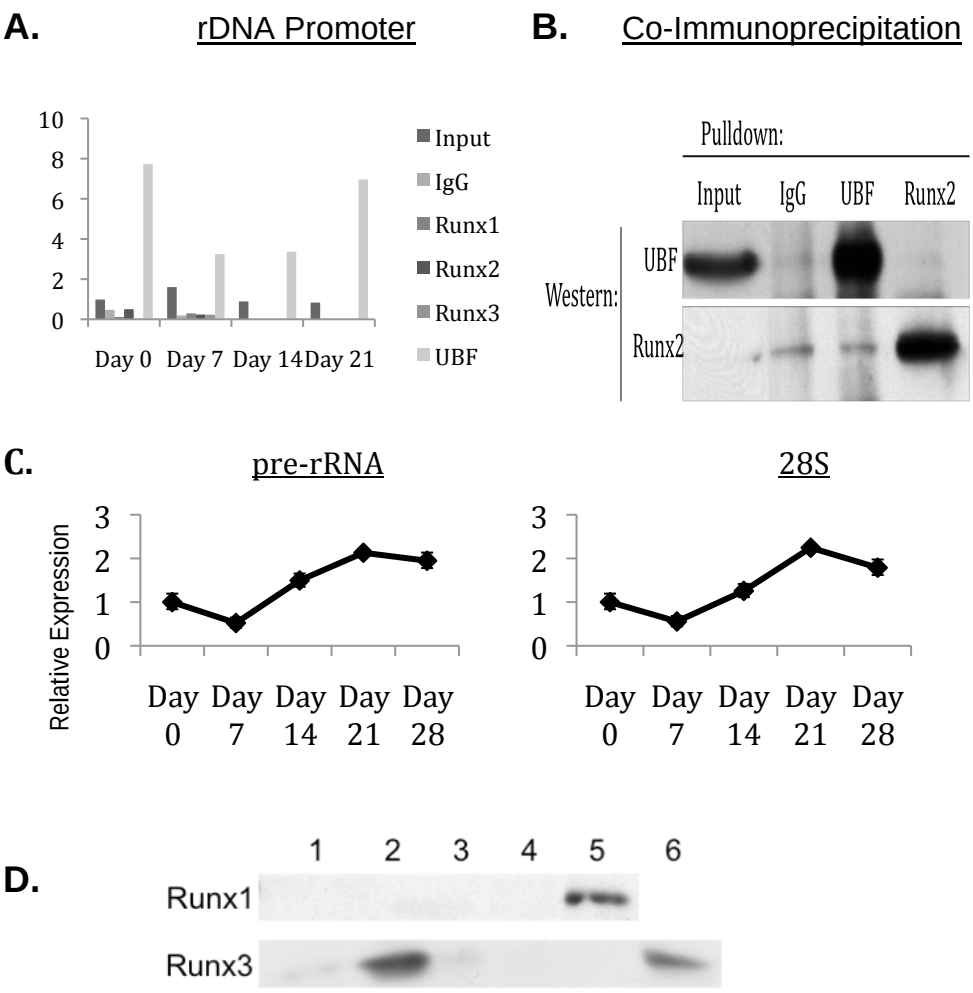

Figure 4.5: Runx Proteins do not Associate with Protein Synthesis Machinery in Chondrocytes

(A) ChIP assessing the presence of Runx proteins and UBF on rDNA repeats throughout chondrogenesis. Values are expressed as enrichment over Day 0 Input. Graph represents one independent experiment. (B) Western blot after immunoprecipitation with UBF, Runx2, or an IgG control. (C) Quantitative RT-PCR analysis showing expression of ribosomal biogenesis markers during ATDC5 differentiation. Values are normalized to mCOX and expressed relative to day 0 values. Graphs represent one independent experiment and error bars represent standard deviation of replicate samples. (D) Western blot data showing pulldown of Runx1 (top) and Runx3 (Bottom) using various Runx antibodies under ChIP conditions. Antibodies used for pulldown are as follows: Runx1; Lane 1 – IgG, Lane 2 – Calbiochem Anti-AML1/RHD (Ab-2), Lane 3 – Cell Signaling Technologies AML1 #4334, Lane 4 – Active Motif AML1 # 39000, Lane 5 – Abcam Runx1 ab50541, Lane 6 – Blank. Runx3; Lane 1 – IgG, Lane 2 Abnova Runx3 #11905, Lane 3 – Abnova Runx3 #49117, Lane 4 – Oncogene AML2 Ab1, Lane 5 – Abcam Runx1 ab50541, Lane 6 – Santa Cruz Runx3 H50.

Runx2 forms distinct foci on metaphase chromosomes.

All three Runx proteins epigenetically regulate their target genes by remaining bound to their promoters throughout mitosis (Runx1 in hematopoietic cells, Runx2 in osteoblasts, and Runx3 in intestinal cells) [122, 123, 134]. To determine if this phenomenon occurs in chondrocytes, immunoflourescense analysis was done on confluent ATDC5 cells to visualize mitotic cells in an untreated proliferating culture. Figure 4.6 shows ATDC5 cells during interphase or mitosis, after immunostaining with an antibody to either Runx1, 2 or 3. Despite punctate foci in interphase cells (bottom panel) neither Runx1 nor Runx3 remains bound to chromosomes during mitosis (top panel); however, distinct Runx2 foci are observed on mitotic chromosomes (Figure 4.6), indicating that Runx2, but not Runx1 or Runx3, is in a position to epigenetically regulate its target genes in a chondrogenic cell line by remaining bound to its target genes throughout the cell cycle, potentially poising then for transcription upon exit from mitosis.

A. Runx Immunofluorescense

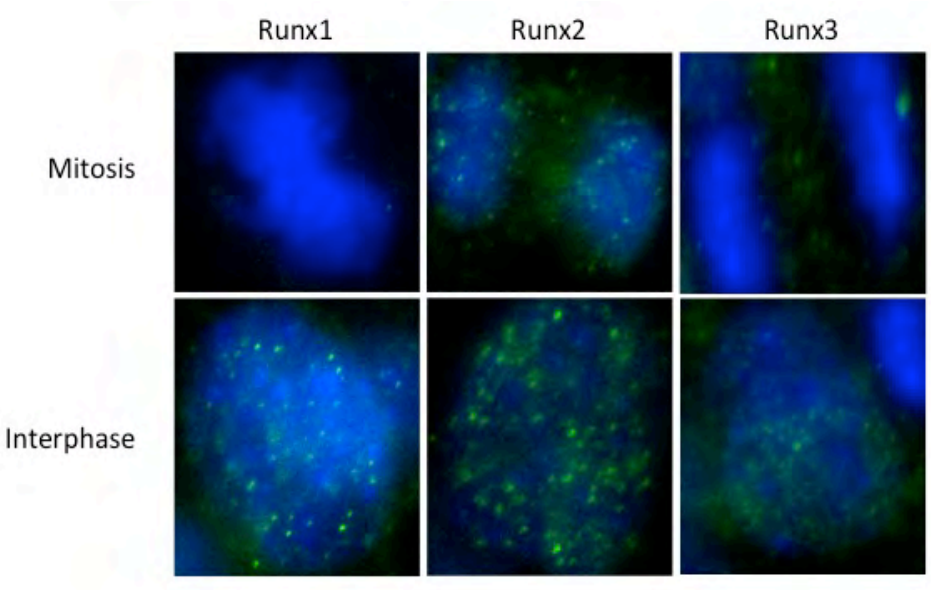

B. Runx2 Metaphase Spread

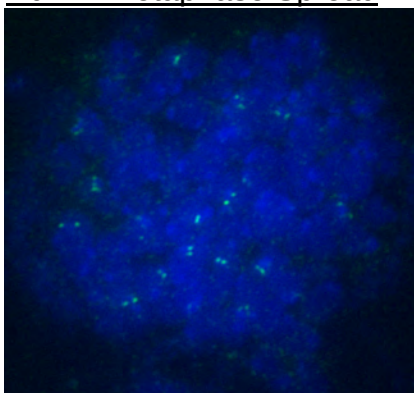

Figure 4.6: Runx2, but not Runx1 or Runx3, remains Bound to DNA during Mitosis
(A) Immunoflourescense of ATDC5 cells in mitosis (top panel) or interphase (bottom panel). Note the presence of Runx proteins [95] in interphase nuclei but the absence of Runx1 and Runx3 from mitotic chromosomes (blue=DAPI to detect chromosomes (B) Metaphase spread of N1511 cells showing distinct foci of Runx2 [95] on mitotic chromosomes (blue).

Conclusion

These preliminary experiments were conducted to determine an appropriate cell line for the study of protein synthesis control by Runx proteins during chondrogenesis. In a number of *in vitro* chondrogenic systems, Runx proteins do not control global protein synthesis. Although no changes in protein synthesis are observed in ATDC5 cells, this observation cannot be generalized to the regulation of protein synthesis and proliferation *in vivo*. ATDC5 cells are derived from a teratocarcinoma [137], a cell line in which cell cycle regulation is already disrupted. The Runx2 knockdown studies were done on N1511 cells, a chondrocyte cell line derived from the rib cartilage of p53-/- mice [135]. Since p53 is able to inhibit protein synthesis, the absence of p53 may result in increased global protein synthesis rates in this cell line at baseline [140]. This may be why Runx2 knockdown did not affect protein synthesis rates in this cell line. The observation that MEFs derived from Runx2-/- mice have similar protein synthesis rates to wild type MEFs is consistent with the observation that proliferation rates are similar in wild type and Runx2-/- MEFs [141]. Thus, while Runx proteins do not control protein synthesis or cell proliferation in these *in vitro* chondrogenic culture systems, one cannot rule out the possibility that they regulate cell proliferation and protein synthesis *in vivo*. These studies may be more appropriate using primary chondrocytes.

During chondrocyte differentiation, pre-rRNA and 28S levels are downregulated during the transition from proliferating to pre-hypertrophic chondrocyte (Figure 4.5C). This is consistent with decreased binding of UBF to rDNA repeats (Figure 4.5A). Upon differentiation into hypertrophic-like chondrocytes, UBF binding to rDNA repeats is restored to the levels found in proliferating chondrocytes, and pre-rRNA and 28S levels are increased 2 fold over those of proliferating chondrocytes. This demonstrates that, in chondrocytes, levels of protein synthesis machinery are higher in proliferating and hypertrophic-like chondrocytes than they are in pre-hypertrophic chondrocytes. To correlate this finding with actual rates of protein synthesis, these experiments need to be repeated, and ^{35}S incorporation assays can be done on proliferating and hypertrophic chondrocytes to determine protein synthesis rates at each stage of chondrogenesis, in a cell that expresses the normal complement of proteins found in hypertrophic chondrocytes.

Exploratory studies designed to assess the presence of Runx proteins on metaphase chromosomes generated a promising result. Runx2 remained bound to chromosomes throughout the cell cycle in chondrocyte cell lines. Thus, Runx2 is in a position to serve an epigenetic function by “bookmarking” its target genes for transcription upon exit from mitosis. Further studies need to be carried out to determine exactly where Runx2 is bound, and whether or not it confers specific histone modifications to repress these target genes in proliferating chondrocytes while enhancing expression of genes at the hypertrophic stage.

CHAPTER V:

Discussion

Summary

This dissertation characterizes the expression of Runx1 in normal articular and osteoarthritic cartilage. The major findings of my thesis studies are the robust expression of Runx1 in superficial zone chondrocytes of articular cartilage, the physiological response of Runx1 to mechanical compression, and the expression of Runx1 in cells that form clusters in response to cartilage damage. In these chondrocyte populations, Runx1 is co-expressed with markers for mesenchymal progenitor cells, alluding to a possible protective role in cartilage tissue. Additionally, Runx1 is associated with markers of proliferation in OA cartilage. It appears that when cartilage tissue is damaged, a response occurs in Runx1 positive cells that have the potential to repopulate the surface. In pursuit of a molecular basis for these functions, the thesis studies addressed the potential for Runx1 in regulatory protein synthesis in chondrocytes. Using a candidate gene approach, many genes that are expressed during chondrogenesis were identified as having the potential to be regulated by Runx genes based on their promoter analysis. However, the small number of candidate genes chosen were not differentially regulated in response to the overexpression of Runx1 in a chondrocyte cell line.

Preliminary experiments were carried out to determine if Runx proteins have novel functions in chondrocytes; namely, global protein synthesis control and epigenetic regulation of target genes. Preliminary experiments in 3 different chondrocyte cell lines failed to associate Runx transcription factors with protein

synthesis control, indicating that either a better chondrocyte model should be used, or that a different transcription factor is responsible for protein synthesis control in the chondrocyte. Interestingly, a pilot study characterizing the expression of Runx proteins throughout the cell cycle in proliferating chondrocytes showed that Runx2 remains bound to mitotic chromosomes, indicating a possible epigenetic function of Runx2 in chondrocytes by "bookmarking" target genes for transcription upon entry into S phase.

The Expression of Runx1 in Superficial Zone Chondrocytes

A number of studies show that Runx1 is detected in pre-chondrocytes, in the mesenchymal condensations of developing cartilage tissue, in suture lines of the calvaria, and in the periosteum [75, 77, 78, 142]. In addition, Runx1 is also the only Runx protein expressed in the chondrocytes of permanent cartilage structures (articular cartilage, hyoid cartilage, xyphoid process) during development [75, 143]. Although Runx1 is essential for hematopoietic cell differentiation, and various mutations in the gene result in leukemias [83], the expression of Runx1 in cartilage tissue suggests a unique, non-hematopoietic, functional role for the protein. The studies carried out in this dissertation show that Runx1 is expressed in the superficial zone chondrocytes of normal articular cartilage, which is similar to its expression in epithelial linings [103]. The most robust Runx1 expression was restricted to the superficial zone, the 1-2 cell layer that is closest to the articular cartilage surface. This surface cell layer is different

from the middle and deep zones of articular cartilage in both morphology with respect to organization of collagen fibrils, and gene expression [97]. When cultured, cells of the superficial zone have higher rates of proliferation than cells of the deep and middle zones [92]. In addition, these superficial zone cells have been shown to express markers of mesenchymal progenitor cells such as Notch-1, Endoglin (CD105), ALCAM (CD166), and VCAM-1 (CD106) [97-99], although, other than VCAM-1, the co-expression of these other proteins with Runx1 in superficial zone chondrocytes was not performed. Runx1 is robustly expressed in the superficial zone cells and, in part, may be responsible for maintaining the phenotype of these cells. Laser capture microdissection is a technique that allows for very small amounts of tissue to be dissected and analyzed. Using this technique to separate superficial, middle, and deep zones of articular cartilage combined with RT-PCR and microarray analysis, it should be possible to identify genes that are present in each zone and quantitate the expression levels of Runx1, as well as MSC markers, in each of the zones.

Runx1 Expression in Osteoarthritic Cartilage

In human OA cartilage, an increase in Runx1 protein levels was observed on the medial side of a varus knee joint, which had damaged cartilage. It has been shown that varying degrees of varus alignment are mirrored by significant differences in medial and lateral stress distribution [144]. As stated previously, varying degrees of mechanical stress cause upregulation of a number of genes

that contribute to the pathogenesis of OA [23, 25]. Additionally, Runx1 is upregulated in response to mechanical loading in an *ex vivo* compression model using bovine articular cartilage. Many studies have documented changes in gene expression in response to articular cartilage compression, with genes differentially expressed under both dynamic and static compression conditions [33, 145-148]. While the expression of Runx1 under dynamic compression conditions was not studied, Runx1 mRNA is increased in as little as 6 hours after the induction of excess loads of static compression (Figure 2.2B). This finding is consistent with several previous studies showing the upregulation of pro-inflammatory cytokines and matrix metalloproteases (MMPs) under loading conditions [33, 149]. It is also known that under compression conditions cell proliferation is increased [100]. MMPs are direct transcriptional targets of Runx proteins [86]. Runx1 also activates genes that support cell differentiation and phenotype maintenance [83]. Thus, compression stimulated upregulation of Runx1 could either contribute to cartilage degeneration or potentially promote expansion of a progenitor cell population in an attempt to repopulate damaged cartilage as documented in previous studies, or both [150].

Striking changes in the expression and distribution of Runx1-positive cells were found in human OA and during disease progression in a mouse model of OA. This provides insight into possible mechanisms related to both degradation and attempted repair of damaged cartilage. Runx1 is expressed in “chondrocyte clones” in human OA and at lesion borders in damaged tissue, rather than a

general upregulation in all chondrocytes of diseased cartilage. Taken together, this expression pattern and the localization of Runx1 in the articular surface of normal cartilage suggests a function in protecting surface integrity and an attempt to increase chondrocyte numbers at the border of degenerating cartilage. Consistent with findings in human patients, the same pattern of Runx1 is observed in OA-like lesions in the mouse model. When monitored during disease progression, Runx1 first decreases in the immediate area of the developing lesion prior to cartilage fibrillation and degeneration. Following this stage, Runx1 positive clusters begin to form at the periphery of the spreading lesion. Given these findings, it is reasonable to hypothesize that Runx1 serves a protective function rather than contributing to cartilage degradation. Its association with MSC markers its and localization at the periphery of OA suggests that it is involved in cartilage regeneration. Further studies need to be done to elicit the exact role of Runx1 in OA cartilage. The most beneficial studies would involve inducing OA in mice overexpressing Runx1 in cartilage, or in mice with Runx1 absent from cartilage, to determine the progression of OA under the influence of altered Runx1 levels. If the above hypothesis is correct, mice with Runx1 upregulated in articular cartilage would show decreased progression of OA lesions when compared to wild-type mice, while mice lacking Runx1 in cartilage would show enhanced development of these lesions.

Runx1 Association with Proliferation and MSC Markers in OA Cartilage

The localization of Runx1 in both diseased OA cartilage and in normal cartilage is consistent with the expression of other markers that have been well characterized. Additionally, certain osteoarthritic “clones” have been shown to express markers for mesenchymal progenitor cells, including VCAM-1[96, 100, 101]. In mouse articular cartilage, VCAM-1 and Runx1 are co-expressed in chondrocytes in normal superficial zone cells as well as in chondrocyte clones in damaged tissue. These clones have also been shown to represent a proliferative cell population [20, 102]. Interestingly, these Runx-1, VCAM-1 expressing chondrocytes in OA cartilage also express proliferation markers such as PCNA and Ki-67. Together, these data indicate that the increase in Runx1 positive chondrocytes in osteoarthritic cartilage represents a proliferative response of a progenitor cell population in response to cartilage damage. However, *in vitro* studies in chondrocyte cell lines did not show a proliferative response to the overexpression of Runx1. This may be because the cell line that was used was derived from a mouse embryonal carcinoma and proliferated rapidly in monolayer. These cells were chosen because they represented a well-differentiated chondrocyte in culture, expressing high levels of Sox9. In contrast to N1511 cells, ATDC5 cells are not known to be deficient in p53, making them a more ideal cell line in which to study proliferation. Other studies in our laboratory show that Runx1 deficiency results in decreased proliferation in MEFs. This, taken with the characterization of Runx1 being co-expressed with markers for

mesenchymal progenitor cells, suggests that Runx1 may have a role in proliferation in chondroprogenitor cells, but not in committed chondrocytes. To confirm this, the MEF studies should be repeated. Additionally, overexpression and knockdown of Runx1 in primary chondrocytes may be able to induce changes in proliferation rates.

In contrast to the concept that the clones represent a proliferation of superficial zone cells, recent studies have suggested that cell clusters in lacunae near OA lesions represent migrated cells [151]. Reminiscent of mesenchymal cell condensations in forming neocartilage (e.g. the embryo anlagen), in which the cells express Runx1, the clones may represent both proliferating and migrated progenitor cells that are attempting to either limit the OA lesion or re-establish the normal cartilage border. Of interest, Runx1 has a role in the regulation of stem cell recruitment and proliferation for regeneration of hematopoietic stem cells and hair follicle stem cells [107, 152]. The finding of robust expression of Runx1 in a population of mesenchymal progenitor cell clusters suggests that Runx1 functions as a compensatory mechanism rather than a matrix-degrading component in response to compressive forces.

Protein Synthesis Control in the Chondrocyte

Although Runx1, Runx2, and Runx3 all bind to rDNA repeats known to regulate ribosomal gene transcription, preliminary experiments show that this novel mechanism of protein synthesis control does not take place in a number of chondrogenic cell lines *in vitro*. Recently, it was observed that other cell fate determining transcription factors regulate global protein synthesis in certain cell types. In myocytes, protein synthesis is regulated by the transcription factors MyoD and Mgn while in adipocytes it is regulated by C/EBP β [153]. If cell fate determining transcription factors are responsible for protein synthesis regulation in their respective cell types, it would follow that either Sox9 or Sox5/6 regulate protein synthesis during chondrocyte maturation.

The dynamic nature of the chondrocyte involves the transition from proliferation to hypertrophy with a subset of stage-specific genes expressed at each stage of chondrocyte maturation. Sox9 is expressed in proliferating chondrocytes, but is downregulated during chondrocyte hypertrophy. If Sox9 were responsible for protein synthesis control at the onset of chondrogenesis, another transcription factor would have to take over upon downregulation of Sox9. The likely candidate for this is Runx2, as it is the transcription factor that is most important for the transition to chondrocyte hypertrophy.

The fact that Runx2-/- mice still exhibit hypertrophic chondrocytes in the tibia/fibula and radius/ulna, but Runx2/Runx3 double knockouts completely lack hypertrophic chondrocytes [67] suggests a functionally redundant role for these

proteins in the hypertrophic chondrocyte. It is possible that upon downregulation of Runx2, Runx3 is able to take over protein synthesis control, and this is why a phenotype is not seen upon downregulation of only Runx2. To test this hypothesis, these experiments can be repeated with Runx2/Runx3 double knockout cells. Additionally, all overexpression experiments were done in proliferating chondrocytes, where it is possible that Sox9 is in control of protein synthesis. This set of experiments can be repeated by overexpressing Sox9 in chondrocyte cell lines to assess changes in rates of global protein synthesis and levels of protein synthesis machinery. The lack of Runx2 or Runx3 binding to rDNA repeats in hypertrophic chondrocytes suggests that neither Runx2 nor Runx3 regulate rDNA transcription during chondrocyte hypertrophy. However, this one observation is not enough to rule out the possibility that they contribute to global protein synthesis control during late stage chondrogenesis.

Because there are few good cell models for culturing primary chondrocytes and maintaining them as either proliferating or hypertrophic chondrocytes, the protein synthesis question is one that is difficult to assess. A combination of laser capture microdissection with chromatin immunoprecipitation would determine if Runx proteins were bound to rDNA promoters in each subpopulation of chondrocytes. Additionally, ChIP experiments on MEFs undergoing chondrogenic differentiation in micromass cultures can be done to determine which transcription factors bind rDNA repeats at each stage of chondrogenesis. Again, since ATDC5 cells are not derived from a primary

chondrocyte source, regulation of protein synthesis control may be altered in this cell line. While this cell line was an appropriate choice for preliminary experiments because of the ease of transfection and committed chondrocyte phenotype, negative results must be confirmed in primary chondrocytes.

Runx and Epigenetics in the Chondrocyte

In interphase ATDC5 cells, Runx1, 2, and 3 all exhibit characteristic distribution in punctate foci throughout the nucleus. In stark contrast, mitotic chromosomes exhibit complete absence of Runx1 and Runx3, while Runx2 foci persist throughout mitosis. In addition to epigenetically regulating target genes by controlling histone modifications, the retention of Runx2 on its target genes throughout mitosis is hypothesized to be a novel epigenetic mechanism by which target genes are poised for transcription upon exit from mitosis [134]. Although most known Runx2 chondrogenic target genes are expressed in post-proliferative hypertrophic chondrocytes, Runx2 is found on mitotic chromosomes in a committed, but proliferating chondrocyte. Although it is not known exactly which genes Runx2 is bound to during mitosis in ATDC5 or N1511 cells, it is possible that Runx2 is on the promoters of genes involved in chondrocyte hypertrophy, poising them for transcription upon exit from the cell cycle and entry into the hypertrophic stage of chondrocyte maturation. The binding of a transcription factor to genes in proliferating chondrocytes, although they are not expressed until hypertrophy, would represent an entirely new level of epigenetic regulation.

FISH experiments would be able determine the genes that are associated with the Runx foci on mitotic chromosomes, first by identifying the specific chromosomes to which Runx2 is bound, then by designing specific probes to Runx target genes known to reside on those chromosomes. The absence of Runx1 and Runx3 on the metaphase chromosomes of these chondrogenic cell lines suggests that these proteins may not function to “bookmark” genes as a means of epigenetic regulation. This is not to say that Runx1 and Runx3 do not function epigenetically in chondrocytes. It is possible that all three Runx proteins confer specific histone modifications to their target genes in chondrocytes. This hypothesis can be tested with ChIP on Chip experiments. As in regular chromatin immunoprecipitation experiments, Runx proteins would be crosslinked with the DNA sequences to which they were bound and isolated by immunoprecipitation. Instead of analyzing the chromatin by RT-PCR, the chromatin can be subjected to microarray analysis to determine direct targets of Runx proteins in chondrogenesis. When target genes are identified, ChIP/re-ChIP experiments can be done, first using a Runx antibody for immunoprecipitation, and then using a modified histone antibody to determine the specific histone modifications with which Runx proteins are associated on the promoters of their target genes. To further ascertain the role of Runx proteins in conferring specific histone modifications in chondrocytes, knockdown studies can be performed to determine if the specific histone modifications identified in the presence of Runx proteins still persist in their absence.

Conclusions

This dissertation characterized the expression of Runx1 in normal and osteoarthritic cartilage, and began to explore potential functions of Runx1 in healthy cartilage and during disease states. Identification of downstream Runx1 target genes, in addition to experimental induction of osteoarthritis in mice either deficient in or overexpressing Runx1 in cartilage, will help ascertain whether Runx1 has a protective effect in cartilage. Additionally, identifying the novel mechanisms by which Runx proteins regulate cartilage maturation will give a greater understanding of the molecular mechanisms that differentiate growth plate chondrocytes from articular chondrocytes, as well as characterizing different sub-populations of articular chondrocytes that may respond differently to the cartilage damage that is characteristic of osteoarthritis. A greater understanding of the contribution of Runx proteins to chondrogenesis could lead to the discovery of potential drug targets to attenuate the severity of cartilage disease, decreasing the need for surgery and improving the quality of life for people with disorders involving chondrocyte misregulation.

Bibliography

1. Kotlarz, H., C.L. Gunnarsson, H. Fang, and J.A. Rizzo, "Insurer and out-of-Pocket Costs of Osteoarthritis in the Us: Evidence from National Survey Data". *Arthritis and rheumatism*, 2009. 60(12): p. 3546-53.
2. Joshua J. Jacobs, G.A., John-Erik Bell, Stuart Weinstein, John Dormans, Steve Gnatz, Nancy Lane, *The Burden of Musculoskeletal Diseases in the United States*2008: American Academy of Orthopaedic Surgeons.
3. Blagojevic, M., C. Jinks, A. Jeffery, and K.P. Jordan, "Risk Factors for Onset of Osteoarthritis of the Knee in Older Adults: A Systematic Review and Meta-Analysis". *Osteoarthritis and cartilage / OARS, Osteoarthritis Research Society*, 2010. 18(1): p. 24-33.
4. Jinks, C., K. Jordan, and P. Croft, "Osteoarthritis as a Public Health Problem: The Impact of Developing Knee Pain on Physical Function in Adults Living in the Community: (Knest 3)". *Rheumatology*, 2007. 46(5): p. 877-81.
5. Issa, R.I. and T.M. Griffin, "Pathobiology of Obesity and Osteoarthritis: Integrating Biomechanics and Inflammation". *Pathobiol Aging Age Relat Dis*, 2012. 2(2012).
6. Kerkhof, H.J., M. Doherty, N.K. Arden, S.B. Abramson, M. Attur, S.D. Bos, C. Cooper, E.M. Dennison, S.A. Doherty, E. Evangelou, D.J. Hart, A. Hofman, K. Javaid, I. Kerna, K. Kisand, M. Kloppenburg, S. Krasnokutsky, R.A. Maciewicz, I. Meulenbelt, K.R. Muir, F. Rivadeneira, J. Samuels, M. Sezgin, E. Slagboom, A.J. Smith, T.D. Spector, A. Tamm, A. Tamm, A.G. Uitterlinden, M. Wheeler, G. Zhai, W. Zhang, J.B. van Meurs, and A.M. Valdes, "Large-Scale Meta-Analysis of Interleukin-1 Beta and Interleukin-1 Receptor Antagonist Polymorphisms on Risk of Radiographic Hip and Knee Osteoarthritis and Severity of Knee Osteoarthritis". *Osteoarthritis Cartilage*, 2011. 19(3): p. 265-71.
7. Hui, W., G.J. Litherland, M.S. Elias, G.I. Kitson, T.E. Cawston, A.D. Rowan, and D.A. Young, "Leptin Produced by Joint White Adipose Tissue Induces Cartilage Degradation Via Upregulation and Activation of Matrix Metalloproteinases". *Ann Rheum Dis*, 2012. 71(3): p. 455-62.
8. Felson, D.T., J. Goggins, J. Niu, Y. Zhang, and D.J. Hunter, "The Effect of Body Weight on Progression of Knee Osteoarthritis Is Dependent on Alignment". *Arthritis Rheum*, 2004. 50(12): p. 3904-9.
9. Sharma, L., C. Lou, S. Cahue, and D.D. Dunlop, "The Mechanism of the Effect of Obesity in Knee Osteoarthritis: The Mediating Role of Malalignment". *Arthritis Rheum*, 2000. 43(3): p. 568-75.
10. Englund, M., A. Guermazi, D. Gale, D.J. Hunter, P. Aliabadi, M. Clancy, and D.T. Felson, "Incidental Meniscal Findings on Knee Mri in Middle-Aged and Elderly Persons". *N Engl J Med*, 2008. 359(11): p. 1108-15.

11. Ruiz-Romero, C., V. Carreira, I. Rego, S. Remeseiro, M.J. Lopez-Armada, and F.J. Blanco, "Proteomic Analysis of Human Osteoarthritic Chondrocytes Reveals Protein Changes in Stress and Glycolysis". *Proteomics*, 2008. 8(3): p. 495-507.
12. Goekoop, R.J., M. Kloppenburg, H.M. Kroon, M. Frolich, T.W. Huizinga, R.G. Westendorp, and J. Gussekloo, "Low Innate Production of Interleukin-1beta and Interleukin-6 Is Associated with the Absence of Osteoarthritis in Old Age". *Osteoarthritis Cartilage*, 2010. 18(7): p. 942-7.
13. Sampson, E.R., M.J. Hilton, Y. Tian, D. Chen, E.M. Schwarz, R.A. Mooney, S.V. Bukata, R.J. O'Keefe, H. Awad, J.E. Puzas, R.N. Rosier, and M.J. Zuscik, "Teriparatide as a Chondroregenerative Therapy for Injury-Induced Osteoarthritis". *Sci Transl Med*, 2011. 3(101): p. 101ra93.
14. Stubendorff, J.J., E. Lammentausta, A. Struglics, L. Lindberg, D. Heinegard, and L.E. Dahlberg, "Is Cartilage Sgag Content Related to Early Changes in Cartilage Disease? Implications for Interpretation of Dgemric". *Osteoarthritis and cartilage / OARS, Osteoarthritis Research Society*, 2012. 20(5): p. 396-404.
15. Verkleij, S.P., P.A. Luijsterburg, A.M. Bohnen, B.W. Koes, and S.M. Bierma-Zeinstra, "Nsaids Vs Acetaminophen in Knee and Hip Osteoarthritis: A Systematic Review Regarding Heterogeneity Influencing the Outcomes". *Osteoarthritis and cartilage / OARS, Osteoarthritis Research Society*, 2011. 19(8): p. 921-9.
16. Singh, J.A., "Stem Cells and Other Innovative Intra-Articular Therapies for Osteoarthritis: What Does the Future Hold?". *BMC Med*, 2012. 10: p. 44.
17. Loughlin, J., "Genetics of Osteoarthritis". *Current opinion in rheumatology*, 2011. 23(5): p. 479-83.
18. Baker-Lepain, J.C., J.A. Lynch, N. Parimi, C.E. McCulloch, M.C. Nevitt, M. Corr, and N.E. Lane, "Variant Alleles of the Wnt Antagonist Frzb Are Determinants of Hip Shape and Modify the Relationship between Hip Shape and Osteoarthritis". *Arthritis and rheumatism*, 2012. 64(5): p. 1457-65.
19. Goldring, M.B. and S.R. Goldring, "Articular Cartilage and Subchondral Bone in the Pathogenesis of Osteoarthritis". *Annals of the New York Academy of Sciences*, 2010. 1192: p. 230-7.
20. Pfander, D., B. Swoboda, and T. Kirsch, "Expression of Early and Late Differentiation Markers (Proliferating Cell Nuclear Antigen, Syndecan-3, Annexin Vi, and Alkaline Phosphatase) by Human Osteoarthritic Chondrocytes". *The American journal of pathology*, 2001. 159(5): p. 1777-83.
21. von der Mark, K., T. Kirsch, A. Nerlich, A. Kuss, G. Weseloh, K. Gluckert, and H. Stoss, "Type X Collagen Synthesis in Human Osteoarthritic Cartilage. Indication of Chondrocyte Hypertrophy". *Arthritis and rheumatism*, 1992. 35(7): p. 806-11.
22. Matyas, J.R., M.E. Adams, D. Huang, and L.J. Sandell, "Discoordinate Gene Expression of Aggrecan and Type Ii Collagen in Experimental Osteoarthritis". *Arthritis and rheumatism*, 1995. 38(3): p. 420-5.

23. Mitchell, P.G., H.A. Magna, L.M. Reeves, L.L. Lopresti-Morrow, S.A. Yocum, P.J. Rosner, K.F. Geoghegan, and J.E. Hambor, "Cloning, Expression, and Type Ii Collagenolytic Activity of Matrix Metalloproteinase-13 from Human Osteoarthritic Cartilage". *The Journal of clinical investigation*, 1996. 97(3): p. 761-8.
24. Bayliss, M.T., S. Hutton, J. Hayward, and R.A. Maciewicz, "Distribution of Aggrecanase (Adamts 4/5) Cleavage Products in Normal and Osteoarthritic Human Articular Cartilage: The Influence of Age, Topography and Zone of Tissue". *Osteoarthritis and cartilage / OARS, Osteoarthritis Research Society*, 2001. 9(6): p. 553-60.
25. Lin, A.C., B.L. Seeto, J.M. Bartoszko, M.A. Khoury, H. Whetstone, L. Ho, C. Hsu, S.A. Ali, and B.A. Alman, "Modulating Hedgehog Signaling Can Attenuate the Severity of Osteoarthritis". *Nature medicine*, 2009. 15(12): p. 1421-5.
26. Kamekura, S., Y. Kawasaki, K. Hoshi, T. Shimoaka, H. Chikuda, Z. Maruyama, T. Komori, S. Sato, S. Takeda, G. Karsenty, K. Nakamura, U.I. Chung, and H. Kawaguchi, "Contribution of Runt-Related Transcription Factor 2 to the Pathogenesis of Osteoarthritis in Mice after Induction of Knee Joint Instability". *Arthritis and rheumatism*, 2006. 54(8): p. 2462-70.
27. Zuscik, M.J., J.F. Baden, Q. Wu, T.J. Sheu, E.M. Schwarz, H. Drissi, R.J. O'Keefe, J.E. Puzas, and R.N. Rosier, "5-Azacytidine Alters Tgf-Beta and Bmp Signaling and Induces Maturation in Articular Chondrocytes". *Journal of cellular biochemistry*, 2004. 92(2): p. 316-31.
28. Barter, M.J., C. Bui, and D.A. Young, "Epigenetic Mechanisms in Cartilage and Osteoarthritis: DNA Methylation, Histone Modifications and Micrornas". *Osteoarthritis and cartilage / OARS, Osteoarthritis Research Society*, 2012.
29. Yu, C., W.P. Chen, and X.H. Wang, "Microrna in Osteoarthritis". *J Int Med Res*, 2011. 39(1): p. 1-9.
30. Millward-Sadler, S.J., M.O. Wright, L.W. Davies, G. Nuki, and D.M. Salter, "Mechanotransduction Via Integrins and Interleukin-4 Results in Altered Aggrecan and Matrix Metalloproteinase 3 Gene Expression in Normal, but Not Osteoarthritic, Human Articular Chondrocytes". *Arthritis and rheumatism*, 2000. 43(9): p. 2091-9.
31. Goldring, M.B. and K.B. Marcu, "Cartilage Homeostasis in Health and Rheumatic Diseases". *Arthritis research & therapy*, 2009. 11(3): p. 224.
32. Jalali, S., M.A. del Pozo, K. Chen, H. Miao, Y. Li, M.A. Schwartz, J.Y. Shyy, and S. Chien, "Integrin-Mediated Mechanotransduction Requires Its Dynamic Interaction with Specific Extracellular Matrix (Ecm) Ligands". *Proceedings of the National Academy of Sciences of the United States of America*, 2001. 98(3): p. 1042-6.
33. Fitzgerald, J.B., M. Jin, D.H. Chai, P. Siparsky, P. Fanning, and A.J. Grodzinsky, "Shear- and Compression-Induced Chondrocyte Transcription Requires Mapk Activation in Cartilage Explants". *The Journal of biological chemistry*, 2008. 283(11): p. 6735-43.

34. Cohen, M.M., Jr., "Perspectives on Runx Genes: An Update". *American journal of medical genetics. Part A*, 2009. 149A(12): p. 2629-46.
35. Wang, Q., T. Stacy, M. Binder, M. Marin-Padilla, A.H. Sharpe, and N.A. Speck, "Disruption of the Cbfa2 Gene Causes Necrosis and Hemorrhaging in the Central Nervous System and Blocks Definitive Hematopoiesis". *Proceedings of the National Academy of Sciences of the United States of America*, 1996. 93(8): p. 3444-9.
36. Komori, T., H. Yagi, S. Nomura, A. Yamaguchi, K. Sasaki, K. Deguchi, Y. Shimizu, R.T. Bronson, Y.H. Gao, M. Inada, M. Sato, R. Okamoto, Y. Kitamura, S. Yoshiki, and T. Kishimoto, "Targeted Disruption of Cbfa1 Results in a Complete Lack of Bone Formation Owing to Maturational Arrest of Osteoblasts". *Cell*, 1997. 89(5): p. 755-64.
37. Lian, J.B., J.L. Stein, G.S. Stein, A.J. van Wijnen, M. Montecino, A. Javed, S. Gutierrez, J. Shen, S.K. Zaidi, and H. Drissi, "Runx2/Cbfa1 Functions: Diverse Regulation of Gene Transcription by Chromatin Remodeling and Co-Regulatory Protein Interactions". *Connect Tissue Res*, 2003. 44 Suppl 1: p. 141-8.
38. Li, Q.L., K. Ito, C. Sakakura, H. Fukamachi, K. Inoue, X.Z. Chi, K.Y. Lee, S. Nomura, C.W. Lee, S.B. Han, H.M. Kim, W.J. Kim, H. Yamamoto, N. Yamashita, T. Yano, T. Ikeda, S. Itohara, J. Inazawa, T. Abe, A. Hagiwara, H. Yamagishi, A. Ooe, A. Kaneda, T. Sugimura, T. Ushijima, S.C. Bae, and Y. Ito, "Causal Relationship between the Loss of Runx3 Expression and Gastric Cancer". *Cell*, 2002. 109(1): p. 113-24.
39. Levanon, D., D. Bettoun, C. Harris-Cerruti, E. Woolf, V. Negreanu, R. Eilam, Y. Bernstein, D. Goldenberg, C. Xiao, M. Fliegauf, E. Kremer, F. Otto, O. Brenner, A. Lev-Tov, and Y. Groner, "The Runx3 Transcription Factor Regulates Development and Survival of Trkc Dorsal Root Ganglia Neurons". *The EMBO journal*, 2002. 21(13): p. 3454-63.
40. Song, W.J., M.G. Sullivan, R.D. Legare, S. Hutchings, X. Tan, D. Kufrin, J. Ratajczak, I.C. Resende, C. Haworth, R. Hock, M. Loh, C. Felix, D.C. Roy, L. Busque, D. Kurnit, C. Willman, A.M. Gewirtz, N.A. Speck, J.H. Bushweller, F.P. Li, K. Gardiner, M. Poncz, J.M. Maris, and D.G. Gilliland, "Haploinsufficiency of Cbfa2 Causes Familial Thrombocytopenia with Propensity to Develop Acute Myelogenous Leukaemia". *Nature genetics*, 1999. 23(2): p. 166-75.
41. Mundlos, S., J.B. Mulliken, D.L. Abramson, M.L. Warman, J.H. Knoll, and B.R. Olsen, "Genetic Mapping of Cleidocranial Dysplasia and Evidence of a Microdeletion in One Family". *Human molecular genetics*, 1995. 4(1): p. 71-5.
42. Mundlos, S., F. Otto, C. Mundlos, J.B. Mulliken, A.S. Aylsworth, S. Albright, D. Lindhout, W.G. Cole, W. Henn, J.H. Knoll, M.J. Owen, R. Mertelsmann, B.U. Zabel, and B.R. Olsen, "Mutations Involving the Transcription Factor Cbfa1 Cause Cleidocranial Dysplasia". *Cell*, 1997. 89(5): p. 773-9.
43. Look, A.T., "Oncogenic Transcription Factors in the Human Acute Leukemias". *Science*, 1997. 278(5340): p. 1059-64.

44. Miyoshi, H., K. Shimizu, T. Kozu, N. Maseki, Y. Kaneko, and M. Ohki, "T(8;21) Breakpoints on Chromosome 21 in Acute Myeloid Leukemia Are Clustered within a Limited Region of a Single Gene, Aml1". *Proceedings of the National Academy of Sciences of the United States of America*, 1991. 88(23): p. 10431-4.
45. Golub, T.R., G.F. Barker, S.K. Bohlander, S.W. Hiebert, D.C. Ward, P. Bray-Ward, E. Morgan, S.C. Raimondi, J.D. Rowley, and D.G. Gilliland, "Fusion of the Tel Gene on 12p13 to the Aml1 Gene on 21q22 in Acute Lymphoblastic Leukemia". *Proceedings of the National Academy of Sciences of the United States of America*, 1995. 92(11): p. 4917-21.
46. Brubaker, K.D., R.L. Vessella, L.G. Brown, and E. Corey, "Prostate Cancer Expression of Runt-Domain Transcription Factor Runx2, a Key Regulator of Osteoblast Differentiation and Function". *The Prostate*, 2003. 56(1): p. 13-22.
47. Barnes, G.L., K.E. Hebert, M. Kamal, A. Javed, T.A. Einhorn, J.B. Lian, G.S. Stein, and L.C. Gerstenfeld, "Fidelity of Runx2 Activity in Breast Cancer Cells Is Required for the Generation of Metastases-Associated Osteolytic Disease". *Cancer research*, 2004. 64(13): p. 4506-13.
48. Akech, J., J.J. Wixted, K. Bedard, M. van der Deen, S. Hussain, T.A. Guise, A.J. van Wijnen, J.L. Stein, L.R. Languino, D.C. Altieri, J. Pratap, E. Keller, G.S. Stein, and J.B. Lian, "Runx2 Association with Progression of Prostate Cancer in Patients: Mechanisms Mediating Bone Osteolysis and Osteoblastic Metastatic Lesions". *Oncogene*, 2010. 29(6): p. 811-21.
49. Pratap, J., J.J. Wixted, T. Gaur, S.K. Zaidi, J. Dobson, K.D. Gokul, S. Hussain, A.J. van Wijnen, J.L. Stein, G.S. Stein, and J.B. Lian, "Runx2 Transcriptional Activation of Indian Hedgehog and a Downstream Bone Metastatic Pathway in Breast Cancer Cells". *Cancer research*, 2008. 68(19): p. 7795-802.
50. Kim, T.Y., H.S. Jong, Y. Jung, G.H. Kang, and Y.J. Bang, "DNA Hypermethylation in Gastric Cancer". *Alimentary pharmacology & therapeutics*, 2004. 20 Suppl 1: p. 131-42.
51. Li, J., J. Kleeff, A. Guweidhi, I. Esposito, P.O. Berberat, T. Giese, M.W. Buchler, and H. Friess, "Runx3 Expression in Primary and Metastatic Pancreatic Cancer". *Journal of clinical pathology*, 2004. 57(3): p. 294-9.
52. Mackie, E.J., L. Tatarczuch, and M. Mirams, "The Growth Plate Chondrocyte and Endochondral Ossification". *The Journal of endocrinology*, 2011.
53. Pazzaglia, U.E., G. Beluffi, A. Benetti, M.P. Bondioni, and G. Zarattini, "A Review of the Actual Knowledge of the Processes Governing Growth and Development of Long Bones". *Fetal and pediatric pathology*, 2011. 30(3): p. 199-208.
54. Bi, W., J.M. Deng, Z. Zhang, R.R. Behringer, and B. de Crombrugghe, "Sox9 Is Required for Cartilage Formation". *Nature genetics*, 1999. 22(1): p. 85-9.
55. Bi, W., W. Huang, D.J. Whitworth, J.M. Deng, Z. Zhang, R.R. Behringer, and B. de Crombrugghe, "Haploinsufficiency of Sox9 Results in Defective Cartilage Primordia and Premature Skeletal Mineralization". *Proceedings of the*

National Academy of Sciences of the United States of America, 2001. 98(12): p. 6698-703.

56. Smits, P., P. Li, J. Mandel, Z. Zhang, J.M. Deng, R.R. Behringer, B. de Crombrugghe, and V. Lefebvre, "The Transcription Factors L-Sox5 and Sox6 Are Essential for Cartilage Formation". *Developmental cell*, 2001. 1(2): p. 277-90.
57. St-Jacques, B., M. Hammerschmidt, and A.P. McMahon, "Indian Hedgehog Signaling Regulates Proliferation and Differentiation of Chondrocytes and Is Essential for Bone Formation". *Genes & development*, 1999. 13(16): p. 2072-86.
58. Maeda, Y., E. Nakamura, M.T. Nguyen, L.J. Suva, F.L. Swain, M.S. Razzaque, S. Mackem, and B. Lanske, "Indian Hedgehog Produced by Postnatal Chondrocytes Is Essential for Maintaining a Growth Plate and Trabecular Bone". *Proceedings of the National Academy of Sciences of the United States of America*, 2007. 104(15): p. 6382-7.
59. Burdan, F., J. Szumilo, A. Korobowicz, R. Farooquee, S. Patel, A. Patel, A. Dave, M. Szumilo, M. Solecki, R. Klepacz, and J. Dudka, "Morphology and Physiology of the Epiphyseal Growth Plate". *Folia Histochem Cytobiol*, 2009. 47(1): p. 5-16.
60. Retting, K.N., B. Song, B.S. Yoon, and K.M. Lyons, "Bmp Canonical Smad Signaling through Smad1 and Smad5 Is Required for Endochondral Bone Formation". *Development*, 2009. 136(7): p. 1093-104.
61. Yoon, B.S., R. Pogue, D.A. Ovchinnikov, I. Yoshii, Y. Mishina, R.R. Behringer, and K.M. Lyons, "Bmps Regulate Multiple Aspects of Growth-Plate Chondrogenesis through Opposing Actions on Fgf Pathways". *Development*, 2006. 133(23): p. 4667-78.
62. Pathi, S., J.B. Rutenberg, R.L. Johnson, and A. Vortkamp, "Interaction of Ihh and Bmp/Noggin Signaling During Cartilage Differentiation". *Developmental biology*, 1999. 209(2): p. 239-53.
63. van der Kraan, P.M., M.J. Goumans, E. Blaney Davidson, and P. ten Dijke, "Age-Dependent Alteration of Tgf-Beta Signalling in Osteoarthritis". *Cell and tissue research*, 2012. 347(1): p. 257-65.
64. Li, W., J. Fan, D. Banerjee, and J.R. Bertino, "Overexpression of P21(Waf1) Decreases G2-M Arrest and Apoptosis Induced by Paclitaxel in Human Sarcoma Cells Lacking Both P53 and Functional Rb Protein". *Molecular pharmacology*, 1999. 55(6): p. 1088-93.
65. Minina, E., C. Kreschel, M.C. Naski, D.M. Ornitz, and A. Vortkamp, "Interaction of Fgf, Ihh/Pthlh, and Bmp Signaling Integrates Chondrocyte Proliferation and Hypertrophic Differentiation". *Developmental cell*, 2002. 3(3): p. 439-49.
66. Inada, M., T. Yasui, S. Nomura, S. Miyake, K. Deguchi, M. Himeno, M. Sato, H. Yamagiwa, T. Kimura, N. Yasui, T. Ochi, N. Endo, Y. Kitamura, T. Kishimoto, and T. Komori, "Maturational Disturbance of Chondrocytes in Cbfa1-Deficient

Mice". *Developmental dynamics : an official publication of the American Association of Anatomists*, 1999. 214(4): p. 279-90.
67. Yoshida, C.A., H. Yamamoto, T. Fujita, T. Furuichi, K. Ito, K. Inoue, K. Yamana, A. Zanma, K. Takada, Y. Ito, and T. Komori, "Runx2 and Runx3 Are Essential for Chondrocyte Maturation, and Runx2 Regulates Limb Growth through Induction of Indian Hedgehog". *Genes & development*, 2004. 18(8): p. 952-63.
68. Liakhovitskaia, A., E. Lana-Elola, E. Stamateris, D.P. Rice, R.J. van 't Hof, and A. Medvinsky, "The Essential Requirement for Runx1 in the Development of the Sternum". *Developmental biology*, 2010. 340(2): p. 539-46.
69. Soung do, Y., L. Talebian, C.J. Matheny, R. Guzzo, M.E. Speck, J.R. Lieberman, N.A. Speck, and H. Drissi, "Runx1 Dose-Dependently Regulates Endochondral Ossification During Skeletal Development and Fracture Healing". *Journal of bone and mineral research : the official journal of the American Society for Bone and Mineral Research*, 2012. 27(7): p. 1585-97.
70. Spender, L.C., H.J. Whiteman, C.E. Karstegl, and P.J. Farrell, "Transcriptional Cross-Regulation of Runx1 by Runx3 in Human B Cells". *Oncogene*, 2005. 24(11): p. 1873-81.
71. Stricker, S., R. Fundele, A. Vortkamp, and S. Mundlos, "Role of Runx Genes in Chondrocyte Differentiation". *Developmental biology*, 2002. 245(1): p. 95-108.
72. Leboy, P., G. Grasso-Knight, M. D'Angelo, S.W. Volk, J.V. Lian, H. Drissi, G.S. Stein, and S.L. Adams, "Smad-Runx Interactions During Chondrocyte Maturation". *The Journal of bone and joint surgery. American volume*, 2001. 83-A Suppl 1(Pt 1): p. S15-22.
73. Higashikawa, A., T. Saito, T. Ikeda, S. Kamekura, N. Kawamura, A. Kan, Y. Oshima, S. Ohba, N. Ogata, K. Takeshita, K. Nakamura, U.I. Chung, and H. Kawaguchi, "Identification of the Core Element Responsive to Runt-Related Transcription Factor 2 in the Promoter of Human Type X Collagen Gene". *Arthritis and rheumatism*, 2009. 60(1): p. 166-78.
74. Hecht, J., V. Seitz, M. Urban, F. Wagner, P.N. Robinson, A. Stiege, C. Dieterich, U. Kornak, U. Wilkening, N. Brieske, C. Zwingman, A. Kidess, S. Stricker, and S. Mundlos, "Detection of Novel Skeletogenesis Target Genes by Comprehensive Analysis of a Runx2(-/-) Mouse Model". *Gene expression patterns : GEP*, 2007. 7(1-2): p. 102-12.
75. Lian, J.B., E. Balint, A. Javed, H. Drissi, R. Vitti, E.J. Quinlan, L. Zhang, A.J. Van Wijnen, J.L. Stein, N. Speck, and G.S. Stein, "Runx1/Aml1 Hematopoietic Transcription Factor Contributes to Skeletal Development in Vivo". *Journal of cellular physiology*, 2003. 196(2): p. 301-11.
76. Kimura, A., H. Inose, F. Yano, K. Fujita, T. Ikeda, S. Sato, M. Iwasaki, T. Jinno, K. Ae, S. Fukumoto, Y. Takeuchi, H. Itoh, T. Imamura, H. Kawaguchi, U.I. Chung, J.F. Martin, S. Iseki, K. Shinomiya, and S. Takeda, "Runx1 and Runx2 Cooperate During Sternal Morphogenesis". *Development*, 2010. 137(7): p. 1159-67.

77. Wang, Y., R.M. Belflower, Y.F. Dong, E.M. Schwarz, R.J. O'Keefe, and H. Drissi, "Runx1/Aml1/Cbfa2 Mediates Onset of Mesenchymal Cell Differentiation toward Chondrogenesis". *Journal of bone and mineral research : the official journal of the American Society for Bone and Mineral Research*, 2005. 20(9): p. 1624-36.
78. Smith, N., Y. Dong, J.B. Lian, J. Pratap, P.D. Kingsley, A.J. van Wijnen, J.L. Stein, E.M. Schwarz, R.J. O'Keefe, G.S. Stein, and M.H. Drissi, "Overlapping Expression of Runx1(Cbfa2) and Runx2(Cbfa1) Transcription Factors Supports Cooperative Induction of Skeletal Development". *Journal of cellular physiology*, 2005. 203(1): p. 133-43.
79. Zeng, L., H. Kempf, L.C. Murtaugh, M.E. Sato, and A.B. Lassar, "Shh Establishes an Nkx3.2/Sox9 Autoregulatory Loop That Is Maintained by Bmp Signals to Induce Somitic Chondrogenesis". *Genes & development*, 2002. 16(15): p. 1990-2005.
80. Lengner, C.J., M.Q. Hassan, R.W. Serra, C. Lepper, A.J. van Wijnen, J.L. Stein, J.B. Lian, and G.S. Stein, "Nkx3.2-Mediated Repression of Runx2 Promotes Chondrogenic Differentiation". *The Journal of biological chemistry*, 2005. 280(16): p. 15872-9.
81. Kumar, D. and A.B. Lassar, "The Transcriptional Activity of Sox9 in Chondrocytes Is Regulated by Rhoa Signaling and Actin Polymerization". *Molecular and cellular biology*, 2009. 29(15): p. 4262-73.
82. Yoshida, C.A. and T. Komori, "Role of Runx Proteins in Chondrogenesis". *Critical reviews in eukaryotic gene expression*, 2005. 15(3): p. 243-54.
83. Swiers, G., M. de Bruijn, and N.A. Speck, "Hematopoietic Stem Cell Emergence in the Conceptus and the Role of Runx1". *The International journal of developmental biology*, 2010. 54(6-7): p. 1151-63.
84. Fanning, P.J., G. Emkey, R.J. Smith, A.J. Grodzinsky, N. Szasz, and S.B. Trippel, "Mechanical Regulation of Mitogen-Activated Protein Kinase Signaling in Articular Cartilage". *The Journal of biological chemistry*, 2003. 278(51): p. 50940-8.
85. Selvamurugan, N., S.C. Jefcoat, S. Kwok, R. Kowalewski, J.A. Tamasi, and N.C. Partridge, "Overexpression of Runx2 Directed by the Matrix Metalloproteinase-13 Promoter Containing the Ap-1 and Runx/Rd/Cbfa Sites Alters Bone Remodeling in Vivo". *Journal of cellular biochemistry*, 2006. 99(2): p. 545-57.
86. Pratap, J., A. Javed, L.R. Languino, A.J. van Wijnen, J.L. Stein, G.S. Stein, and J.B. Lian, "The Runx2 Osteogenic Transcription Factor Regulates Matrix Metalloproteinase 9 in Bone Metastatic Cancer Cells and Controls Cell Invasion". *Molecular and cellular biology*, 2005. 25(19): p. 8581-91.
87. Rutges, J.P., R.A. Duit, J.A. Kummer, F.C. Oner, M.H. van Rijen, A.J. Verbout, R.M. Castelein, W.J. Dhert, and L.B. Creemers, "Hypertrophic Differentiation and Calcification During Intervertebral Disc Degeneration". *Osteoarthritis and cartilage / OARS, Osteoarthritis Research Society*, 2010. 18(11): p. 1487-95.

88. Gabay, O., D.J. Hall, F. Berenbaum, Y. Henrotin, and C. Sanchez, "Osteoarthritis and Obesity: Experimental Models". *Joint Bone Spine*, 2008. 75(6): p. 675-9.
89. Gregory, M.H., N. Capito, K. Kuroki, A.M. Stoker, J.L. Cook, and S.L. Sherman, "A Review of Translational Animal Models for Knee Osteoarthritis". *Arthritis*, 2012. 2012: p. 764621.
90. Pritzker, K.P., "Animal Models for Osteoarthritis: Processes, Problems and Prospects". *Annals of the rheumatic diseases*, 1994. 53(6): p. 406-20.
91. Glasson, S.S., T.J. Blanchet, and E.A. Morris, "The Surgical Destabilization of the Medial Meniscus (Dmm) Model of Osteoarthritis in the 129/Svev Mouse". *Osteoarthritis and cartilage / OARS, Osteoarthritis Research Society*, 2007. 15(9): p. 1061-9.
92. Hidaka, C., C. Cheng, D. Alexandre, M. Bhargava, and P.A. Torzilli, "Maturational Differences in Superficial and Deep Zone Articular Chondrocytes". *Cell and tissue research*, 2006. 323(1): p. 127-35.
93. Schmitz, N., S. Laverty, V.B. Kraus, and T. Aigner, "Basic Methods in Histopathology of Joint Tissues". *Osteoarthritis and cartilage / OARS, Osteoarthritis Research Society*, 2010. 18 Suppl 3: p. S113-6.
94. Abouheif, M.M., T. Nakasa, H. Shibuya, T. Niimoto, W. Kongcharoensombat, and M. Ochi, "Silencing Microrna-34a Inhibits Chondrocyte Apoptosis in a Rat Osteoarthritis Model in Vitro". *Rheumatology*, 2010. 49(11): p. 2054-60.
95. Zusso, M., L. Methot, R. Lo, A.D. Greenhalgh, S. David, and S. Stifani, "Regulation of Postnatal Forebrain Amoeboid Microglial Cell Proliferation and Development by the Transcription Factor Runx1". *J Neurosci*, 2012. 32(33): p. 11285-98.
96. Grogan, S.P., S. Miyaki, H. Asahara, D.D. D'Lima, and M.K. Lotz, "Mesenchymal Progenitor Cell Markers in Human Articular Cartilage: Normal Distribution and Changes in Osteoarthritis". *Arthritis research & therapy*, 2009. 11(3): p. R85.
97. Dowthwaite, G.P., J.C. Bishop, S.N. Redman, I.M. Khan, P. Rooney, D.J. Evans, L. Haughton, Z. Bayram, S. Boyer, B. Thomson, M.S. Wolfe, and C.W. Archer, "The Surface of Articular Cartilage Contains a Progenitor Cell Population". *Journal of cell science*, 2004. 117(Pt 6): p. 889-97.
98. Arufe, M.C., A. De la Fuente, I. Fuentes, F.J. de Toro, and F.J. Blanco, "Chondrogenic Potential of Subpopulations of Cells Expressing Mesenchymal Stem Cell Markers Derived from Human Synovial Membranes". *Journal of cellular biochemistry*, 2010. 111(4): p. 834-45.
99. Pretzel, D., S. Linss, S. Rochler, M. Endres, C. Kaps, S. Alsalameh, and R.W. Kinne, "Relative Percentage and Zonal Distribution of Mesenchymal Progenitor Cells in Human Osteoarthritic and Normal Cartilage". *Arthritis research & therapy*, 2011. 13(2): p. R64.
100. Fickert, S., J. Fiedler, and R.E. Brenner, "Identification of Subpopulations with Characteristics of Mesenchymal Progenitor Cells from Human Osteoarthritic

Cartilage Using Triple Staining for Cell Surface Markers". *Arthritis research & therapy*, 2004. 6(5): p. R422-32.
101. Alsalameh, S., R. Amin, T. Gemba, and M. Lotz, "Identification of Mesenchymal Progenitor Cells in Normal and Osteoarthritic Human Articular Cartilage". *Arthritis and rheumatism*, 2004. 50(5): p. 1522-32.
102. Lee, D.A., G. Bentley, and C.W. Archer, "The Control of Cell Division in Articular Chondrocytes". *Osteoarthritis and cartilage / OARS, Osteoarthritis Research Society*, 1993. 1(2): p. 137-46.
103. Scheitz, C.J. and T. Tumbar, "New Insights into the Role of Runx1 in Epithelial Stem Cell Biology and Pathology". *Journal of cellular biochemistry*, 2012.
104. Tsuzuki, S. and M. Seto, "Expansion of Functionally Defined Mouse Hematopoietic Stem and Progenitor Cells by a Short Isoform of Runx1/Aml1". *Blood*, 2012. 119(3): p. 727-35.
105. Bernardin, F. and A.D. Friedman, "Aml1 Stimulates G1 to S Progression Via Its Transactivation Domain". *Oncogene*, 2002. 21(20): p. 3247-52.
106. Strom, D.K., J. Nip, J.J. Westendorf, B. Linggi, B. Lutterbach, J.R. Downing, N. Lenny, and S.W. Hiebert, "Expression of the Aml-1 Oncogene Shortens the G(1) Phase of the Cell Cycle". *The Journal of biological chemistry*, 2000. 275(5): p. 3438-45.
107. Hoi, C.S., S.E. Lee, S.Y. Lu, D.J. McDermitt, K.M. Osorio, C.M. Piskun, R.M. Peters, R. Paus, and T. Tumbar, "Runx1 Directly Promotes Proliferation of Hair Follicle Stem Cells and Epithelial Tumor Formation in Mouse Skin". *Molecular and cellular biology*, 2010. 30(10): p. 2518-36.
108. Wotton, S.F., K. Blyth, A. Kilbey, A. Jenkins, A. Terry, F. Bernardin-Fried, A.D. Friedman, E.W. Baxter, J.C. Neil, and E.R. Cameron, "Runx1 Transformation of Primary Embryonic Fibroblasts Is Revealed in the Absence of P53". *Oncogene*, 2004. 23(32): p. 5476-86.
109. James, C.G., C.T. Appleton, V. Ulici, T.M. Underhill, and F. Beier, "Microarray Analyses of Gene Expression During Chondrocyte Differentiation Identifies Novel Regulators of Hypertrophy". *Molecular biology of the cell*, 2005. 16(11): p. 5316-33.
110. !!! INVALID CITATION !!!
111. Surrall, K.E., H.A. Bird, and J.S. Dixon, "Caeruloplasmin, Prealbumin and Alpha 2-Macroglobulin as Potential Indices of Disease Activity in Different Arthritides". *Clin Rheumatol*, 1987. 6(1): p. 64-9.
112. Bock, H.C., P. Michaeli, C. Bode, W. Schultz, H. Kresse, R. Herken, and N. Miosge, "The Small Proteoglycans Decorin and Biglycan in Human Articular Cartilage of Late-Stage Osteoarthritis". *Osteoarthritis and cartilage / OARS, Osteoarthritis Research Society*, 2001. 9(7): p. 654-63.
113. Kan, A., T. Ikeda, A. Fukai, T. Nakagawa, K. Nakamura, U.I. Chung, H. Kawaguchi, and C.J. Tabin, "Sox11 Contributes to the Regulation of Gdf5 in Joint Maintenance". *BMC Dev Biol*, 2013. 13(1): p. 4.

114. Lee, M.S., M.T. Sun, S.T. Pang, S.W. Ueng, S.C. Chen, T.L. Hwang, and T.H. Wang, "Evaluation of Differentially Expressed Genes by Shear Stress in Human Osteoarthritic Chondrocytes in Vitro". *Chang Gung Med J*, 2009. 32(1): p. 42-50.
115. Gavenis, K., T. Pufe, L.O. Brandenburg, K. Schiffl, and B. Schmidt-Rohlfing, "Effects of Controlled Released Bmp-7 on Markers of Inflammation and Degradation During the Cultivation of Human Osteoarthritic Chondrocytes". *J Biomater Appl*, 2011. 26(4): p. 419-33.
116. Endres, M., K. Andreas, G. Kalwitz, U. Freymann, K. Neumann, J. Ringe, M. Sittinger, T. Haupl, and C. Kaps, "Chemokine Profile of Synovial Fluid from Normal, Osteoarthritis and Rheumatoid Arthritis Patients: Ccl25, Cxcl10 and Xcl1 Recruit Human Subchondral Mesenchymal Progenitor Cells". *Osteoarthritis and cartilage / OARS, Osteoarthritis Research Society*, 2010. 18(11): p. 1458-66.
117. Baserga, R., "Is Cell Size Important?". *Cell cycle*, 2007. 6(7): p. 814-6.
118. Russell, J. and J.C. Zomerdijk, "Rna-Polymerase-I-Directed Rdna Transcription, Life and Works". *Trends in biochemical sciences*, 2005. 30(2): p. 87-96.
119. Bruce Alberts, A.J., Julian Lewis, Martin Raff, Keith Roberts, and Peter Walter., *Molecular Biology of the Cell, 4th Edition*2002, New York: Garland Science.
120. Moss, T., "At the Crossroads of Growth Control; Making Ribosomal Rna". *Current opinion in genetics & development*, 2004. 14(2): p. 210-7.
121. Bakshi, R., S.K. Zaidi, S. Pande, M.Q. Hassan, D.W. Young, M. Montecino, J.B. Lian, A.J. van Wijnen, J.L. Stein, and G.S. Stein, "The Leukemogenic T(8;21) Fusion Protein Aml1-Eto Controls Rrna Genes and Associates with Nucleolar-Organizing Regions at Mitotic Chromosomes". *Journal of cell science*, 2008. 121(Pt 23): p. 3981-90.
122. Pande, S., S.A. Ali, C. Dowdy, S.K. Zaidi, K. Ito, Y. Ito, M.A. Montecino, J.B. Lian, J.L. Stein, A.J. van Wijnen, and G.S. Stein, "Subnuclear Targeting of the Runx3 Tumor Suppressor and Its Epigenetic Association with Mitotic Chromosomes". *Journal of cellular physiology*, 2009. 218(3): p. 473-9.
123. Young, D.W., M.Q. Hassan, J. Pratap, M. Galindo, S.K. Zaidi, S.H. Lee, X. Yang, R. Xie, A. Javed, J.M. Underwood, P. Furcinitti, A.N. Imbalzano, S. Penman, J.A. Nickerson, M.A. Montecino, J.B. Lian, J.L. Stein, A.J. van Wijnen, and G.S. Stein, "Mitotic Occupancy and Lineage-Specific Transcriptional Control of Rrna Genes by Runx2". *Nature*, 2007. 445(7126): p. 442-6.
124. Darzynkiewicz, Z., D.P. Evenson, L. Staiano-Coico, T.K. Sharpless, and M.L. Melamed, "Correlation between Cell Cycle Duration and Rna Content". *Journal of cellular physiology*, 1979. 100(3): p. 425-38.
125. Hannan, R.D., A. Jenkins, A.K. Jenkins, and Y. Brandenburger, "Cardiac Hypertrophy: A Matter of Translation". *Clinical and experimental pharmacology & physiology*, 2003. 30(8): p. 517-27.

126. Hirata, M., F. Kugimiya, A. Fukai, S. Ohba, N. Kawamura, T. Ogasawara, Y. Kawasaki, T. Saito, F. Yano, T. Ikeda, K. Nakamura, U.I. Chung, and H. Kawaguchi, "C/Ebpbeta Promotes Transition from Proliferation to Hypertrophic Differentiation of Chondrocytes through Transactivation of P57". *PloS one*, 2009. 4(2): p. e4543.
127. Lee, M.H., I. Reynisdottir, and J. Massague, "Cloning of P57kip2, a Cyclin-Dependent Kinase Inhibitor with Unique Domain Structure and Tissue Distribution". *Genes & development*, 1995. 9(6): p. 639-49.
128. Zaidi, S.K., D.W. Young, M. Montecino, A.J. van Wijnen, J.L. Stein, J.B. Lian, and G.S. Stein, "Bookmarking the Genome: Maintenance of Epigenetic Information". *The Journal of biological chemistry*, 2011. 286(21): p. 18355-61.
129. Fazzari, M.J. and J.M. Greally, "Epigenomics: Beyond Cpg Islands". *Nature reviews. Genetics*, 2004. 5(6): p. 446-55.
130. Deaton, A.M. and A. Bird, "Cpg Islands and the Regulation of Transcription". *Genes & development*, 2011. 25(10): p. 1010-22.
131. David L. Nelson, M.M.C., *Lehninger Principles of Biochemistry, Third Edition*2000: W. H. Freeman.
132. Berger, S.L., "The Complex Language of Chromatin Regulation During Transcription". *Nature*, 2007. 447(7143): p. 407-12.
133. Mellor, J., P. Dudek, and D. Clynes, "A Glimpse into the Epigenetic Landscape of Gene Regulation". *Current opinion in genetics & development*, 2008. 18(2): p. 116-22.
134. Young, D.W., M.Q. Hassan, X.Q. Yang, M. Galindo, A. Javed, S.K. Zaidi, P. Furcinitti, D. Lapointe, M. Montecino, J.B. Lian, J.L. Stein, A.J. van Wijnen, and G.S. Stein, "Mitotic Retention of Gene Expression Patterns by the Cell Fate-Determining Transcription Factor Runx2". *Proceedings of the National Academy of Sciences of the United States of America*, 2007. 104(9): p. 3189-94.
135. Kamiya, N., A. Jikko, K. Kimata, C. Damsky, K. Shimizu, and H. Watanabe, "Establishment of a Novel Chondrocytic Cell Line N1511 Derived from P53-Null Mice". *Journal of bone and mineral research : the official journal of the American Society for Bone and Mineral Research*, 2002. 17(10): p. 1832-42.
136. Lengner, C.J., C. Lepper, A.J. van Wijnen, J.L. Stein, G.S. Stein, and J.B. Lian, "Primary Mouse Embryonic Fibroblasts: A Model of Mesenchymal Cartilage Formation". *Journal of cellular physiology*, 2004. 200(3): p. 327-33.
137. Atsumi, T., Y. Miwa, K. Kimata, and Y. Ikawa, "A Chondrogenic Cell Line Derived from a Differentiating Culture of At805 Teratocarcinoma Cells". *Cell differentiation and development : the official journal of the International Society of Developmental Biologists*, 1990. 30(2): p. 109-16.
138. Akhtar, N., Z. Rasheed, S. Ramamurthy, A.N. Anbazhagan, F.R. Voss, and T.M. Haqqi, "Microrna-27b Regulates the Expression of Matrix Metalloproteinase 13 in Human Osteoarthritis Chondrocytes". *Arthritis and rheumatism*, 2010. 62(5): p. 1361-71.

139. Javed, A., S.K. Zaidi, S.E. Gutierrez, C.J. Lengner, K.S. Harrington, H. Hovhannisyan, B.C. Cho, J. Pratap, S.M. Pockwinse, M. Montecino, A.J. van Wijnen, J.B. Lian, J.L. Stein, and G.S. Stein, "Chromatin Immunoprecipitation". *Methods Mol Biol*, 2004. 285: p. 41-4.
140. Constantinou, C., M. Bushell, I.W. Jeffrey, V. Tilleray, M. West, V. Frost, J. Hensold, and M.J. Clemens, "P53-Induced Inhibition of Protein Synthesis Is Independent of Apoptosis". *Eur J Biochem*, 2003. 270(15): p. 3122-32.
141. Pratap, J., M. Galindo, S.K. Zaidi, D. Vradii, B.M. Bhat, J.A. Robinson, J.Y. Choi, T. Komori, J.L. Stein, J.B. Lian, G.S. Stein, and A.J. van Wijnen, "Cell Growth Regulatory Role of Runx2 During Proliferative Expansion of Preosteoblasts". *Cancer research*, 2003. 63(17): p. 5357-62.
142. Sato, S., A. Kimura, J. Ozdemir, Y. Asou, M. Miyazaki, T. Jinno, K. Ae, X. Liu, M. Osaki, Y. Takeuchi, S. Fukumoto, H. Kawaguchi, H. Haro, K. Shinomiya, G. Karsenty, and S. Takeda, "The Distinct Role of the Runx Proteins in Chondrocyte Differentiation and Intervertebral Disc Degeneration: Findings in Murine Models and in Human Disease". *Arthritis and rheumatism*, 2008. 58(9): p. 2764-75.
143. Levanon, D., O. Brenner, V. Negreanu, D. Bettoun, E. Woolf, R. Eilam, J. Lotem, U. Gat, F. Otto, N. Speck, and Y. Groner, "Spatial and Temporal Expression Pattern of Runx3 (Aml2) and Runx1 (Aml1) Indicates Non-Redundant Functions During Mouse Embryogenesis". *Mechanisms of development*, 2001. 109(2): p. 413-7.
144. Werner, F.W., D.C. Ayers, L.P. Maletsky, and P.J. Rullkoetter, "The Effect of Valgus/Varus Malalignment on Load Distribution in Total Knee Replacements". *Journal of biomechanics*, 2005. 38(2): p. 349-55.
145. Lee, C.R., S. Grad, J.J. Maclean, J.C. Iatridis, and M. Alini, "Effect of Mechanical Loading on Mrna Levels of Common Endogenous Controls in Articular Chondrocytes and Intervertebral Disk". *Analytical biochemistry*, 2005. 341(2): p. 372-5.
146. Upton, M.L., J. Chen, F. Guilak, and L.A. Setton, "Differential Effects of Static and Dynamic Compression on Meniscal Cell Gene Expression". *Journal of orthopaedic research : official publication of the Orthopaedic Research Society*, 2003. 21(6): p. 963-9.
147. Tomiyama, T., K. Fukuda, K. Yamazaki, K. Hashimoto, H. Ueda, S. Mori, and C. Hamanishi, "Cyclic Compression Loaded on Cartilage Explants Enhances the Production of Reactive Oxygen Species". *The Journal of rheumatology*, 2007. 34(3): p. 556-62.
148. Knobloch, T.J., S. Madhavan, J. Nam, S. Agarwal, Jr., and S. Agarwal, "Regulation of Chondrocytic Gene Expression by Biomechanical Signals". *Critical reviews in eukaryotic gene expression*, 2008. 18(2): p. 139-50.
149. Murata, M., L.J. Bonassar, M. Wright, H.J. Mankin, and C.A. Towle, "A Role for the Interleukin-1 Receptor in the Pathway Linking Static Mechanical

Compression to Decreased Proteoglycan Synthesis in Surface Articular Cartilage". *Archives of biochemistry and biophysics*, 2003. 413(2): p. 229-35.
150. Ryan, J.A., E.A. Eisner, G. DuRaine, Z. You, and A.H. Reddi, "Mechanical Compression of Articular Cartilage Induces Chondrocyte Proliferation and Inhibits Proteoglycan Synthesis by Activation of the Erk Pathway: Implications for Tissue Engineering and Regenerative Medicine". *Journal of tissue engineering and regenerative medicine*, 2009. 3(2): p. 107-16.
151. Khan, I.M., R. Williams, and C.W. Archer, "One Flew over the Progenitor's Nest: Migratory Cells Find a Home in Osteoarthritic Cartilage". *Cell stem cell*, 2009. 4(4): p. 282-4.
152. Osorio, K.M., K.C. Lilja, and T. Tumbar, "Runx1 Modulates Adult Hair Follicle Stem Cell Emergence and Maintenance from Distinct Embryonic Skin Compartments". *The Journal of cell biology*, 2011. 193(1): p. 235-50.
153. Ali, S.A., S.K. Zaidi, C.S. Dacwag, N. Salma, D.W. Young, A.R. Shakoori, M.A. Montecino, J.B. Lian, A.J. van Wijnen, A.N. Imbalzano, G.S. Stein, and J.L. Stein, "Phenotypic Transcription Factors Epigenetically Mediate Cell Growth Control". *Proceedings of the National Academy of Sciences of the United States of America*, 2008. 105(18): p. 6632-7.